

DIFFERENTIAL RESPONSES TO *SALMONELLA* TYPHIMURIUM INFECTION IN
THE COLLABORATIVE CROSS MOUSE POPULATION

A Dissertation

by

KRISTIN MOZELLE SCOGGIN

Submitted to the Graduate and Professional School of
Texas A&M University
in partial fulfillment of the requirements for the degree of

DOCTOR OF PHILOSOPHY

Chair of Committee,	David Threadgill
Co-Chair of Committee,	Helene Andrews-Polymenis
Committee Members,	Mark Heise Phillip West
Head of Department,	David Threadgill

December 2021

Major Subject: Genetics

Copyright 2021 Kristin Mozelle Scoggin

ABSTRACT

Salmonella Typhimurium (STm) usually cause self-limiting gastroenteritis. In some individuals, these bacteria can spread systemically and cause disseminated disease. Rising incidence of antibiotic resistance in STm is a world-wide health concern. Exploration of disease phenotypes that differ between individuals may offer alternative pathways for treatment of infections that do not rely on traditional antibiotics. We screened 32 Collaborative Cross (CC) lines for their responses to oral infection with STm to discover new pathways involved in response to infection and host disease outcome. Eighteen CC lines survived to day 7, while fourteen required euthanasia before day 7. The surviving 18 lines were infected and monitored for three weeks. Five of these lines reduced the bacterial load and were called resistant, 6 lines maintained a bacterial load and were categorized as tolerant, and 7 lines succumbed to infection before three-weeks and were called delayed susceptible. The tolerant lines maintained bacterial burdens in Peyer's patches (PP), mesenteric lymph node (MLN), spleen, and liver, while resistant lines had significantly lower colonization in multiple tissues. Surviving mice had lower baseline temperatures than susceptible mice at one week post-infection and tolerant lines had lower baseline temperatures than both delayed susceptible and resistant. Resistant lines reduced tissue damage in spleen and liver while tolerant lines did not repair tissue damage between one and three weeks post-infection. We identified four suggestive loci for one-week survival, and one significant and six suggestive associations for three-week phenotypes. CC045 was particularly unusual as it survived

one-week infections with high bacterial loads and modest weight loss, unlike other lines carrying the *Slc11a1* mutation. We generated an *Slc11a1*⁻ F2 population between CC045 and CC061. F1s all survived infection as did the majority of the F2s, supporting a dominant phenotype. The F2s were highly colonized in spleen and liver while maintaining body weight better than CC061, the parental susceptible line. Genetic analysis was performed on the survival data and four significant associations, and one significant allele interaction were identified.

ACKNOWLEDGEMENTS

First and foremost, I would like to thank my committee chairs Dr. David Threadgill and Dr. Helene Andrews-Polymenis and my committee members Dr. Phillip West and Dr. Mark Heise who have challenged and guided me through the ups and downs of this project.

I would also like to thank my lab mates, past and present, who have helped me through tough times, whether it be an assay that would not quite work or prelims, they are always there to lend an ear.

Thanks also goes to Dr. Michael Kirby and his group, particularly Dr. Manuchehr Aminian and Dr. Amy Peterson, who have helped me analyze the overwhelming amounts of data generated throughout this project.

Finally, I would like to thank my parents, my husband, and my dog for their emotional support, encouragement, and unyielding belief in my abilities. Without them, there is no way I could have completed my dissertation and kept my sanity!

CONTRIBUTORS AND FUNDING SOURCES

Contributors

This work was supported by a dissertation committee consisting of Dr. David Threadgill (chair), Dr. Helene Andrews-Polymenis (co-chair), Dr. Phillip West, and Dr. Mark Heise. The telemetry data in chapters 1 and 2 was analyzed by Dr. Manuchehr Aminian and the RNA-seq analysis in chapters 1 and 2 was performed by Dr. Amy Peterson, both under the supervision of Dr. Michael Kirby. The histopathology scoring was done by Dr. Garry Adams, an expert board-certified pathologist. The QTL analysis in chapter 3 was performed by Aravindh Nagarajan. All RNA sequencing data was generated by the Texas A&M Institute for Genome Sciences and Society (TIGSS).

Funding Source

This work was funded by the Department of Defense (DoD) grant DARPA D17AP00004.

NOMENCLATURE

CBC	Complete Blood Count
CC	Collaborative Cross
CFU	Colony Forming Unit
Chr	Chromosome
ENA-78	Epithelial Neutrophil-Activating Protein 78
F1	First Filial Generation
F2	Second Filial Generation
IFN-gamma	Interferon-gamma
LB	Luria-Bertani
LPS	Lipopolysaccharide
LYM	Lymphocytes
MCP-1	Monocyte Chemoattractant Protein-1
MLN	Mesenteric Lymph Node
MON	Monocytes
NADPH	Nicotinamide adenine dinucleotide phosphate
Nal	Nalidixic acid
NEU	Neutrophils
<i>Ncf2</i>	Neutrophil Cytosolic Factor 2
NTS	Non-typhoidal Salmonella
PBS	Phosphate-buffered saline

PP	Peyer's Patches
QTL	Quantitative Trait Loci
<i>Slc11a1</i>	Solute Carrier Family 11 Member 1
SNP	Single Nucleotide Polymorphisms
STm	<i>Salmonella enterica</i> serotype Typhimurium
<i>Tlr4</i>	Toll-like Receptor 4
VEP	Ensembl Variant Effect Predictor
WBC	White Blood Cell

TABLE OF CONTENTS

	Page
ABSTRACT	ii
ACKNOWLEDGEMENTS	iv
CONTRIBUTORS AND FUNDING SOURCES.....	v
NOMENCLATURE.....	vi
TABLE OF CONTENTS	viii
LIST OF FIGURES.....	x
LIST OF TABLES	xiii
CHAPTER I INTRODUCTION	1
<i>Salmonella enterica</i>	1
<i>Salmonella</i> susceptibility genes in mice.....	3
The Collaborative Cross.....	4
Tolerance.....	6
Aims of this study	8
CHAPTER II GENETIC BACKGROUND INFLUENCES SURVIVAL TO <i>SALMONELLA ENTERICA</i> SEROVAR TYPHIMURIUM INFECTION IN THE COLLABORATIVE CROSS.....	10
Overview	10
Introduction	11
Results.....	14
Discussion	44
Materials/Methods.....	51
CHAPTER III ELUCIDATING TOLERANCE MECHANISMS TO <i>SALMONELLA</i> TYPHIMURIUM ACROSS LONG-TERM INFECTIONS USING THE COLLABORATIVE CROSS.....	60
Overview	60
Introduction	61

Results	63
Discussion	86
Materials/Methods.....	90
CHAPTER IV CC045 SURVIVES <i>SALMONELLA</i> TYPHIMURIUM INFECTION DESPITE CARRYING THE SUSCEPTIBLE MUTATION IN <i>SLC11A1</i>	99
Overview	99
Introduction	100
Results	102
Discussion	115
Materials/Methods.....	120
CHAPTER V CONCLUSIONS AND FUTURE DIRECTIONS.....	123
REFERENCES	136
APPENDIX A	158

LIST OF FIGURES

	Page
Figure 1: Salmonella pathogenesis in invasive disease.....	2
Figure 2: Generation of the Collaborative Cross	5
Figure 3: Infectious disease outcomes in mice.....	7
Figure 4: Survival is correlated to CFU and % weight change.....	14
Figure 5: CC lines have variable responses to STm infection.	15
Figure 6: Survival for susceptible lines is correlated to CFU and % weight change.....	17
Figure 7: Sex differences found in 8 CC lines.	19
Figure 8: Each line has a unique circadian pattern before infection.	22
Figure 9: At pre-infection baseline, susceptible lines have higher body temperatures, are more active during normal rest period, and maintain activity patterns longer than temperature patterns than surviving lines.	25
Figure 10: Intestinal organs were minimally damaged after STm infections.	26
Figure 11: Spleen and liver damage weakly correlate with survival time.	27
Figure 12: White blood cells are not significantly different between surviving and susceptible lines.	31
Figure 13: QTLs for 30 CC lines, excluding CC042 and CC045.	38
Figure 14: QTL of slope of survival, or how quickly each line succumbed to infection.	39
Figure 15: Founder effects plots for QTL of median time survived.	40
Figure 16: Founder effect plots of QTL of percent of mice surviving to day 7.....	41
Figure 17: CC mice infected orally with STm are more highly and variably colonized than after IV infection.....	48
Figure 18: Delayed susceptible, tolerant, and resistant lines show distinct responses to STm infections.....	66

Figure 19: Ileum, cecum, and colon CFU/g are not significantly different.	67
Figure 20: CC lines resistant to STm infection have lower MLN and PP colonization compared to tolerant strains.....	68
Figure 21: Tolerant mice have cooler body temperatures and deviate from normal body temperature patterns sooner than resistant mice.	71
Figure 22: Activity levels and off-pattern time is not significantly different between groups.	72
Figure 23: Tolerant mice have higher WBC and higher NEU than resistant mice.	75
Figure 24: Tolerant lines have more INF- γ and MCP-1, but less ENA-78 at 3 weeks post-infection than resistant lines.	77
Figure 25: Histopathology scores for all organs.	79
Figure 26: QTLs for CFU for 18 CC lines.	83
Figure 27: QTLs for resistances for 32 CC lines.	84
Figure 28: QTLs for tolerance for 27 CC lines.	85
Figure 29: Liver and spleen colonization is significantly lower in resistant lines three- weeks post-infection.	86
Figure 30: CC045 survives longer and loses less weight while maintaining a similar bacterial burden in spleen and liver.	103
Figure 31: CC045 does not have a different baseline CBC.	104
Figure 32: CC045 has some differences in CBC change post-infection.....	106
Figure 33: F2 survival, weight change, and bacterial burdens in spleen and liver.	108
Figure 34: F2 survival, weight change, and bacterial burdens in spleen and liver separated by sex.....	109
Figure 35: Survival is strongly correlated to weight change and weakly correlated to CFU for F2.....	110
Figure 36: Survival QTL for 245 F2 mice.	111
Figure 37: Allele effect plots for significant QTL regions.....	113

Figure 38: Allele interaction plots for top SNPs on significant QTL regions.....	114
Figure 39: CC045 did not have any differences in INF- γ levels post-infection.....	119
Figure A1: Histopathology scoring matrix with descriptions	159
Figure A2: Graphical representation of how telemetry models were run	160

LIST OF TABLES

	Page
Table 1: Uninfected baseline Complete Blood Counts	29
Table 2: Infected Complete Blood Counts at necropsy time minus uninfected mean for respective line.	30
Table 3: Uninfected baseline for 36 cytokines.	32
Table 4: Infected cytokine values taken at necropsy time minus uninfected mean values for respective line.	33
Table 5: QTL associations for median survival time and percent survived to day 7 after STm infections.	37
Table 6: Median Survival Time QTL Candidate Genes.	42
Table 7: % Survived to Day 7 QTL Candidate Genes.	43
Table 8: Number of mice used and facility of origin for 2 control strains and 32 CC lines.	52
Table 9: Median values of temperature for rest period, 24-hour period, and active period.	70
Table 10: Infected Complete Blood Counts taken at necropsy time minus uninfected mean for respective line.	74
Table 11: 36 Infected Cytokines taken at necropsy time minus uninfected mean for respective line.	78
Table 12: QTLs for resistance and tolerance categorization and spleen/liver CFU after STm infections.	82
Table 13: Number of mice used and facility origin for 18 CC lines.	91
Table 14: Significant survival QTL associations for CC061xCC045 F2 mice.	112
Table 15: Number of mice used for infections and facility of origin.	120
Table A1: Representative images of spleen and liver histology scoring matrix	158

CHAPTER I

INTRODUCTION

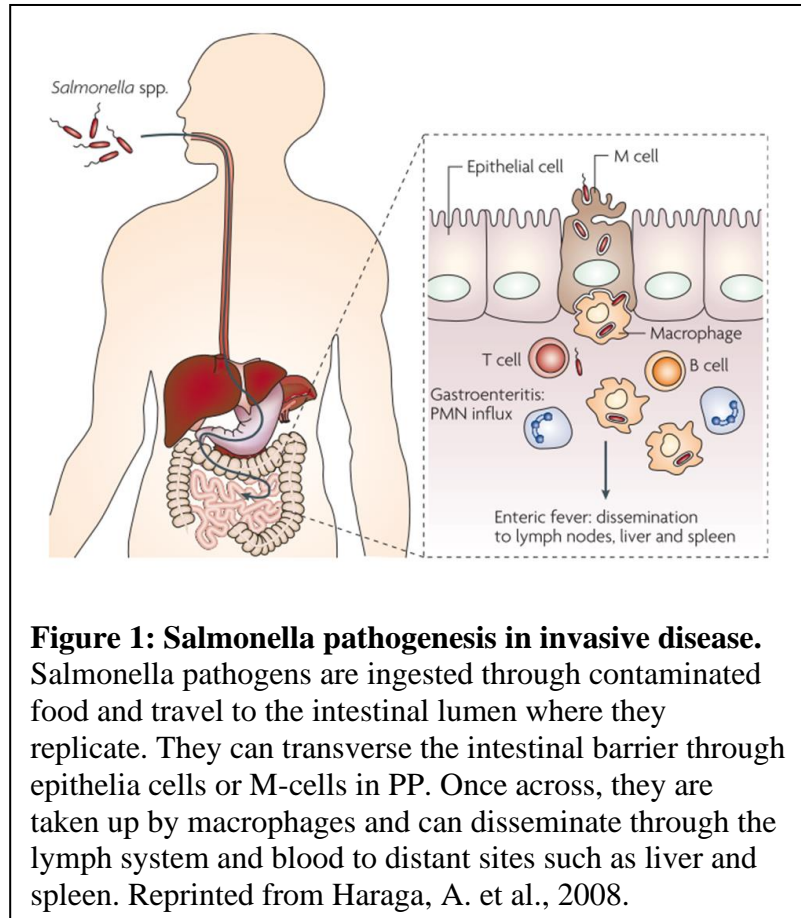
Salmonella enterica

Non-typhoidal *Salmonella* (NTS) are estimated to cause 93.8 million human cases per year, resulting in 155,000 deaths worldwide (1). While NTS infection is typically limited to the intestine and causes diarrheal disease, it can also cause more severe disseminated disease in some individuals, depending on the *Salmonella* serotype and host factors such as age, immune status, and genetics (2–5). Immunosuppressive infections and conditions such as HIV, diabetes mellitus, and malaria make individuals especially susceptible to severe disseminated infections that require treatment (6, 7). Worldwide, 535,000 human cases of disseminated disease, either *Salmonella* bacteremia or invasive non-typhoidal salmonellosis, occur annually and cause 77,500 deaths (4).

Salmonella enterica are Gram negative facultative intracellular bacteria that cause a wide range of disease phenotypes such as gastroenteritis, typhoid fever, bacteremia, and sepsis in hosts ranging from chicken to mice and humans (3, 8–10). Typically, a host will ingest the bacteria through contaminated food or water (8, 11). Once inside the intestinal tract, the bacteria invade epithelial cells, including the intestinal microfold (M) cells of the Peyer's patches (PP) (3, 11–13) (Fig. 1). From there, the bacteria are engulfed by phagocytic cells such as macrophages. Once inside macrophages, *Salmonella* modify the phagosome that they reside and replicate in into a *Salmonella* containing vacuole (SCV). In invasive disease, the bacteria will migrate to

the mesenteric lymph nodes (MLN) and drain into the bloodstream where it can enter the reticuloendothelial system and infect the spleen and liver causing disseminated disease (3, 14) (Fig. 1).

Although antibiotics are not generally used to treat patients with NTS gastroenteritis, they are used to treat patients with NTS bacteremia or invasive non-typhoidal salmonellosis. Thus, a concern of increasing importance is development of multi-



drug resistant strains of *Salmonella* that cause 212,500 human cases per year in the US alone, with 16% of all NTS cases resistant to at least one antibiotic as of 2017 (15). In addition, antibiotics also kill the host's natural microbiota, a vital component to limiting the growth of intestinal pathogens such as *Salmonella* (16, 17). Exploitation of differences in host immunity may help identify new interventions that could become better treatment alternatives to antibiotics (18–20).

***Salmonella* susceptibility genes in mice**

Salmonella enterica serotype Typhimurium (STm) is one of the most common serotypes of non-typhoidal *Salmonella* and infection in mice models severe invasive human infections (10, 21). Some mouse strains are particularly susceptible (C57BL/6J and BALB/cJ), while others are able to resist severe systemic disease (CBA/J, 129/SvJ, and A/J) (10, 12, 22). Response to infection with STm in mice has historically been categorized as either resistant or susceptible, based primarily on a mutation in the gene Solute Carrier Family 11 Member 1 (*Slc11a1*) that encodes a metal cation pump in macrophages reducing intracellular growth of bacteria (3, 23–27). This pump extrudes divalent cations, such as iron and manganese, that are often the limiting resource for intracellular pathogens and for enhancing pro-inflammatory immune pathways (28, 29). There are two forms of *Slc11a1*: a wild type “resistant” allele and a mutated “susceptible” allele with a glycine to aspartic amino acid substitution at position 169, rendering the protein non-functional (29).

Natural variation in other murine genes has also played a role in survival after STm infection, including Neutrophil Cytosolic Factor 2 (*Ncf2*) and Toll-like Receptor 4 (*Tlr4*) and has also been linked to survival to STm infections in mice (27, 30–32). *Ncf2* encodes a component of the Nicotinamide adenine dinucleotide phosphate (NADPH) complex in neutrophils that generates superoxide and is vital to neutrophil’s killing ability (27, 30). In fact, humans with defects in neutrophil function are more susceptible to various pathogens including invasive *Salmonella* (25). Toll-like receptor 4 (*Tlr4*)

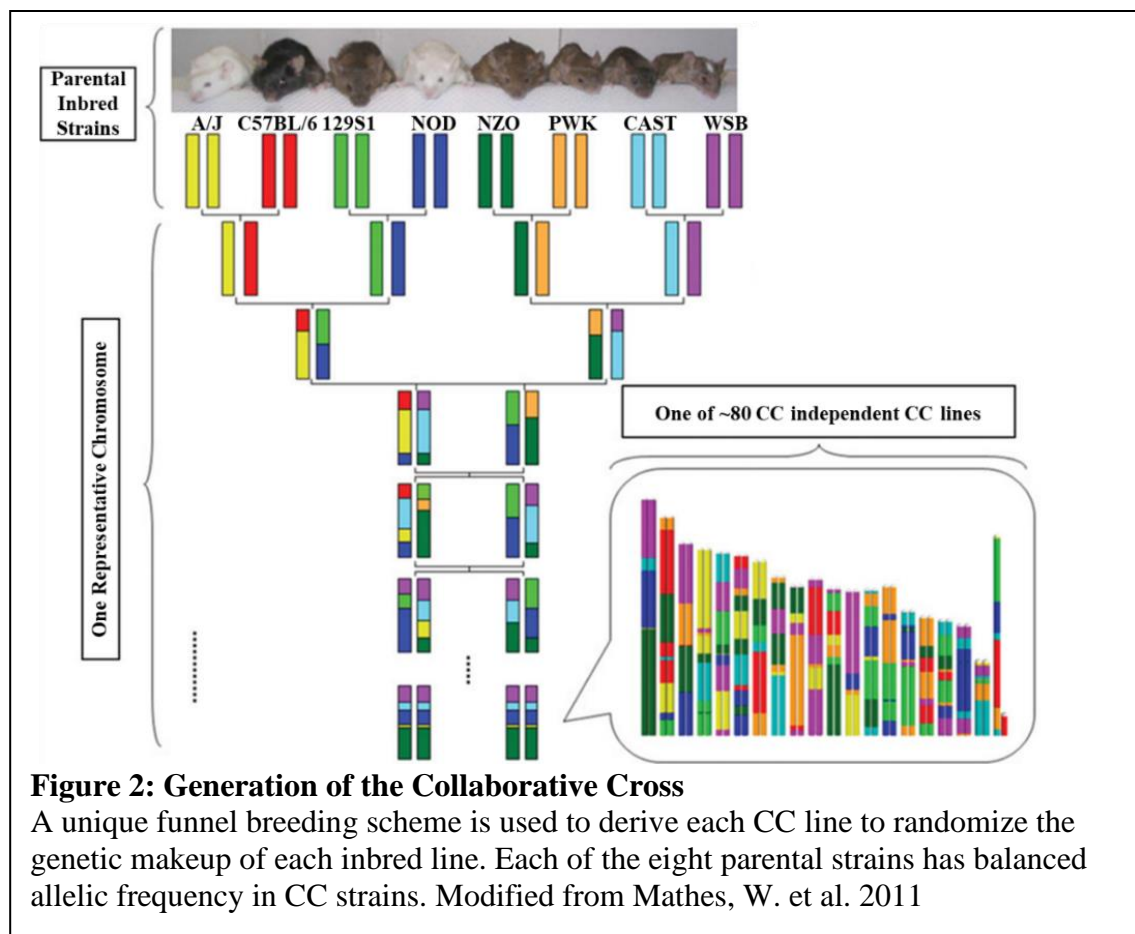
recognizes lipopolysaccharide (LPS) and is a key component of innate immune response activation and cytokine production (31, 32). Even more genes have been linked to poor outcomes after STm infection including Bruton agammaglobulinemia tyrosine kinase (*Btk*), needed for proper B-cell development and later phase control of STm infections, and Lipopolysaccharide-binding protein (*Lbp*) and CD14 antigen (*Cd14*) which are involved in innate immune response to LPS in early infection (10, 25, 33). While mutations in these genes and others have been linked to poor survival outcomes after STm infection, mutations in *Slc11a1* are the most detrimental (27, 29, 32).

Many cytokines and the genes encoding them have also been linked to STm infection outcome including TNF- α , IFN- γ , IL-12, and IL-1 (10, 12, 34, 35). However, there is a growing appreciation that response to infection is complex, and not simply binary. Our understanding of host responses is expanding beyond the binary parameters of susceptibility and resistance with increasing use of hosts of different genetic backgrounds, including the diverse mouse population called The Collaborative Cross (CC).

The Collaborative Cross

Traditional inbred strains allow for replication of experiments, but limit the genetic diversity tested, while outbred populations capture genetic diversity but are not replicable. The Collaborative Cross mouse reference population was created to overcome this challenge, as a mouse population that is both diverse and allows replication (36, 37). The CC is a diverse panel of recombinant inbred mouse lines that

recapitulates the genetic diversity found in human populations (38–41). The collaborative cross was generated using a funnel breeding scheme and the eight founder strains capture 90% of all genetic diversity found in mice. While typical recombinant inbred lines start with two parental strains, the CC has eight founder strains: five traditional laboratory mouse strains (A/J, C57BL/6J, 129S1/SvImJ, NOD/SHiLtJ, NZO/HILtJ) and three wild derived strains (CAST/EiJ, PWK/PhJ, WSB/EiJ) (42) (Fig. 2).



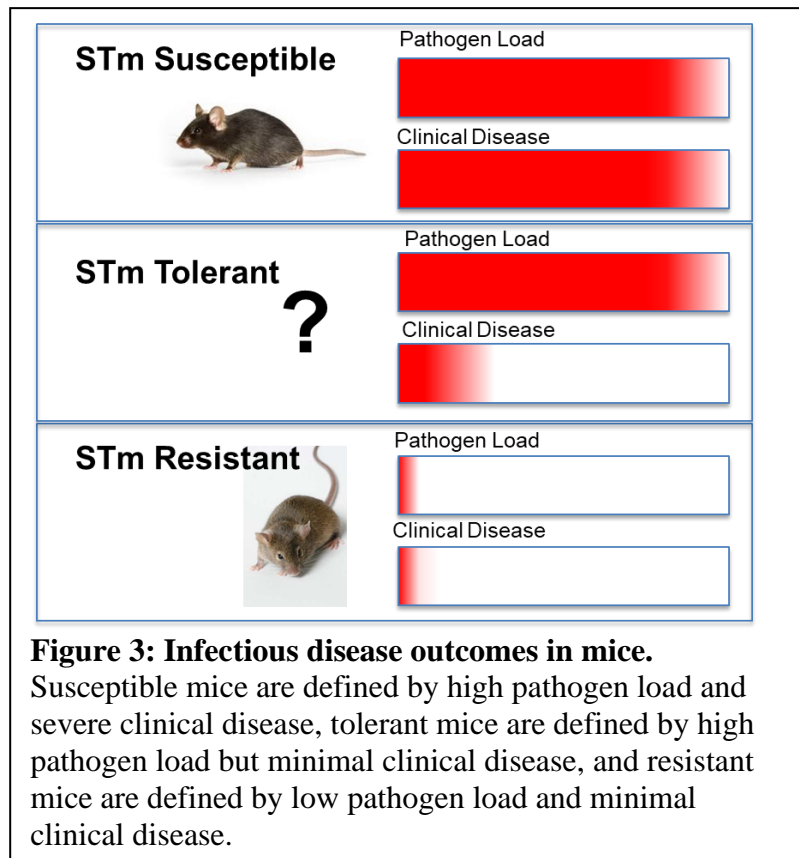
Only one of the CC founders (C57BL/6J) carries the *Slc11a1* mutation, three (PWK/PhJ, CAST/EiJ, NZO/ HILtJ) carry the *Ncf2* mutation, and none carry the *Tlr4*

mutation. This diversity allows us to capture new phenotypic combinations not present in other mouse strains and can reveal new phenotypes (37–39, 43). The CC has greater variability across all parameters than traditional lines, including baseline immune phenotypes such as B and T cell populations and natural killer and dendritic cells (2, 36, 44–46). This population has been used to identify novel genetic variants and new phenotypes in mice, including infectious agents (47–50). Viral infections have been the most heavily studied using the CC and include West Nile virus (51, 52), Influenza A (53–55), Ebola (56, 57), Theiler’s murine encephalomyelitis virus (58), and SARS-Corona virus (59, 60). The CC has also been used to study various bacterial pathogens including *Klebsiella pneumoniae* (61), *Pseudomonas aeruginosa* (62), periodontal bacterial populations (63), *Mycobacterium tuberculosis* (64), and most recently *Salmonella* Typhimurium (65, 66). These new mouse phenotypes can model human disease more precisely and potentially become new mouse models (50). This population has even enabled researchers to identify unique de-novo mutations, such as a new *Mx1* mutant for susceptibility to influenza infection and *Itgal* mutation for susceptibility to *Salmonella* infections (53, 66).

Tolerance

In mammalian systems, host response to infections has been categorized as susceptible and resistant, based on the host’s ability to clear the infection; either the host is able to kill the invading pathogen and survive, or the host is unable to fight off the infection and becomes ill (10, 67) (Fig. 3). However, a third response called tolerance

has been acknowledged in plant systems for many years and is now being applied to other systems such as *Drosophila* and mice (47, 49, 68–72). Tolerance is now being thought of as a quintessential part of immunity and is perhaps as important as resistance (73). In



tolerance, the host tolerates damage done by either the pathogen or the immune system thus preventing serious illness during infection (72–74) (Fig. 3). Minimizing tissue damage through immune modulation or toxin neutralization are classic tolerance mechanisms, allowing the host to maintain homeostasis in the face of high pathogen burden (73, 75). However, tolerance can also be induced by food intake modulation and thermoregulatory changes (76–78). Tolerance can even be promoted by commensal intestinal organisms such as *Escherichia coli* (79). While tolerance helps a host survive, it does not prevent the host from infecting other hosts, thus tolerance is not beneficial for eradicating diseases (80).

Tolerance has been described for influenza virus in some CC lines, where these lines had a high viral titer but also maintained their weight (81). Tolerance was also identified when CC mice were exposed to Ebola virus, with similar high viral titer and low weight loss (41, 56).

Aims of this study

To screen for new phenotypes suggesting new mechanisms underlying diverse host responses to STm infections in mice, we infected CC lines and monitored infected lines for one week. We took many measurements before and after infection including baseline body temperature and activity, bacterial burden in various tissues, and both uninfected and infected complete blood counts (CBC) and cytokine levels. Lines that survived to day 7 had lower baseline temperatures but deviated from their normal pattern of body temperature and activity similarly to susceptible lines. All parameters were line dependent, but in general, mice were colonized in systemic organs independent of survival time, spleen damage was most correlated to survival, and cytokines and CBC parameters were not predictive of survival. QTLs associated with survival time showed three significant and two suggestive associations, confirming known loci and detecting previously unknown variants providing new candidate genes not previously associated with STm.

Since colonization levels at one-week post-infection for surviving lines were indistinguishable, we infected the surviving 18 lines and monitored them over three-weeks. Tolerant lines maintained a significantly higher bacterial burden in PP, MLN,

spleen, and liver than resistant lines. Tolerant lines also lost more weight than resistant lines despite surviving the infections. Resistant lines reduced tissue damage in spleen and liver significantly more than tolerant lines between one- and three- weeks post-infection. Whole blood and serum were also collected at this time, and tolerant lines had more circulating total white blood cells, neutrophils, Interferon-gamma (IFN-gamma), and Monocyte Chemoattractant Protein-1 (MCP-1) than resistant lines. Resistant lines had significantly more circulating Epithelial Neutrophil-Activating Protein 78 (ENA-78) than tolerant lines. Quantitative trait loci (QTL) analysis was also performed and one significant association, *Scq1*, and six suggestive association were found.

During one-week infections, one line, CC045, survived to day 7 despite carrying the *Slc11a1* mutation, while maintaining high bacterial loads in spleen and liver. We measured bacterial burden, weight change, and baseline and infected white blood cells across the five *Slc11a1* CC mutants and C57BL/6J after one-week infections with STm and found no differences. We generated an F2 population with CC045 and CC061 to identify what makes CC045 unique. F1s survived to day 7 and lost less weight than CC061 but were colonized to a lower degree in spleen and liver than CC045. This finding suggests that the genetic component supporting CC045 survival after infection with STm is dominant. When F2s were infected, most survived to day 7 and were highly colonized in spleen and liver. Bacterial burden in both spleen and liver were weakly correlated with survival time. When R/qt12 was used to analyze the survival time, 4 significant associations and one allele interaction were identified.

CHAPTER II

GENETIC BACKGROUND INFLUENCES SURVIVAL TO *SALMONELLA* *ENTERICA* SEROVAR TYPHIMURIUM INFECTION IN THE COLLABORATIVE CROSS

Overview

Salmonella infections typically cause self-limiting gastroenteritis, but in some individuals these bacteria can spread systemically and cause disseminated disease. *Salmonella* Typhimurium (STm) causes severe systemic disease in most inbred mice. To screen for new infection phenotypes across a range of host genetics, we infected 32 Collaborative Cross (CC) mouse lines orally with STm and monitored their disease progression for seven days. Eighteen CC lines survived to day 7, while fourteen susceptible lines succumbed to infection before day 7. Our data revealed a broad range of phenotypes across many parameters including survival, bacterial colonization, tissue damage, complete blood counts (CBC), and cytokines in serum. Several lines showed sex differences across several parameters. Surviving lines had lower baseline temperatures pre-infection and were less active during their active period. Temperature disruptions were detected earlier than activity disruptions, making temperature a better detector of illness. All lines had STm in spleen and liver, but susceptible lines had higher levels than surviving lines. Tissue damage was weakly negatively correlated to survival, while CBC and cytokines were not. We identified loci associated with survival on Chromosomes (Chr) 1, 2, 4, 7. Polymorphisms in *Ncf2* and *Slc11a1*, known to reduce

survival in mice after STm infections, are located in the Chr 1 interval we identified, and the Chr 7 association overlaps with a previously identified QTL peak called Ses2. We identified the genetic regions on Chr 2 and 4 associated with susceptibility to STm infection for the first time. Our data reveal the diversity of responses to STm infection across a range of host genetics and identified new candidate regions for survival after STm infection.

Introduction

Salmonellae are Gram negative facultative intracellular bacteria that cause self-limiting gastroenteritis, typhoid fever, or sepsis (3, 8, 9). Non-typhoidal *Salmonella* (NTS) infections are estimated to cause 93.8 million human cases per year, resulting in 155,000 deaths worldwide (1). While NTS infection is typically limited to the intestine and causes diarrheal disease, NTS can also cause more severe disseminated disease, depending on the *Salmonella* serotype and host factors such as age, immune status, and genetics (2). Worldwide, 535,000 human cases of NTS disseminated disease, either *Salmonella* bacteremia or invasive non-typhoidal salmonellosis, occur annually and cause 77,500 deaths (4).

Although antibiotics are not generally used to treat patients with NTS gastroenteritis, they are used to treat patients with NTS bacteremia and invasive non-typhoidal salmonellosis. Thus, a concern of increasing importance is development of multi-drug resistant strains of *Salmonella* that cause 212,500 human cases per year in the US alone, with 16% of all NTS cases resistant to at least one antibiotic as of 2017 (15).

Exploitation of differences in host immunity may help identify new interventions that could become treatment alternatives to antibiotics (18–20).

Salmonella enterica serotype Typhimurium (STm) is a serotype of non-typhoidal *Salmonella* that causes murine typhoid resembling severe invasive human infections. Some mouse strains are particularly susceptible (C57BL/6J and BALB/cJ), while others are able to resist severe systemic disease (CBA/J, 129/SvJ, and A/J) (10, 12, 22). Previous studies have largely attributed differential susceptibility to a mutation in Solute Carrier Family 11 Member 1 (*Slc11a1*) encoding a metal cation pump in macrophages that reduces intracellular growth of bacteria (3, 23–25). Natural variation in other genes has also been shown to play a role in differential survival after STm infection, including Neutrophil Cytosolic Factor 2 (*Ncf2*) and Toll-like Receptor 4 (*Tlr4*). *Ncf2* encodes a component of the NADPH complex in neutrophils that generates superoxide and is vital to neutrophil's killing ability (27, 30). Toll-like receptor 4 (*Tlr4*) recognizes lipopolysaccharide (LPS) and is a key component of innate immune response activation and cytokine production (31, 32).

To identify new host genetic mechanisms that could influence differential susceptibility to STm infections, we used the Collaborative Cross (CC) mouse genetic reference population (37–39, 43). The CC has greater variability across all parameters than traditional lines, including immune phenotypes, because of its genetic diversity (36, 44, 45). This population has been used to identify novel genetic variants and discover new phenotypes in mice, such as tolerance (high pathogen load with minimal disease) (47–49) for infectious agents including Influenza A, Ebola, Mycobacterium

Tuberculosis, Theiler's murine encephalomyelitis virus, SARS-Corona virus, and West Nile virus (54–56, 58, 64, 82, 83).

To identify new mechanisms underlying diverse host responses to STm infections in mice, we infected CC lines orally and monitored infected animals for one-week post-infection using telemetry to track temperature and activity levels. At necropsy, organs and blood were collected to analyze colonization, RNA levels, histopathology, complete blood counts (CBC), and cytokine levels. Lines that survived to day 7 had lower baseline uninfected body temperatures and were less active during their active period pre-infection. Temperature patterns were disrupted earlier than activity patterns, suggesting that temperature is a more sensitive measurement for illness. All parameters were line dependent, but in general, mice were colonized in systemic organs independent of survival time, spleen damage was most correlated to survival, and cytokines and CBC parameters were not predictive of survival. Several lines showed sex differences across survival, weight change, and bacterial burden, but one line, CC027, showed stark sex-dependence across all parameters. QTLs analysis for survival time revealed three significant and two suggestive associations, confirming known loci and detecting previously unknown variants providing new candidate genes not previously associated with STm. Furthermore, despite having susceptible alleles in both *Slc11a1* and *Ncf2* that are linked to early death from *Salmonella* infection, CC045 mice were able to survive 7 days with a high bacterial load and exhibited tolerance to systemic *Salmonella* infection.

Results

Response to oral *Salmonella* Typhimurium infection is variable across CC lines.

Thirty-two Collaborative Cross (CC) lines were infected with *S. Typhimurium* (STm) ATCC14028 and monitored for up to one week to identify variable susceptibility to STm infection. Due to their well-characterized response to STm infection, C57BL/6J (B6) mice, which develop systemic murine typhoid, and CBA/J (CBA) mice, which are resistant to systemic infection, were used as infection controls. At the time of necropsy,

sections of ileum,

cecum, colon, liver, and

spleen were collected to

determine bacterial load.

We focused our analysis

on the systemic phase of

infection. Using sex-

combined median data,

the correlation between

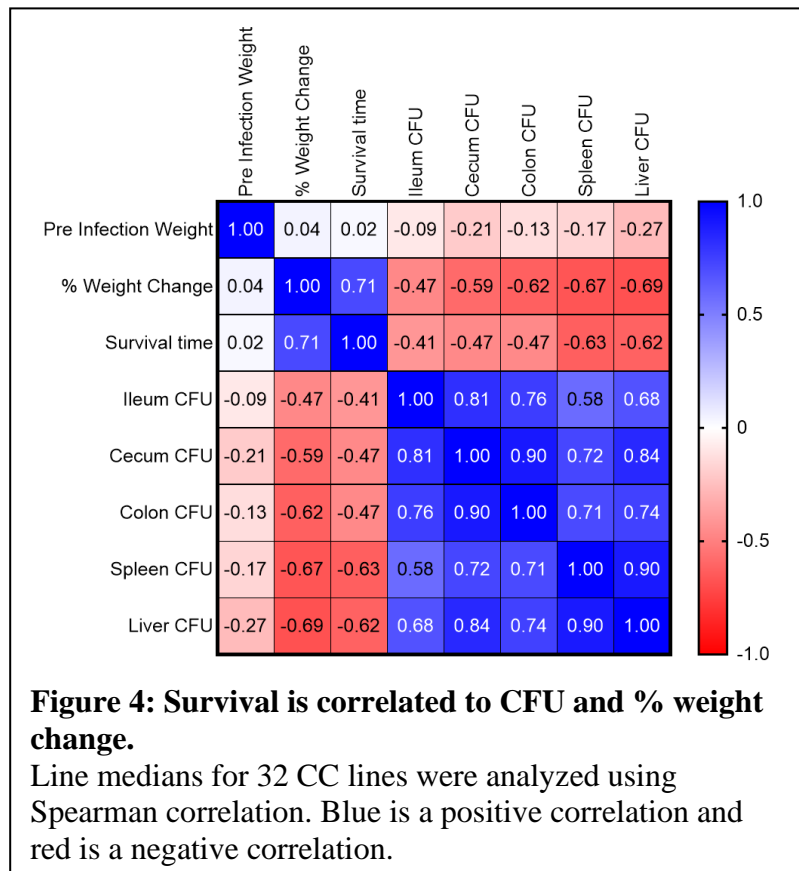
liver and spleen

colonization with

survival time was $R = -$

0.62 and -0.63,

respectively (Fig. 4).



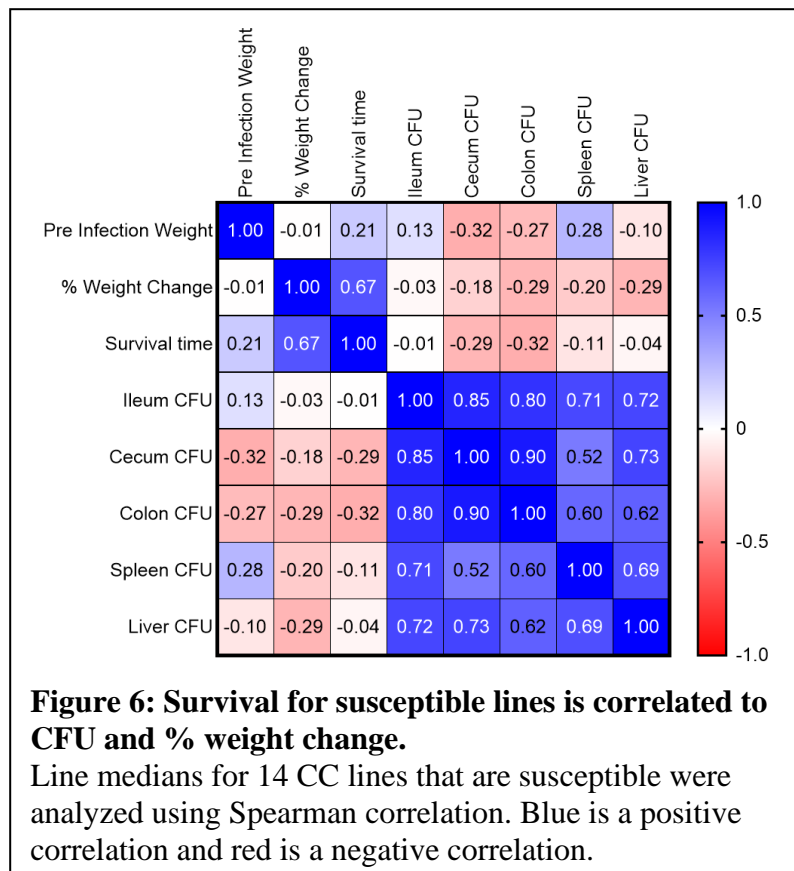
All B6 mice met the euthanasia criteria between day 3 and 6 post-infection with a median at day 4 and were classified as highly susceptible (Fig. 5A). B6 mice lost a median of 20.73% of their body weight during infection (Fig. 5B). CBA mice survived to day 7 and were classified as resistant (Fig. 5A). CBA mice lost a median of 7.92% of their body weight during infection (Fig. 5B). B6 mice were highly colonized in the liver and spleen with medians of 2.56×10^6 and 1.21×10^7 , respectively (Fig. 5C, D), while CBA mice were colonized at least two orders of magnitude lower with medians of 5.45×10^3 and 1.84×10^4 , respectively (Fig. 5C, D).

Of the 32 CC lines evaluated, 14 were categorized as susceptible, as 3 or more mice met the euthanasia criteria prior to day 7 post-infection (Fig. 5A). In general, susceptible lines that suffered earlier mortality also had greater weight loss (Fig. 5B) with a correlation of $R = 0.67$ (Fig. 6). Additionally, lines in the susceptible category had a least 10-fold lower bacterial burden in liver than B6 control mice, with the exception of CC013, CC027, and CC042 (Fig. 5C). CC013 and CC027 had comparable colonization in liver to B6, and CC042 had 100-fold higher with a median colonization of 1.02×10^8 (Fig. 5C), consistent with previous reports (65, 66). In spleen, all lines had at least a 10-fold lower bacterial burden than B6 mice, with the exception of CC042 (Fig. 5D), which were colonized 100-fold higher than B6 mice (Fig. 5D). The high colonization of CC042 has been previously attributed to a de novo mutation in Integrin Alpha (*Itgal*) (66). The susceptible lines were also colonized at least 10-fold higher than CBA control mice, with the exception of CC032 (Fig. 5C, D). CC032 mice were

colonized in both liver and spleen similarly to CBA with a median of 4.11×10^3 and 3.96×10^4 , respectively, yet succumbed to infection before day 7 (Fig. 5C, 2D).

An additional 18 lines were categorized as resistant or tolerant. Resistance was defined

as surviving infection by preventing colonization or by clearing the bacteria. Tolerance was defined as surviving infection while maintaining high bacterial burden. Both resistant and tolerant lines had ≤ 2 mice meeting euthanasia criteria prior to day 7. Of these 18 lines, all 6 mice lived to day 7 in 12 lines (Fig. 5A). Lines that survived longer lost less weight than those that did not with a correlation of $R = 0.71$ across all lines (Fig. 4 and Fig. 5B). However, CC011 lost substantially more weight than expected for a surviving line. All of the resistant and tolerant lines, with two exceptions (CC045 and CC051), were equally colonized across systemic organs, thus making the phenotypes difficult to differentiate.

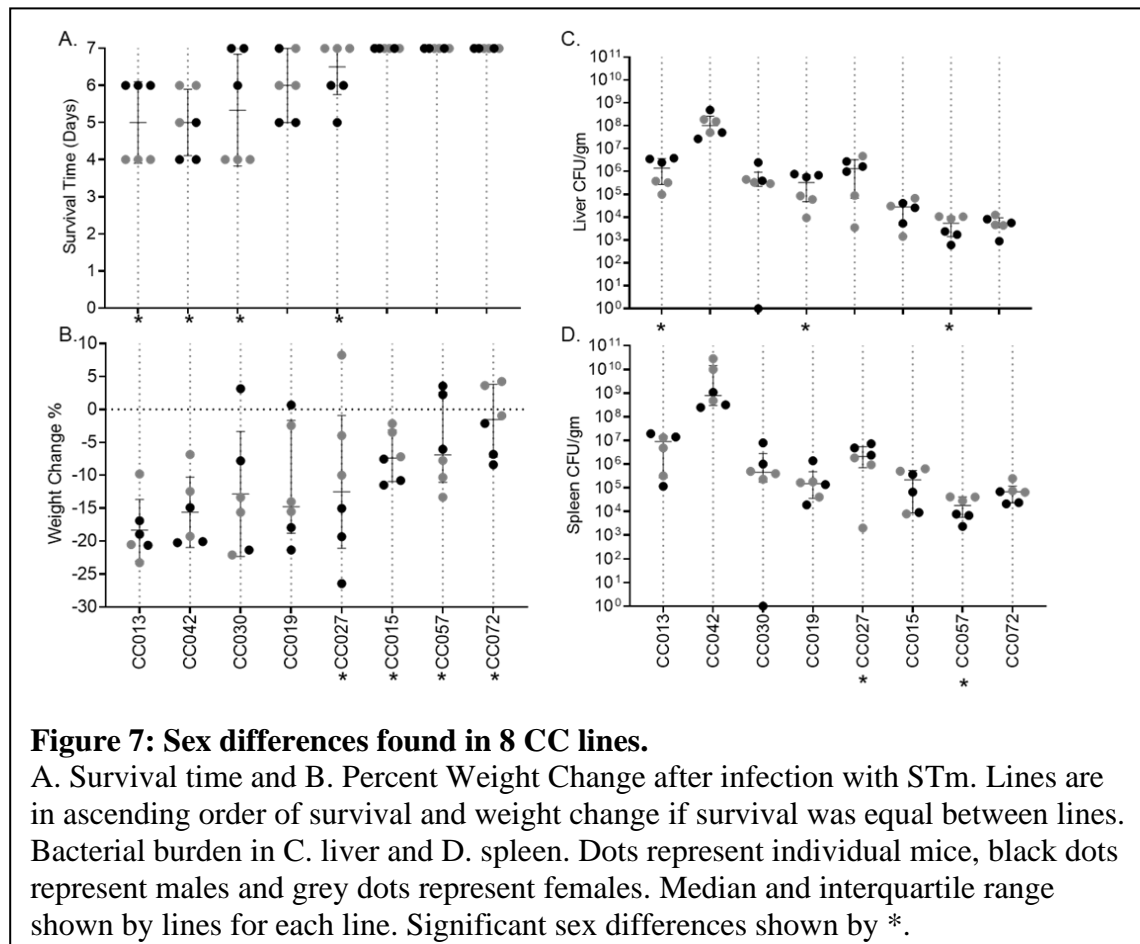


One line – CC051 – had 100-fold lower bacterial burden than CBA in both liver and spleen with medians of 9.30×10^1 and 2.92×10^2 , respectively, and it therefore meets the criteria for resistance (Fig. 5C, D). Another line – CC045 – had a 100-fold higher bacterial burden than CBA mice with 3.31×10^5 and 4.83×10^6 , respectively, making it the strongest candidate for tolerance (Fig. 5C, D). Eight CC lines were colonized in the liver to the same level as CBA mice, while eight additional lines were colonized in the liver 10-fold higher than CBA mice (Fig. 5C). In spleen, one line had a 10-fold lower bacterial burden than CBA mice, ten lines were colonized to the same level as CBA mice, and five lines were colonized 10-fold higher (Fig. 5D).

Sex-dependent variation in susceptibility is line dependent

Sex has been shown to be an influencing factor in many phenotypes, including response to infection, but there are many contradicting reports on which sex is better at surviving infections (45, 84–88). Across the entire CC population tested, sex did not significantly influence survival time ($P = 0.8149$), weight change post-infection ($P = 0.9764$), spleen CFU ($P = 0.7289$), or liver CFU ($P = 0.5571$). However, when individual lines were examined, sex-dependent variation was evident in several lines. CC013 and CC030 males survived longer than females and CC027 and CC042 females survived longer than males (Fig. 7A). CC015, CC027, and CC072 females lost less weight than males and CC057 males lost less than females (Fig 7B). CC027 was the only line where weight loss influenced survival in a sex-dependent manner.

CC013, CC019, and CC027 males were more colonized than females, while CC057 females were more highly colonized than males (Fig 7C, D). CC013 and CC019 had different liver colonization (Fig. 7C), while CC027 had different spleen colonization (Fig. 7D), and CC057 had differences in both organs (Fig. 7C, D). CC027 was the sole line where bacterial burden influenced survival time in a sex-dependent manner. CC027 females survived to day 7, had a lower bacterial burden, and lost less weight than males. As such, CC027 males would be classified as susceptible to STm infection, while females would be classified as tolerant or resistant.



Surviving mice have lower baseline body temperatures and stay on circadian pattern longer for activity levels

Implantable telemetry devices were used to track body temperature and activity levels at one-minute intervals both before and throughout infections. Each line had unique uninfected baseline temperature and activity profiles (Fig. 8). When lines were grouped by survival outcome, differences between groups became apparent (Fig. 9). Resistant/tolerant mice that survived the infection had a baseline pre-infection median minimum temperature of 36.32 °C during their resting period compared to susceptible non-surviving mice with a pre-infection median minimum temperature of 36.67 °C at rest (Fig. 9A, $P = <0.0001$). The pre-infection median overall temperature for surviving versus susceptible mice was 36.61 °C and 36.95 °C, respectively (Fig. 9A, $P = <0.0001$). This significant difference was also found in maximum temperature reached during the active periods with medians of 37.08 °C and 37.35 °C, for surviving versus non-surviving mice respectively (Fig. 9A, $P = 0.0025$). Thus, surviving lines had a small but significantly lower pre-infection baseline body temperature relative to susceptible lines.

Pre-infection activity measurements were analyzed by what fraction of the time the mouse was active, with a higher fraction suggesting more activity. Before infection, all mice had maximal activity during their active period at night. During the most active periods for the mice, lines that did not survive STm infection spent significantly more time active than lines that survived STm infection (0.83 versus 0.74, Fig. 9B, $P = 0.0139$). Considering an entire 24-hour period prior to infection, there was no statistically significant difference in activity between susceptible and surviving lines.

Furthermore, in pre-infection periods where mice were minimally active (day), both susceptible lines and surviving lines were active for equal amounts of time (Fig 9B). Thus, at pre-infection baseline, surviving lines appeared to spend more time at rest during the normal waking period of the mouse (night).

Post-infection telemetry data was analyzed using sinusoidal math models to pinpoint when mice deviated from their circadian pattern of body temperature and activity after infection with STm (“off-pattern”) (89). For temperature measurements, surviving and susceptible lines did not differ significantly for their time to circadian pattern disruption after infection (Fig 9C, $P = 0.3961$). Susceptible and surviving lines also did not differ significantly for time to off pattern for activity either (Fig 9C, $P = >0.9999$). However, susceptible lines did stay on their normal activity pattern significantly longer than they stayed on their normal temperature pattern with medians of 1789 minutes (1.24 days) and 770.75 minutes (0.54 days) (Fig. 9C, $P = 0.0397$). Survived lines did not stay on either activity or temperature pattern significantly longer (Fig 9C, $P = 0.1057$).

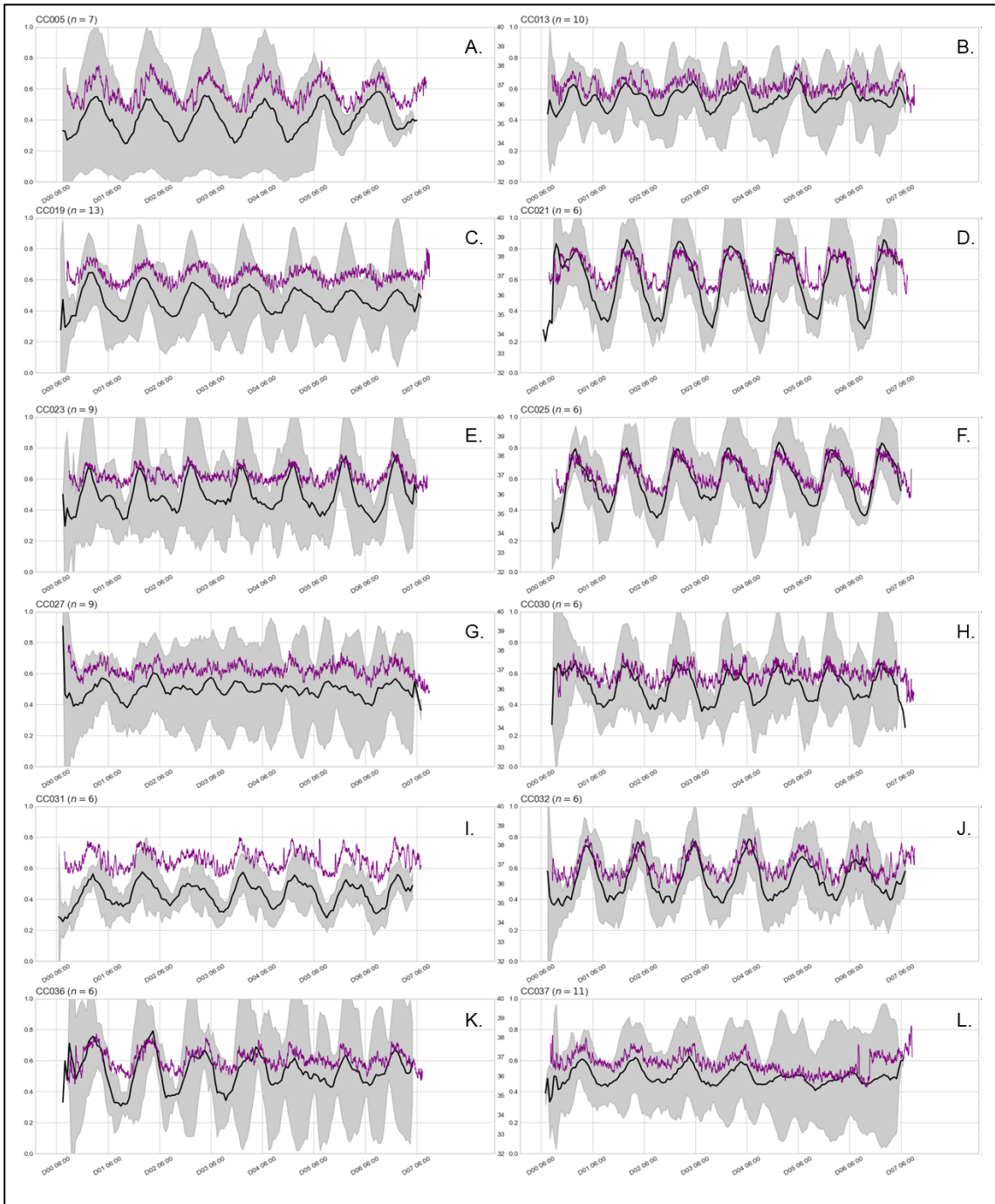


Figure 8: Each line has a unique circadian pattern before infection. Purple lines represent the average temperature and black lines represent the average fraction of time the mouse is active pre-infection for 7 days. The gray area represents +/- 2SD. A-N are susceptible lines, O-AF are survived lines, and AG-AH are control strains.

Figure 8 Continued

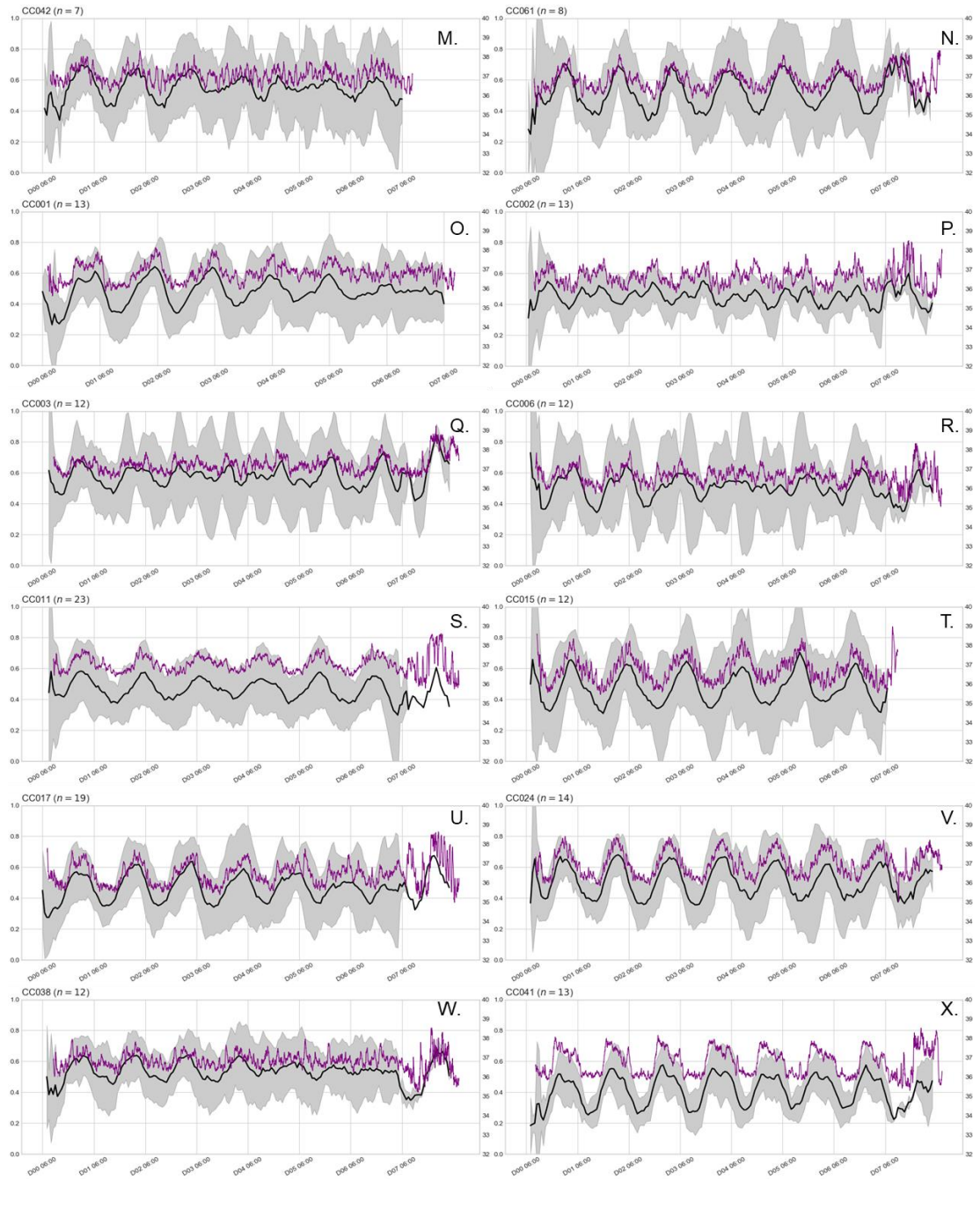
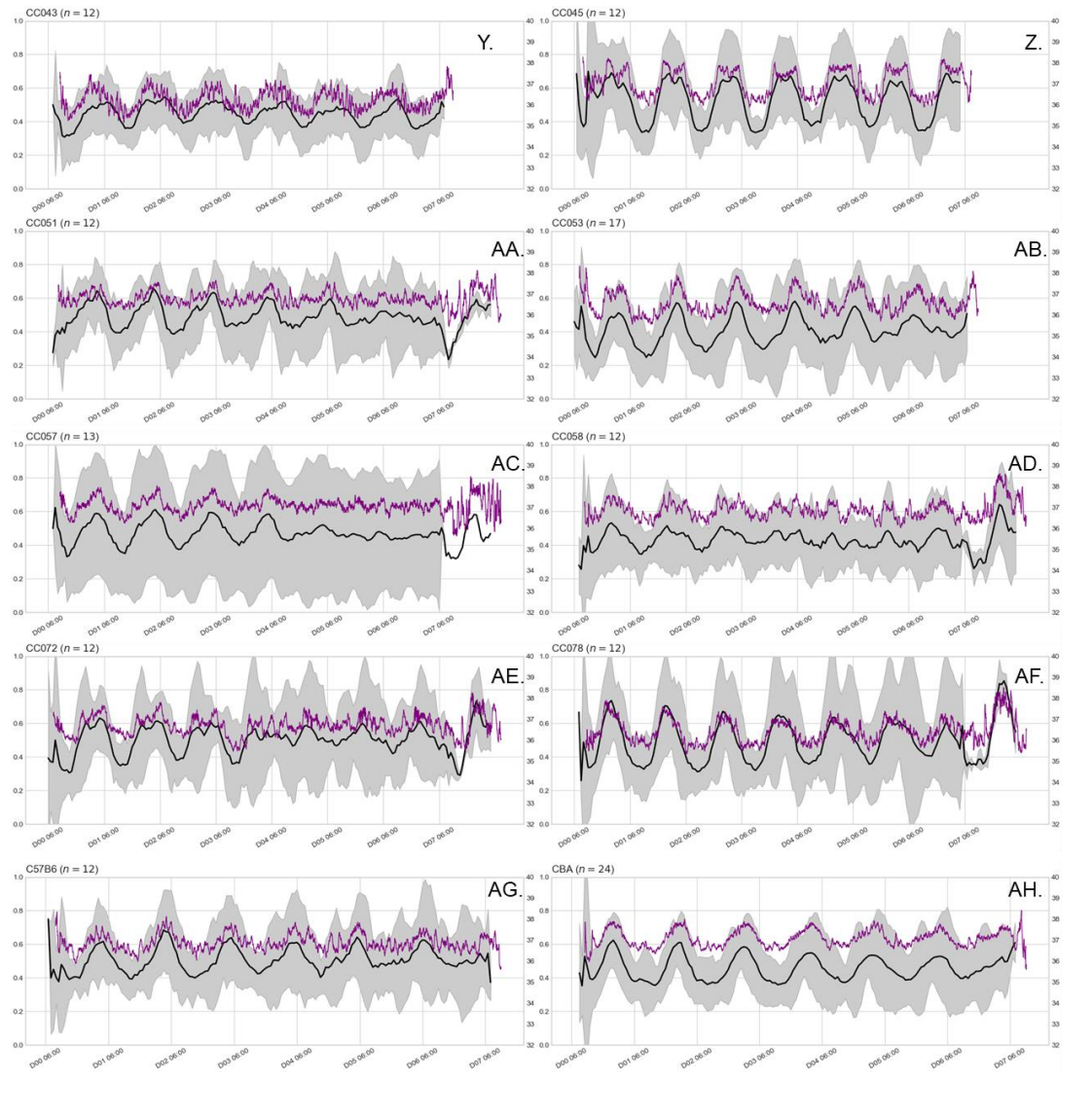


Figure 8 Continued



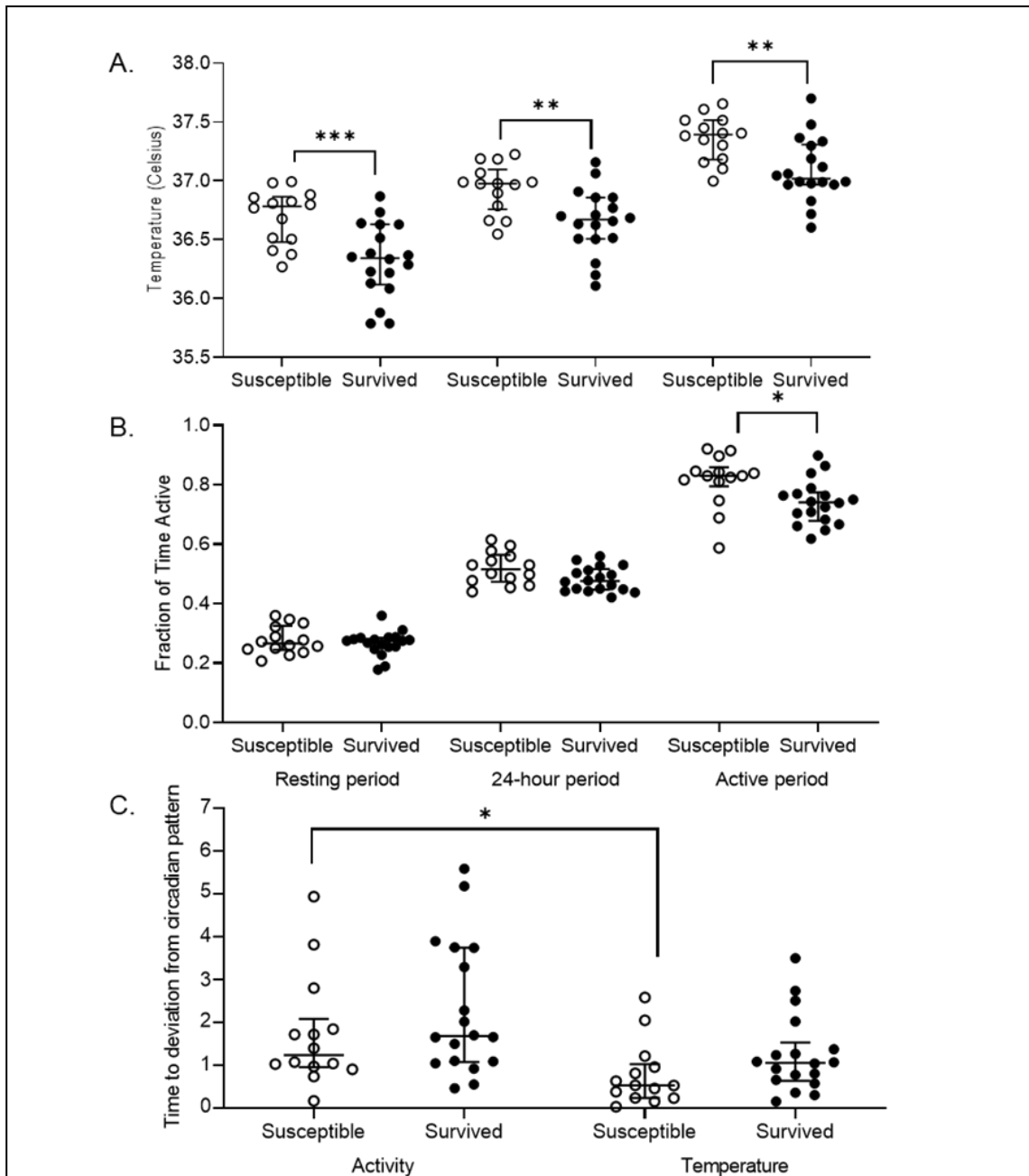


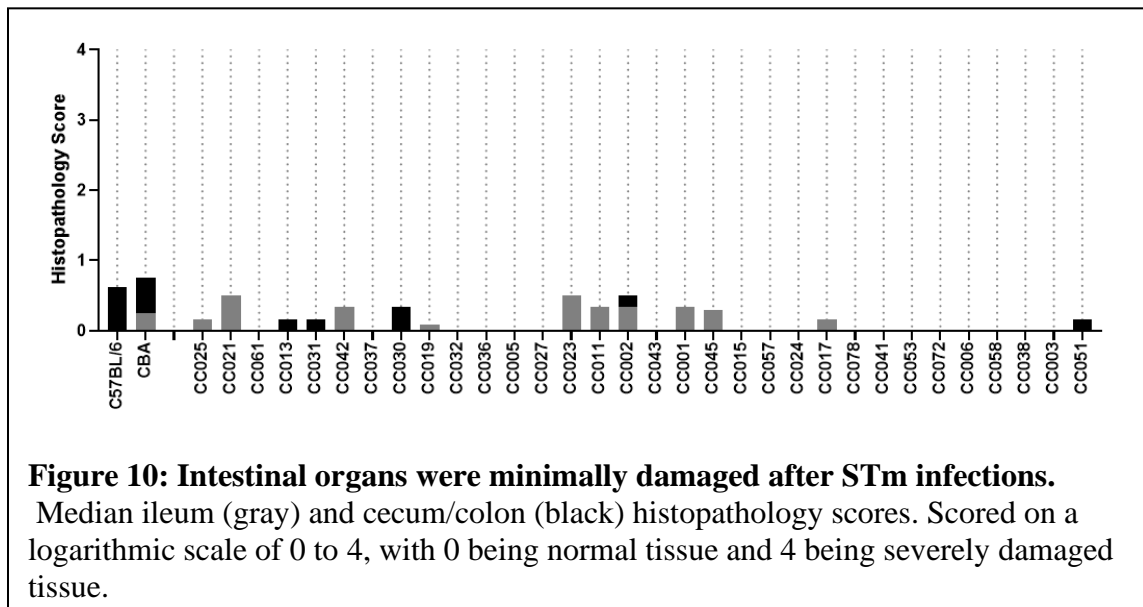
Figure 9: At pre-infection baseline, susceptible lines have higher body temperatures, are more active during normal rest period, and maintain activity patterns longer than temperature patterns than surviving lines.

Resting period, 24-hour period, and active period strain medians shown for A. temperature and B. fraction of time active (0-1). C. Time to deviation from baseline activity and temperature post-infection (days). Lines are grouped by survival status. Median overall values and interquartile range are indicated. (* P < 0.05, ** P < 0.01, *** P < 0.001).

Tissue damage is weakly correlated to survival time and is driven by splenic damage

Tissue sections were stained with H&E, and a board-certified pathologist scored each tissue blindly for damage using a scale of 0 to 4 (0 = normal, 4 = severe damage, Table A1 and Fig. A1). Minimal damage was noted in the intestinal sections examined (ileum, cecum, and colon, scores 0-1) and these were excluded from further analyses (Fig. 10). To assess the relationship between survival and tissue damage, linear regression was performed showing survival and combined spleen and liver pathology scores with $R^2 = 0.1256$, while the spleen pathology score alone was 0.1323 and the liver pathology score alone was 0.08382 (Fig. 11B, C, D, all $P = <0.001$).

Thus, damage to the spleen appears to be driving the small but significant correlation between histopathology scores and survival. Organs from susceptible lines were not necessarily more damaged than those from surviving lines, perhaps because the mice succumbed to infection before more severe damage could occur (Fig. 11A).



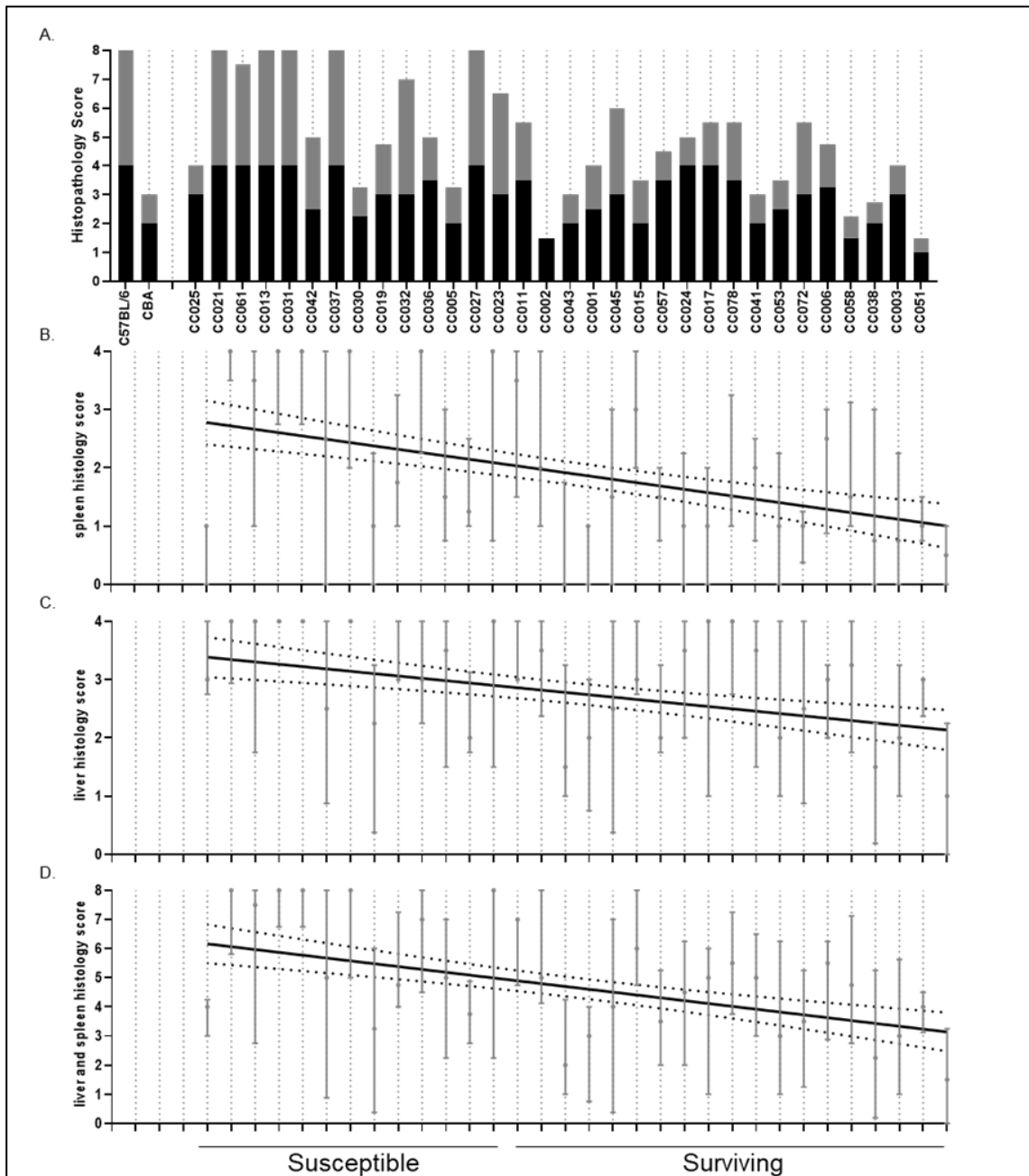


Figure 11: Spleen and liver damage weakly correlate with survival time.

A. Median Liver (black) and spleen (grey) histopathology scores for each line. Scored on a logarithmic scale of 0 to 4, with 0 being normal tissue and 4 being severely damaged tissue B. Spleen ($R^2 = 0.1323$, $P = <0.0001$) and C. liver ($R^2 = 0.08382$, $P = <0.0001$) individual linear regression of histopathology scores. D. Linear regression of CC strains on combined spleen and liver histopathology scores ($R^2 = 0.1256$, $P = <0.0001$). 95% confidence interval of regression lines are shown by dotted lines. Medians and interquartile ranges indicated.

Complete Blood Counts and circulating cytokines/chemokines do not explain differential host response to STm infection

Complete blood counts (CBC) were performed on pre-infection blood and on blood collected at necropsy (Table 1 and 2). The differential counts for white blood cell (WBC), neutrophils (NEU), monocytes (MON), lymphocytes (LYM) were analyzed. No significant differences were observed between surviving and non-surviving lines (Fig. 12, $P = 0.4415, 0.2833, 0.9031, \text{ and } 0.2505$). The levels of 36 serum cytokines and chemokines were also determined from serum collected at necropsy and compared to those of uninfected control animals from each line (Table 3 and 4). Susceptibility or survival was not significantly correlated to the cytokine profile. The profile was influenced more by line than infection status. Highly STm susceptible CC042 mice had high levels of almost every cytokine, suggesting that the mice were suffering a cytokine storm (Table 4).

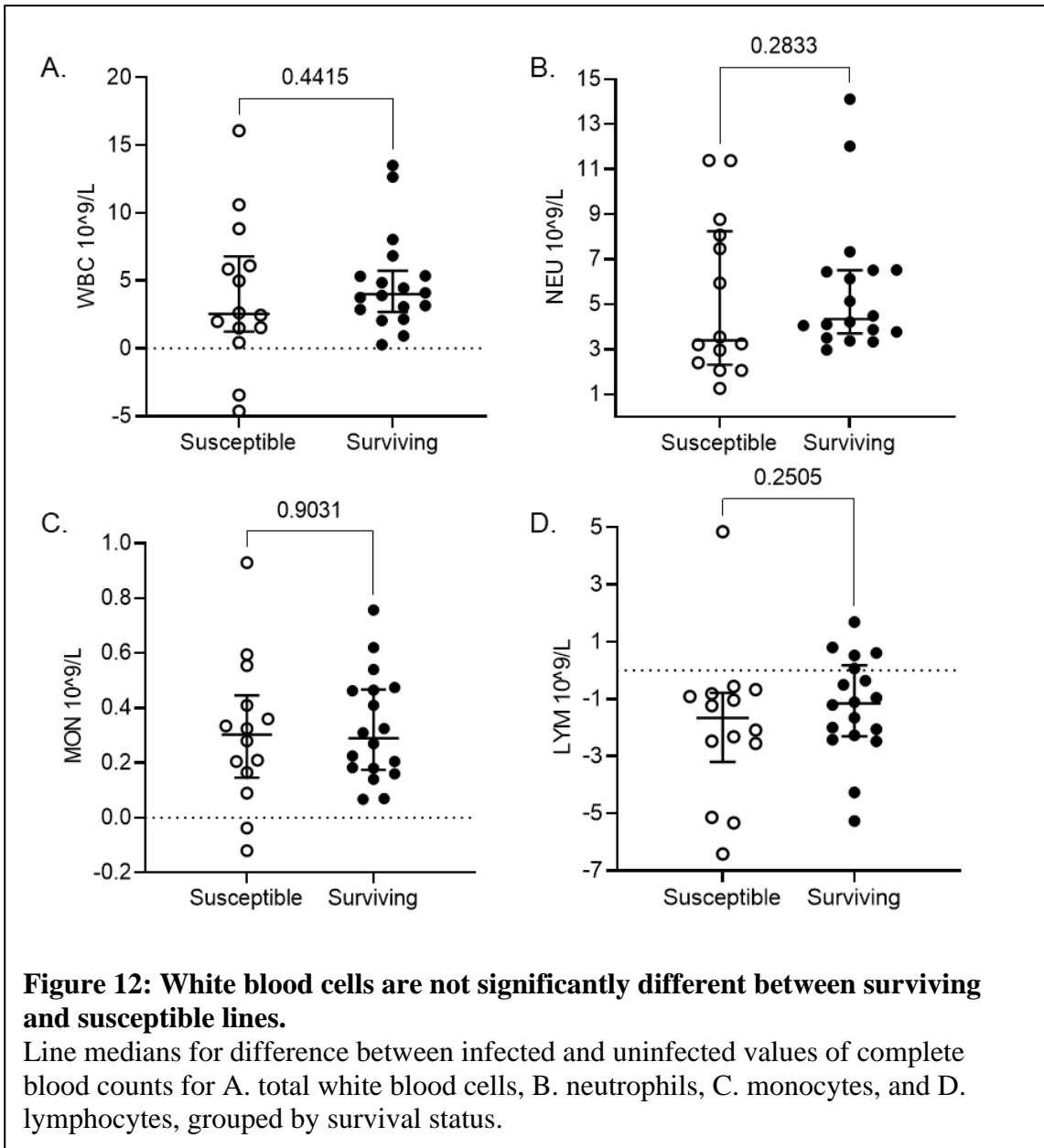


Table 4: Infected cytokine values taken at necropsy time minus uninfected mean values for respective line. Includes 28 CC lines and 2 control liens (B6 and CBA). Mean and standard deviation shown.

Cytokine	BS	CBA	CC001	CC002	CC003	CC005	CC006	CC011	CC013	CC015	CC017	CC019	CC024	CC025
	Mean	SD	Mean	SD	Mean	SD	Mean	SD	Mean	SD	Mean	SD	Mean	SD
IL-1	430.14	115.93	1073.36	5970.38	4772.24	1710.93	169.93	721.17	27.66	53.18	35.65	564.24	309.02	604.86
IL-2	20.48	466.45	61.41	286.38	566.58	53.14	415.45	146.05	676.42	123.26	459.14	241.03	267.65	180.15
IL-3	841.94	1120.07	294.88	681.11	310.64	670.11	615.88	89.11	310.64	150.46	47.86	69.13	208.23	485.11
IL-4	8.72	9.44	1.84	3.11	1.77	1.55	0.38	0.02	0.38	0.02	0.38	0.02	0.38	0.02
IL-5	705.51	705.51	21.74	28.51	18.24	24.67	21.74	18.24	24.67	21.74	18.24	24.67	21.74	18.24
IL-6	769.13	654.93	688.33	659.33	1068.22	659.33	209.33	1057.24	844.11	719.12	592.45	209.33	780.33	659.33
IL-7	73.74	161.12	38.12	91.70	594.42	447.82	4.31	4.41	5.41	2.31	4.41	3.01	4.41	3.01
IL-8	9.34	77.83	2.10	0.00	0.00	0.00	0.00	0.00	0.00	0.00	0.00	0.00	0.00	0.00
IL-9	182.19	2122.83	12.70	41.38	17.91	32.42	0.00	0.00	17.91	32.42	25.64	48.74	36.42	11.31
IL-10	0.14	2.34	1.21	3.28	0.29	0.00	0.10	0.00	1.10	0.00	0.00	0.00	0.00	0.00
IL-11	0.41	0.58	0.18	1.14	0.00	0.00	0.10	0.00	0.00	0.00	0.00	0.00	0.00	0.00
IL-12	109.34	90.58	35.02	46.51	99.51	136.74	0.14	0.35	35.24	21.41	10.61	52.91	17.41	12.41
IL-13	13.74	25.32	32.75	1.82	1.21	0.38	3.33	0.02	5.14	0.69	7.01	0.02	2.38	3.44
IL-14	9898.52	11654.17	4699.64	147.78	135.98	131.02	464.48	188.57	416.53	78.28	1148.48	457.78	209.13	184.03
IL-15	1.12	0.10	0.12	1.91	3.22	0.44	0.00	0.13	1.58	0.38	0.72	0.61	1.56	0.00
IL-16	487.68	502.46	233.88	360.36	14.26	35.02	5.30	79.35	15.34	58.81	58.18	13.02	57.28	72.78
IL-17	29.64	42.22	33.80	75.88	7.81	21.42	30.32	17.17	71.47	130.97	15.04	37.88	2.97	16.15
IL-18	39.02	61.13	15.50	22.54	8.64	16.14	1.85	3.65	27.36	21.48	40.43	9.87	8.47	21.88
IL-19	206.59	726.14	417.36	1064.38	2859.65	4660.74	29.14	47.57	94.75	169.53	28.14	140.24	6.72	89.00
IL-20	0.93	17.28	10.76	10.28	112.02	188.77	3.86	10.02	12.83	12.43	14.48	12.28	2.24	3.11
IL-21	88.57	175.04	33.87	51.98	458.71	564.17	0.21	6.92	26.56	27.09	20.92	7.02	9.82	16.26
IL-22	2.88	4.66	0.72	2.11	0.18	0.46	0.98	0.11	0.98	1.46	0.68	1.46	0.72	0.98
IL-23	20.16	39.46	1.83	8.02	11.96	1.46	7.22	1.51	10.10	1.41	4.96	5.92	1.83	4.96
IL-24	1675.56	2864.45	165.36	900.27	291.57	34.90	10.90	13.70	47.46	11.74	124.46	60.28	136.70	117.46
IL-25	31.64	60.72	144.03	169.87	65.83	31.11	17.24	7.02	57.02	121.83	31.03	141.83	8.42	141.83
IL-26	324.93	591.92	170.42	174.68	174.68	174.68	174.68	174.68	174.68	174.68	174.68	174.68	174.68	174.68
IL-27	69.14	69.14	19.42	75.93	26.33	43.14	75.93	0.00	19.42	75.93	26.33	43.14	75.93	0.00
IL-28	250.83	474.15	258.11	278.11	182.88	143.58	258.11	182.88	143.58	258.11	182.88	143.58	258.11	182.88
IL-29	335.38	457.10	153.11	145.11	23.94	96.61	19.75	61.10	88.10	58.84	105.66	88.10	58.84	105.66
IL-30	0.00	0.00	0.38	0.98	0.42	1.38	0.00	0.00	0.10	0.00	0.42	0.00	0.00	0.00
IL-31	41.20	101.15	1.96	1.94	0.20	0.32	0.05	0.00	0.11	0.22	0.11	0.32	0.54	1.17
IL-32	107.74	177.02	1.74	0.72	2.02	0.87	1.78	3.05	4.68	11.84	0.34	1.42	0.34	1.42
IL-33	72.01	171.82	1.47	7.51	2.89	5.68	10.72	6.12	3.82	4.18	5.78	4.08	11.46	6.42
IL-34	615.54	775.02	21.71	63.67	25.18	34.18	2.17	4.02	14.92	17.27	32.78	30.32	43.11	8.38
IL-35	312.08	388.44	19.81	29.42	7.02	17.37	3.88	0.02	0.02	15.71	23.14	23.98	33.87	53.13

Cytokine	CC027	CC028	CC029	CC030	CC031	CC032	CC033	CC034	CC035	CC036	CC037	CC038	CC039	CC040
	Mean	SD	Mean	SD	Mean	SD	Mean	SD	Mean	SD	Mean	SD	Mean	SD
IL-1	120.10	40.11	272.22	110.76	942.51	3331.93	1519.10	3838.86	40.11	28.51	146.96	65.72	680.53	1015.56
IL-2	330.17	175.48	822.88	374.65	4735.38	4529.68	1861.97	417.58	382.47	219.11	282.44	138.70	1484.78	1330.11
IL-3	193.43	175.88	38.73	30.38	219.13	297.98	1280.33	88.33	34.92	34.92	183.88	68.33	34.92	183.88
IL-4	9.87	6.42	2.64	4.04	3.04	1.96	1.20	0.41	3.04	1.96	1.20	0.41	3.04	1.96
IL-5	100.94	148.70	11.38	34.96	14.07	57.62	39.33	40.00	15.24	53.24	32.11	1144.48	670.18	13.33
IL-6	951.13	1395.05	431.98	546.31	1040.11	907.86	477.97	698.78	183.18	193.17	366.94	771.62	2497.44	1382.14
IL-7	1.52	3.52	4.64	2.11	84.21	131.04	60.38	98.62	0.00	1.02	3.64	1.12	124.83	74.02
IL-8	6.06	74.07	12.62	19.33	40.33	10.41	37.72	38.33	0.72	0.72	3.62	0.00	1.02	3.62
IL-9	0.00	0.12	5.33	1.93	0.11	0.11	0.00	0.00	0.00	0.00	0.00	0.00	0.00	0.00
IL-10	0.00	0.00	0.00	0.00	23.53	0.00	1.96	0.00	0.00	0.00	0.00	0.00	0.00	0.00
IL-11	28.44	21.74	24.66	100.79	118.33	143.33	77.72	4.26	3.77	4.26	3.77	4.26	3.77	4.26
IL-12	0.88	1.42	26.68	0.43	48.87	14.60	14.60	7.45	0.00	0.00	0.00	0.00	0.00	0.00
IL-13	717.29	693.78	1174.93	723.38	3055.58	471.18	1169.12	542.58	179.18	374.42	835.34	3144.98	2959.52	391.52
IL-14	0.00	0.00	0.41	1.74	0.18	0.28	0.32	1.52	0.00	0.42	0.00	0.00	0.00	0.00
IL-15	312.08	440.15	79.24	43.66	231.20	57.88	203.02	179.02	84.05	64.04	313.15	387.24	4284.63	55.62
IL-16	17.78	17.02	17.88	34.11	29.97	12.00	39.38	67.08	30.02	27.92	21.94	23.98	723.02	15.31
IL-17	22.40	24.78	19.50	16.02	18.84	9.12	22.00	18.38	79.48	31.62	40.22	82.38	14.10	19.46
IL-18	38.21	41.88	32.54	145.14	9.08	447.53	91.10	155.85	37.02	58.11	20.30	348.18	349.42	118.51
IL-19	11.64	6.72	16.14	19.33	75.87	166.88	15.18	23.72	7.89	1.76	1.02	207.64	224.64	59.88
IL-20	2.33	2.04	0.78	1.24	0.92	2.37	1.77	0.68	0.42	0.40	0.50	0.47	40.00	50.00
IL-21	2.60	7.02	6.11	9.23	8.38	1.95	4.26	4.26	3.10	53.34	104.98	76.04	0.38	1.04
IL-22	353.31	262.00	488.68	853.84	74.24	133.66	101.00	92.82	35.92	37.00	184.18	3724.00	30296.58	72.71
IL-23	96.14	78.00	100.00	197.46	204.82	77.58	142.11	47.17	53.62	102.86	284.26	462.61	284.26	462.61
IL-24	284.88	307.72	7.85	166.88	331.13	472.16	636.77	118.72	91.46	150.44	165.66	995.65	71.52	112.11
IL-25	0.78	3.45	8.71	20.55	42.72	49.04	55.92	3.00	17.52	3.00	17.52	3.00	17.52	3.00
IL-26	912.26	1129.00	384.94	171.11	323.97	264.84	269.84	174.11	181.00	172.62	172.62	172.62	172.62	172.62
IL-27	422.26	393.88	970.88	110.88	62.84	246.11	80.00	263.88	145.88	63.71	137.00	2477.24	853.24	669.24
IL-28	0.00	0.00	0.00	0.00	0.00	0.00	0.00	0.00	0.00	0.00	0.00	0.00	0.00	0.00
IL-29	1.86	1.42	0.54	0.33	0.21	0.11	0.11	0.11	0.11	0.11	0.11	0.11	0.11	0.11
IL-30	24.72	32.82	1.21	7.21	5.04	6.61	0.14	7.20	7.08	7.11	5.91	18.96	880.88	687.02
IL-31	18.87	11.17	8.33	3.00	27.04	8.63	5.17	4.83	5.02	8.36	4484.84	2198.12	8.63	5.17
IL-32	237.74	205.48	1.65	20.18	97.60	83.88	104.54	7.15	37.21	14.24	67.00	796.42	416.92	1.65
IL-33	88.64	57.04	13.44	54.28	0.21	55.91	38.18	75.52	0.00	51.71	91.02	2077.72	2280.72	14.11

Known polymorphisms do not always predict infection outcome

A point mutation in *Slc11a1* (previously named *Nramp1*, or *Ity*) is associated with susceptibility to lethal systemic STm infection (3, 23, 25). B6 is the only CC founder strain to carry this mutation, and B6 is susceptible to systemic STm infection. Only 5 CC lines in the panel analyzed – CC021, CC031, CC042, CC045, and CC061 – carry the *Slc11a1* mutation (Fig. 5). All of these lines were highly colonized in liver and spleen, and, with the exception of one line, succumbed to infection before day 7. CC045 had a high bacterial burden but survived to day 7 post-infection. This result suggests that CC045 has compensatory mechanisms to overcome STm susceptibility caused by the *Slc11a1* mutation.

Another mutation previously linked to STm susceptibility is in *Ncf2*, although it is not as detrimental to murine survival after *Salmonella* infection as the *Slc11a1* mutation (27, 30). Three of the CC founders (PWK, CAST, NZO) carry the *Ncf2* mutation, and 12 of the CC lines in the current panel – CC013, CC015, CC023, CC025, CC030, CC032, CC036, CC038, CC045, CC058, CC072, CC078 – also carry the *Ncf2* mutation (Fig. 5). Six out of these 12 lines did not survive to day 7 post-infection (CC013, CC023, CC025, CC030, CC032, CC036).

Tlr4 also has a known point mutation linked to STm susceptibility, but none of the CC founder strains carry the mutation, making it impossible to verify the effect of this mutation on STm infection using CC mice (31, 32).

Ncf2 and *Slc11a1* combined explained 10 of the 14 susceptible lines, but 4 of the lines – CC005, CC019, CC027, CC037 – are not explained by mutations in either of

these genes, suggesting that other genetic factors contribute to their susceptibility to STm infection. CC045, the only line to carry both mutations, is particularly unusual since 4 out of 6 mice survived STm infections to day 7.

Genetic basis for variable response to infection with *Salmonella* Typhimurium.

We used gQTL analysis (90) to identify genetic regions associated with survival after oral STm infection. Since CC042 has a de novo mutation that explains its extreme susceptibility to STm infections, it was excluded from genetic analysis. CC045 was also excluded, as it carries mutations in *Slc11a1* and *Ncf2*, yet survives infection. Using median survival time and percent of mice surviving to day 7 post-infection, significant associations were detected on Chromosomes (Chr) 4, 6, and 7 and suggestive associations on Chr 1 and 2 (Fig. 13A and C, Table 5). We called the significant association on Chr 4 *Stq1* (Survival Time QTL) and the significant association on Chr 7 *Stq2*. The heritability of survival time was 45.55. Although the slope of survival percentages over time did not return significant temporal QTL, suggestive associations overlapped with those from the other survival parameters (Fig. 14). Other parameters such as weight change, CFUs, and CBCs were also analyzed using gQTL with no significant or suggestive associations detected, further supporting their independence from STm infection survival.

Chr 1 has two suggestive associations that overlapped with the previously implicated genes *Slc11a1* and *Ncf2*, suggesting that these genes underlie these associations. The significant association on Chr 6 has four annotated genes, three are

hypothetical genes and one, *Cntn3*, is involved in nervous system development (Fig. 15A). However, no SNP differences were found in *Cntn3* that were consistent with founder haplotype effects. Although genes on Chr 2 and 4 have previously been shown to be involved in STm infections, the QTL regions we identified do not overlap with the previously detected loci. The association on Chr 7 overlaps with a previously detected QTL region called *Ses2*, but the causative gene in this region remains unknown (91, 92).

Using founder effect plots (Fig. 13, 15, and 16), haplotype effects were determined for each QTL association. Haplotypes with low effects lead to poor survival and high effect haplotypes correspond to longer survival. For median survival time, the association on Chr 2 had low effect haplotypes (poor survival) for PWK and CAST (Fig. 13B, Table 5). *Stq1* (Chr 4) had low haplotype effects for WSB and NZO (Fig 13B, Table 5). B6, NOD, and WSB had low effect haplotypes for *Stq2* (Chr 7) (Fig. 15B, Table 5). For percent of mice that survived to day 7, Chr 2 had low haplotype effects for PWK and CAST (Fig. 16A, Table 5), *Stq1* (Chr 4) had low haplotype effects for B6, WSB, and NOD (Fig. 16B, Table 5), and *Stq2* (Chr 7) had low haplotypes effects for B6, NOD, and WSB (Fig 13D, Table 5). No high haplotype effects were found in these associations.

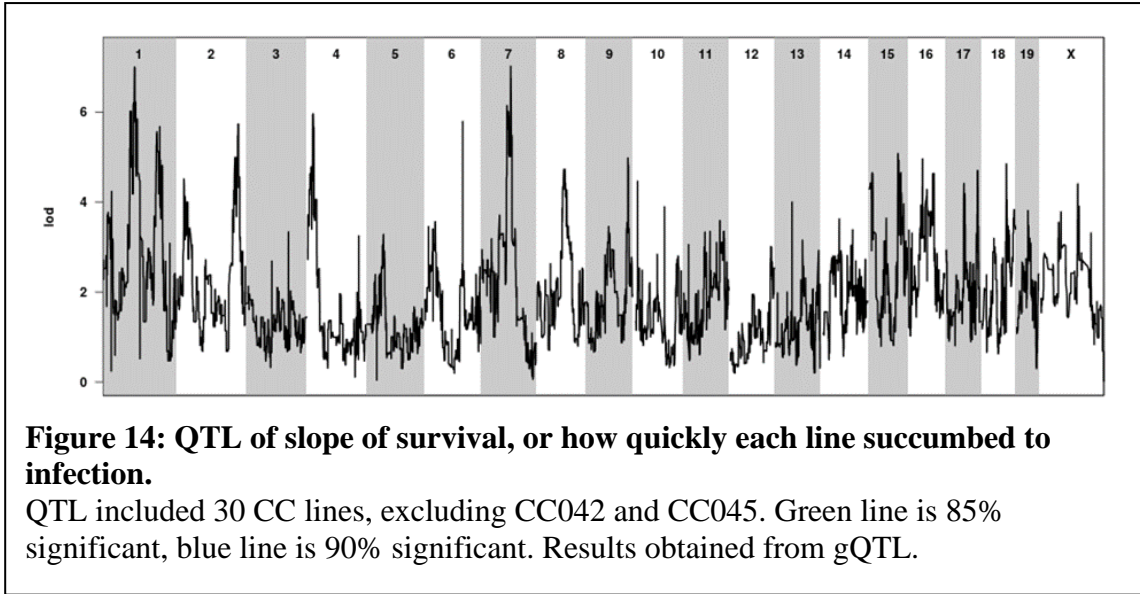
To narrow down the number of candidate genes for each association, SNP differences in coding regions in the CC founder strains were identified using the Mouse Phenome Database (The Jackson Laboratory). Ensembl Variant Effect Predictor (VEP) was used to identify if the SNP difference had an effect at the protein level. Haplotype effects for each locus were used to filter candidate genes that had differences in their

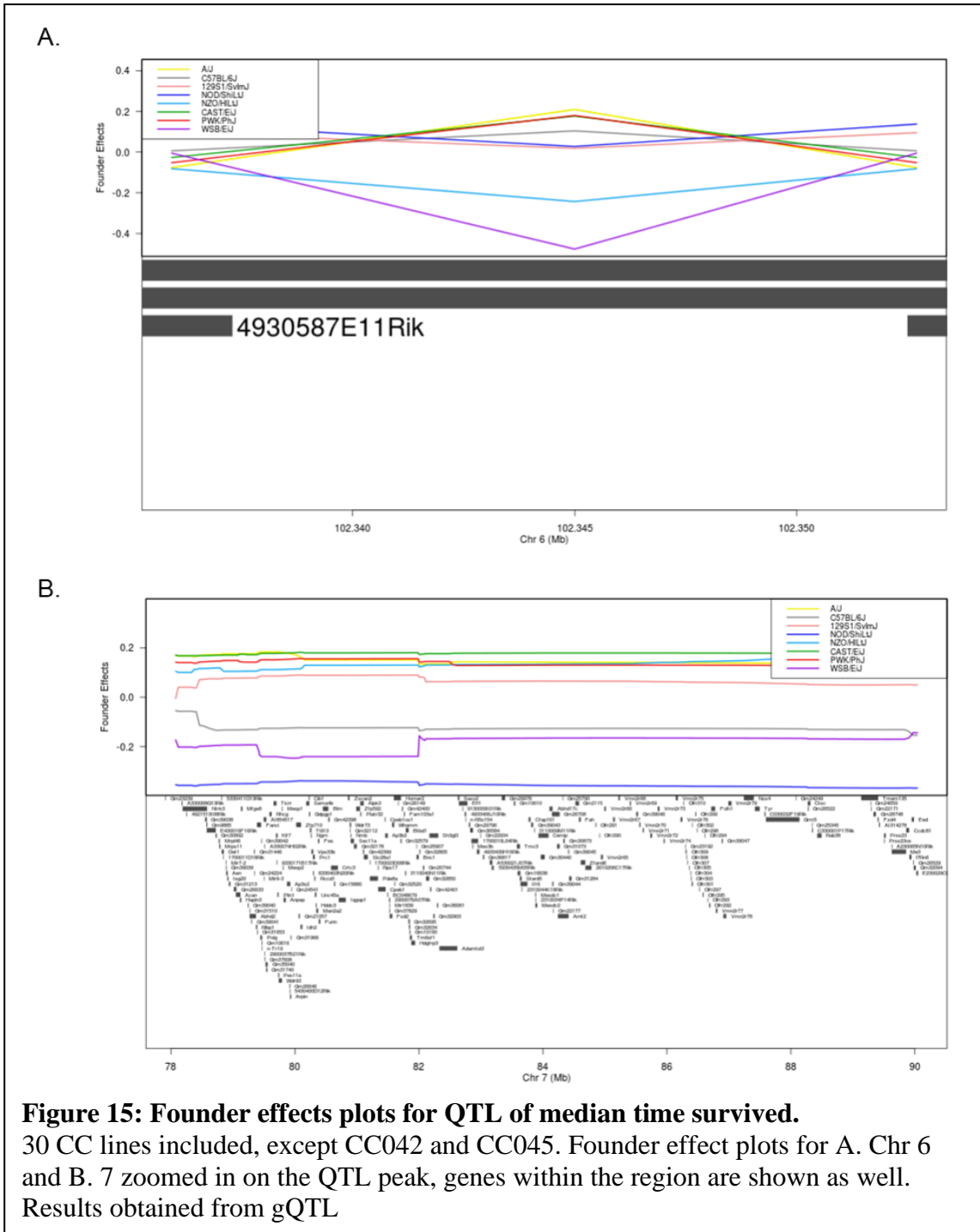
sequences. For median survival time, Chr 2 had 259 genes with 13 SNP differences in genes that matched haplotype differences (Table 6). *Stq1*, with 23 genes, and Chr 7, with 232 genes, had no candidate genes with SNP differences. For percent survived to day 7, the Chr 2 region had 503 genes, of these genes 51 had SNP differences matching haplotype effects (Table 7). The Chr 4 region had 28 genes and *Stq2* had 115 genes, but neither region had SNP differences corresponding to haplotype differences.

Table 5: QTL associations for median survival time and percent survived to day 7 after STm infections.

30 CC lines were included in the run, excluding CC042 and CC045. Ran using gQTL.

QTL name	Phenotype	SNP ID	Chr	LOD	P-value	Proximal (Mb)	Max (Mb)	Distal (Mb)	Haplotype Effects
	survival time	CEBJAX00271542	1	8.242557876	3.09E-06	73.965322	152.072538	152.077538	
	survival time	UNC4305092	2	7.643011274	1.03E-05	151.393943	157.792225	158.057682	low: PWK, CAST
Stq1	survival time	UNC6840265	4	9.42603847	2.78E-07	16.302261	19.511363	19.630331	low: WSB, NZO
	survival time	UNC13209247	7	7.242908516	2.27E-05	78.07569	79.711974	90.041534	low: WSB, NOD, B6
	% survived to day 7	CEBJAX00271542	1	6.918303094	4.31E-05	73.977655	152.072538	154.462237	
	% survived to day 7	UNC4305092	2	6.664908806	7.08E-05	151.018857	157.792225	166.407037	low: PWK, CAST
	% survived to day 7	UNC6817353	4	6.915843372	4.33E-05	16.129434	17.671082	19.725082	low: WSB, NOD, B6
Stq2	% survived to day 7	UNC13206400	7	9.112015614	5.29E-07	78.407671	79.427009	82.005976	low: WSB, NOD, B6





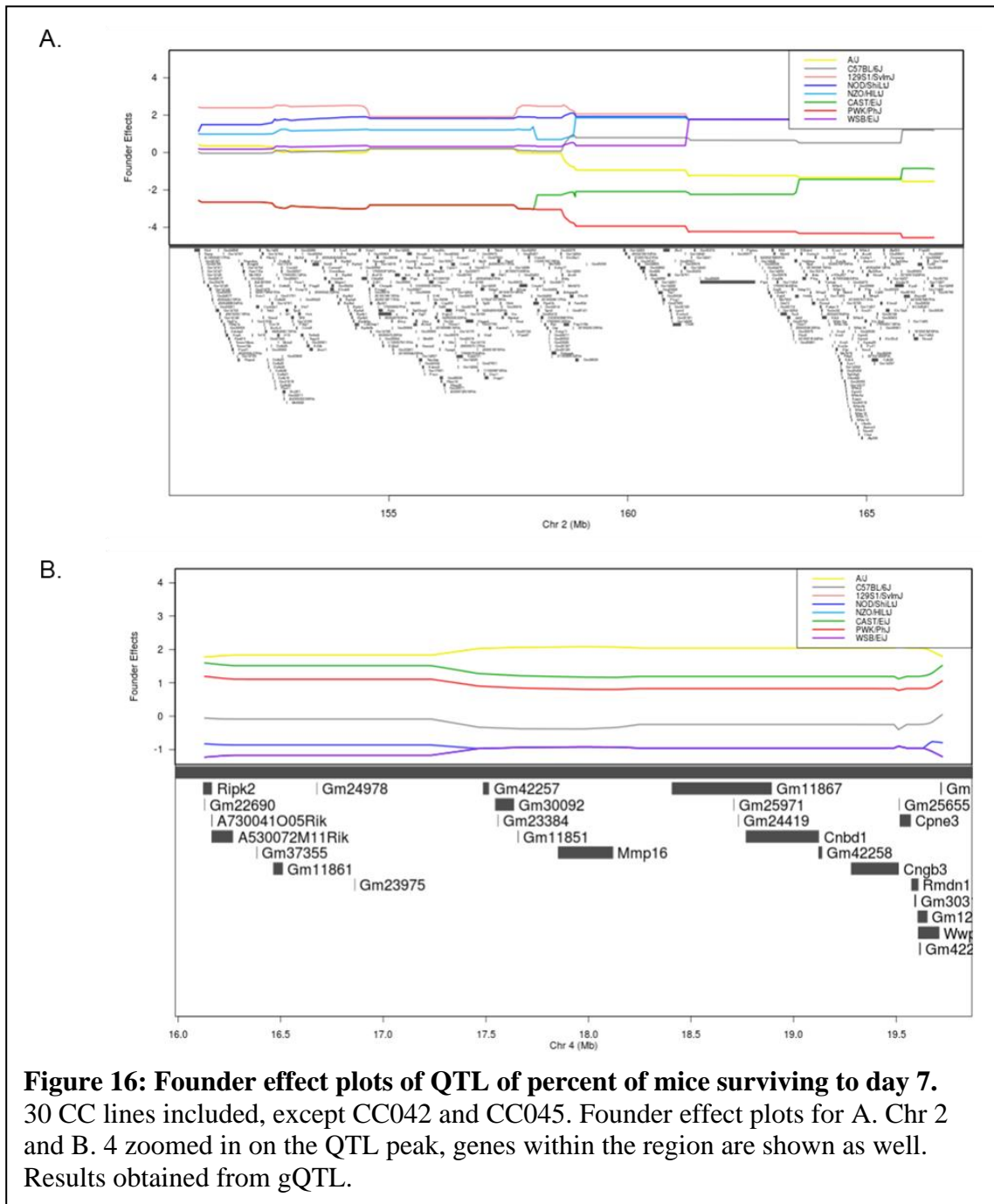


Table 6: Median Survival Time QTL Candidate Genes.

Candidate genes from median survival QTL associations that had SNP differences corresponding to haplotype differences. The predicted impact of the SNP difference on the resulting protein is shown as well.

Gene	Impact on protein
<i>6430550D23Rik</i>	moderate
<i>Bpifb2</i>	moderate
<i>Fer1l4</i>	modifier
<i>Myh7b</i>	modifier
<i>Nrsn2</i>	modifier
<i>Rbl1</i>	modifier, moderate
<i>Rpn2</i>	modifier
<i>Samhd1</i>	moderate
<i>Soga1</i>	moderate
<i>Sun5</i>	modifier
<i>Tlhc2</i>	low, modifier
<i>Tmem74bos</i>	moderate
<i>Tti1</i>	moderate

Table 7: % Survived to Day 7 QTL Candidate Genes.

Candidate genes from percent survived to day 7 QTL associations that had SNP differences corresponding to haplotype differences. The predicted impact of the SNP difference on the resulting protein is shown as well.

Gene	Impact on protein
<i>6430550D23Rik</i>	moderate
<i>Arhgap40</i>	moderate
<i>Bpi</i>	modifier, moderate
<i>Bpifb2</i>	moderate
<i>Cd40</i>	moderate
<i>Dbndd2</i>	modifier
<i>Dhx35</i>	modifier
<i>Emilin3</i>	moderate
<i>Fer114</i>	modifier
<i>Jph2</i>	moderate
<i>L3mbtl1</i>	modifier
<i>Lbp</i>	moderate
<i>Lpin3</i>	moderate
<i>Mafb</i>	moderate
<i>Mmp9</i>	moderate
<i>Mybl2</i>	moderate
<i>Myh7b</i>	low, modifier
<i>Nrsn2</i>	modifier
<i>Ocstamp</i>	moderate
<i>Oser1</i>	moderate
<i>Pltp</i>	moderate
<i>Ptprt</i>	moderate
<i>R3hdml</i>	moderate
<i>Rbl1</i>	modifier, moderate
<i>Rpn2</i>	modifier
<i>Samhd1</i>	moderate
<i>Slc13a3</i>	moderate
<i>Snhg11</i>	moderate
<i>Soga1</i>	moderate
<i>Spata25</i>	moderate
<i>Sulf2</i>	modifier
<i>Sun5</i>	modifier
<i>Svs2</i>	moderate
<i>Sys1</i>	modifier
<i>Tldc2</i>	low, modifier
<i>Tmem74bos</i>	moderate
<i>Tomm34</i>	moderate
<i>Tox2</i>	modifier, moderate
<i>Trp53rka</i>	moderate
<i>Trp53tg5</i>	modifier
<i>Tti1</i>	moderate
<i>Wfdc15b</i>	moderate
<i>Wfdc5</i>	moderate
<i>Wfdc6b</i>	moderate
<i>Wfdc8</i>	moderate
<i>Zfp334</i>	moderate
<i>Zfp335</i>	moderate
<i>Zfp663</i>	moderate
<i>Zhx3</i>	moderate
<i>Zmynd8</i>	moderate
<i>Zswim1</i>	moderate

Discussion

Salmonella is a serious human health concern, with rising multi-drug resistance, that has primarily been studied in inbred mice. We used 32 genetically diverse CC lines to capture a greater range of phenotypes than is possible with traditional inbred laboratory mice. Our goal is to identify mechanisms behind these new phenotypes.

We identified 14 lines that did not survive to day seven post STm infection, and thus were called “susceptible.” The remaining 18 lines survived the full study period. The range of median CC line survivals was four to seven days, similar to that observed in B6 and CBA mice. This similar range may be due to technical parameters of our experiment: seven days may not be a long enough window to capture variable survival at the higher end, and four days may be the quickest a mouse can succumb to STm using the current infection paradigm. Weight change ranged in the CC mice from 23.08% loss to a gain of 2.75%, while the control mice ranged from a loss of 20.73% to a loss of 7.92%. The control strains, B6 and CBA, ranged in STm colonization in spleen and liver from 1.84×10^4 to 1.21×10^7 and 5.45×10^3 to 2.56×10^6 , respectively. The 32 CC lines differed in their range in colonization in spleen and liver from 2.92×10^2 to 7.8×10^8 and 9.3×10^1 to 1.02×10^8 , respectively. This much wider range of colonization phenotypes reflects the genetic diversity of the CC.

There were a few CC lines that had unique infection profiles different from those of traditional inbred mouse lines. CC051 mice were poorly colonized relative to CBA mice (resistant control) and gained weight, while CBA mice lost weight. This data suggests that CC051 mice are more resistant to STm infection than previously studied

strains. CC042 mice were significantly more highly colonized than the susceptible control B6 mice, supporting previous studies (65, 66). CC045 mice had bacterial loads of STm more like susceptible mice yet survived to day 7 and only lost a median of 7.44% of weight, similar to CBA mice. Unlike CBA, CC045 mice also have mutations in both *Slc11a1* and *Ncf2*, both typically leading to worse survival outcomes to STm infections due to an inability to control intracellular bacterial growth (23–25, 27, 30). CC045 is a candidate “tolerant” line, as it survives STm infection in the face of heavier colonization. CC045 mice must have compensatory mechanisms for survival in the face of the *Slc11a1* and *Ncf2* mutations that would normally make it susceptible to STm infection.

In past experiments, sex has influenced many different phenotypes from core body temperature and circadian patterns to infection outcome (45, 84–87). Female mice are more resistant to LPS challenge than males (45), but were more susceptible to viral infections (86). Work in this area is contradictory, and does not have a clear consensus on which sex is most at risk for adverse response to infection (88). We identified several CC lines that exhibited sex differences, with CC027 having the starkest sex differences. CC027 females survived to day 7 post-infection and males survived to day 6. CC027 females lost 3.97% of their weight compared to males that lost 19.31%. Consistent with this data, CC027 males were considerably more heavily colonized in spleen and liver than females: (males: 4.80×10^6 and 1.63×10^6 , females: 9.33×10^5 and 8.87×10^4 , respectively). CC027 offers a unique opportunity to explore how sex can influence

outcome to disease, as it was the only line to exhibit completely opposite phenotypes between males and females.

Telemetry provides unique insight into each mouse's minute-by-minute temperature and activity. This minute-by-minute reading allowed us to establish each mouse's unique circadian rhythm and to pinpoint the exact minute that each mouse started to develop disease, even before symptoms were otherwise detectable. Interestingly, mice that survived infection had a lower uninfected baseline temperature during rest periods, during active periods, and overall. Because fever is generally thought to be disease fighting (78, 93–95), we expected mice with higher baseline temperatures to be better equipped to mount a quicker fever response. When evaluating pre-infection baseline activity, surviving mice spent more time at rest during periods of the day when mice were the most active than susceptible mice. The increased time at rest in surviving lines is unlikely to be the cause of lower body temperature in these lines because surviving lines maintained a lower body temperature even during periods when susceptible and surviving mice spent equal time at rest (during their most restful period). Furthermore, there was no significant difference in how rapidly surviving and susceptible infected mice left their normal circadian pattern of activity after infection. However, susceptible mice deviated from their temperature pattern significantly earlier than their activity pattern, suggesting that temperature is a more sensitive measurement to detect early disease.

Tissue damage had a small but significant correlation with survival time. Spleen and liver exhibited severe damage across most lines. Splenic damage drove the small

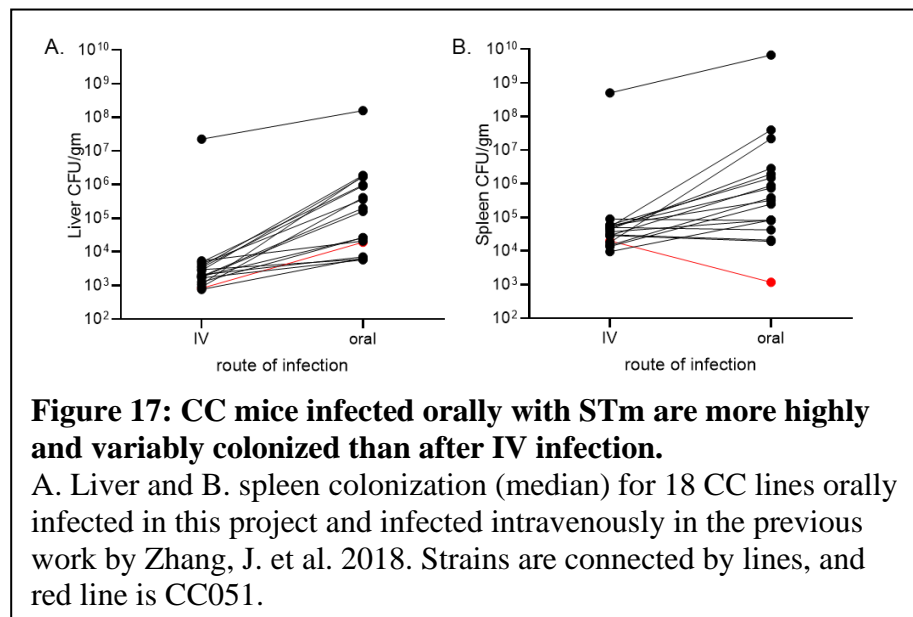
correlation suggesting that liver damage, while more severe, is better tolerated than splenic damage. Interestingly, there were some lines that exhibited quite severe damage in both organs yet survived (CC011, CC017, CC045, CC072, and CC078) and some lines that did not have as severe of damage and did not survive (CC005, CC025, and CC030). While mice are typically categorized into resistant and susceptible, this variable damage data supports a heterogeneity in responses to infection and suggests that there is more than one way to respond to infection. Discovery of these phenotypes highlights the usefulness of the CC as a way to assay responses that may be influenced by genetic diversity.

Complete blood counts and cytokine levels were also assessed in these animals but were not significantly different in surviving versus non-surviving lines. Differences appeared to originate from underlying line differences rather than from differential response to STm infection, highlighting the diversity of even baseline immune parameters in the CC.

While we are focused on the response to an oral STm infection, other studies have examined STm colonization after intravenous injection. Intravenous injection bypasses the intestine and host defenses present in this niche entirely. In a previous study using STm infection in the CC model, mice were infected intravenously, bypassing the intestinal barrier (65). Although the two studies used similar total numbers of CC lines, only 18 lines were shared between the two studies. When median colonization in liver and spleen was compared for these lines, the oral infection route (current infection) produced higher bacterial burdens in both organs and a wider range of colonization in

general (liver: 10^4 to 10^6 vs 10^3 to 10^4 and spleen: 10^3 to 10^7 vs 10^4 vs 10^5 , excluding CC042) (Fig. 17). CC051 was an exception, with lower bacterial counts in the spleen after the oral infection. This finding suggests that the intestinal barrier in CC051 is harder for STm to transverse or that this line is better at clearing the infection prior to sustained systemic infection. CC051 presents a potential model to explore the resistance mechanisms in the intestinal phase of STm infections as it was the only line that appeared to control systemic spread of STm after oral infection (8, 96). Both studies also showed that CC042 was more heavily colonized than all other lines (65). Possible

reasons for the differences in colonization levels include time of necropsy and bacterial strain differences. In the intravenous



infection study, all mice were necropsied on day 4 post-infection (65), while the mice in the current study were necropsied when they met euthanasia criteria or at day 7 post-infection. Furthermore, the two studies used different bacterial strains: oral infections used *S. Typhimurium* ATCC14028 while the IV infections used *S. Typhimurium* SL1344.

All of the collected parameters were analyzed to identify genes using gQTL (90), but only survival time yielded significant associations. Intervals on Chr 1 corresponded to *Slc11a1* and *Ncf2*, previously known genes that have mutations linked to poor survival after STm infection. While these mutations are detrimental to survival after STm infection, this was not universal for all CC lines. One line with an *Slc11a1* mutation (of five lines) was able to survive the entire study period as did six out of twelve lines with *Ncf2* mutations. These lines must have alternative/compensatory mechanisms that allow them to overcome these *Slc11a1* and *Ncf2* mutations. One line, CC045, had a mutation in both *Slc11a1* and *Ncf2* and was able to survive for the duration of the experiment and was highly colonized in both spleen and liver, making it the most interesting tolerant candidate. The genetic basis for the ability of CC045 to survive STm infection in the face of these two mutations requires further exploration.

In addition to the intervals on Chr 1, suggestive and significant intervals on Chr 2, 4, and 7 were also identified in the gQTL analysis. The intervals on Chr 2 and 4 do not contain any genes previously linked to STm infection, but the interval on Chr 7 overlaps with a previously discovered QTL region, *Ses2* (91, 92). Genes linked to STm susceptibility underlying *Ses2* interval have not been identified. These regions were narrowed further using the method described above into a candidate gene list.

For median survival time, the suggestive QTL interval on Chr 2 had 13 candidate genes after considering haplotypes (Table 6). The suggestive interval on Chr 2 for percent of mice surviving to day seven had 51 candidate genes left (Table 7). A few of these genes are the most promising: BPI fold containing family B, member 2 (*Bpifb2*),

and SAM domain and HD domain, 1 (*Samhd1*). *Bpifb2* is a member of the lipid-transfer protein family and is predicted to have bactericidal and permeability-increasing properties, making it a good candidate for further investigation (97). *Samhd1* is involved in regulating interferon pathways in response to viral infections, through NF-KB (98, 99). While *Samhd1* has been linked to the immune response, it has only been implicated in viral infections, but could have a previously unknown role in bacterial immunity. Further investigation would be needed to prove such a link.

In both median survival and percent survived to day seven QTL intervals for Chr 4 and 7, the filtering process did not yield any candidate genes with haplotype differences. RNA expression analysis will be needed to identify candidate genes for these intervals.

Utilizing a subset of the CC mouse population, we have identified novel responses to STm infection as well as previously known and novel regions of the genome associated with survival time after infection. We found that parameters, such as CBC and cytokines, were driven more by inter-line variations than by infection status. We also found that histology, while weakly correlated with survival was also line-dependent as several lines were outliers. Overall, this research has identified potential new targets for further research into the complex host response to bacterial infections.

Materials/Methods

Bacterial strains and media

The *Salmonella enterica* ser. Typhimurium strain (HA420) used for this study was derived from ATCC14028. HA420 is a fully virulent, spontaneous nalidixic acid resistant derivative of ATCC14028 (100). Strains were routinely cultured in Luria-Bertani (LB) broth and plates, supplemented with antibiotics when needed at 50 mg/L nalidixic acid (Nal).

For murine infections, strains were grown aerobically at 37°C to stationary phase in LB broth with nalidixic acid and diluted to generate an inoculum of $2-5 \times 10^7$ organisms in 100 microliters. Bacterial cultures used as inocula were serially diluted and plated to enumerate colony forming units (CFU) and determine the exact titer.

Murine Strains

Both conventional mice (C57BL/6J and CBA/J) and collaborative cross (CC) mice were utilized in these experiments. Most animals were bred and maintained (on 2919 chow or 4% based on strain requirements) in the Division of Comparative Medicine at Texas A&M University. The remaining animals were obtained from UNC Collaborative Cross Core. Our experiments utilized 32 lines of CC mice, 3 females and 3 males per line for a total of 228 mice (CC045 only had 2 females due to a surgical complication) (Table 8). All animal experiments were conducted in accordance with the Guide for the Care and Use of Laboratory Animals, and with the TAMU IACUC (AUP# 2018-0488 D and 2015-0315 D).

Table 8: Number of mice used and facility of origin for 2 control strains and 32 CC lines.

Strain	Male	Female	Origin
B6	14	5	TAMU
CBA	14	2	TAMU
CC001	3	3	TAMU
CC002	3	3	TAMU
CC003	3	3	TAMU
CC005	3	3	TAMU
CC006	3	3	TAMU
CC011	3	3	TAMU
CC013	3	3	TAMU
CC015	3	3	TAMU
CC017	3	3	TAMU
CC019	3	3	TAMU
CC021	3	3	UNC
CC023	3	3	TAMU
CC024	4	3	TAMU
CC025	3	3	TAMU
CC027	3	3	TAMU
CC030	3	3	TAMU
CC031	3	3	UNC
CC032	3	3	TAMU
CC036	3	3	TAMU
CC037	4	3	TAMU
CC038	3	3	TAMU
CC041	3	3	TAMU
CC042	3	3	TAMU
CC043	3	3	TAMU
CC045	3	2	UNC
CC051	3	3	TAMU
CC053	3	3	TAMU
CC057	3	3	TAMU
CC058	3	3	TAMU
CC061	3	3	TAMU
CC072	3	3	TAMU
CC078	3	3	TAMU

Placement of Telemetry Devices

5 to 9-week-old mice (C57BL/6, CBA, CC) were anesthetized with isoflurane anesthesia. The abdomen was opened with a midline abdominal incision (up to 2 cm). Starr life science G2 E-mitter devices were loosely sutured to the ventral abdominal wall. The abdominal muscle layer was closed with 5-0 vicryl, and the skin layer was closed using stainless steel wound clips (FST 9mm). Animals were given an intraperitoneal injection of Buprenorphine (0.0001 mg/g) for pain prior to recovery from anesthesia, and every 8 hours thereafter as necessary for pain control. After recovery from anesthesia, implanted mice were group-housed and monitored twice daily for pain and wound closure for 7 days post-surgery, when the clips were removed. Any animals found to have serious complications after surgery were humanely euthanized.

Infection with *Salmonella* Typhimurium

After 4-7 days of acclimation in the BSL-2 facility, 8 to 12-week-old implanted mice were weighed and infected by gavage with a dose of $2-5 \times 10^7$ CFU of *S. Typhimurium* HA420 in 100 microliters of LB broth. Infected mice were monitored twice daily for signs of disease and activity by visual inspection. When telemetry and health condition data suggested the development of clinical disease from infection, mice were humanely euthanized. Animals that remained clinically healthy throughout the duration of the experiment were humanely euthanized at 7 days post-infection.

Bacterial load determination

Mice were humanely euthanized, and the spleen, liver, ileum, cecum, and colon were collected. A third of each organ was collected in 3 mL of ice-cold PBS, weighed,

homogenized, serially diluted in PBS, and plated on Nal plates for enumeration of *S. Typhimurium* in each organ. Data are expressed as CFU/g of tissue.

Telemetry Monitoring

Prior to placing implanted mice on telemetry platforms, mice were moved into individual cages and provided with a cardboard hut and bedding material. Individual cages containing implanted, uninfected mice were placed onto ER4000 receiver platforms, and the collection of body temperature (once per minute), and gross motor activity (continuous measurement summed each minute) data was initiated. Body temperature and gross motor activity data was collected for 4-7 days from uninfected mice. Mice were removed briefly from the receiver platforms for infection and then were placed back on the platforms and data collection by telemetry was resumed. Infected animals were continuously monitored by telemetry in addition to twice daily visual monitoring.

Identification of deviation from circadian pattern of body temperature

Additional clinical information, such as the time of inoculation relative to the start of the experiment (denoted T), was reported and used in centering time series for comparison between mice (typically, seven days after the beginning of monitoring). Quantitative detection of deviation from the baseline “off-pattern,” using temperature data was calculated on an individual basis. A temperature time series was filtered, a definition of healthy variation was defined, then the time of first “off-pattern” was calculated using that definition on post-inoculation data.

Each mouse time series was preprocessed using a moving median filter with a one-day window. For a specific minute t , the median collection of temperature values from $[t-720, t+720]$ was used in calculating a median for the value t . After this processing, healthy variation was defined as any temperature falling within the range of minimum to maximum values during the pre-inoculation phase $[T-5760, T]$ (5760 minutes=4 days). This choice allowed for enough data to account for natural inter-day variation due to potential factors such as inter-line variation, epigenetic differences, and sex differences, while avoiding bias due to observed acclimation time after transfer to a new facility in some mice in the first few days of observation (Fig. A2 A).

Identifying post-inoculation off-pattern behavior was done by identifying temperature values that fall outside the interval of healthy variation. The post-inoculation interval ranges from $[T+60, T+10080]$ (7 days), where the one hour gap was used to avoid false positive detection due to the physical disturbance associated with inoculation (Fig. A2 A).

Detection of deviation from circadian pattern of activity

While activity data does exhibit circadian patterns, this data necessitated a different approach to preprocessing because activity values are inherently non-negative and have a modal value of zero. Hence, we approached the analysis of activity data from the perspective of determining the parameters of a stochastic process. For a time interval t , we worked from the assumption that the number of activity values observed to be i obeys the following distribution:

$$\ln(p(A(t) = i)) = \alpha + \beta i$$

where the coefficient β , expected to be negative, corresponds to the modeling assumption that the relative drop in observed activity counts ought to decay (note $0 < e^\beta < 1$ if β is negative). For instance, if the value of $\beta = -0.693$, so that $e^\beta \approx 1/2$, this would represent an assumption that there are half as many activity values observed to be 1 (one movement per minute) than 2 (two movements per minute). In actuality, this decay coefficient is typically seen to be $\beta \approx -0.025$ to $\beta \approx -0.015$, representing that observed activity values decay by half around every 27-46 values.

This theory is implemented in practice by windowing a mouse's activity time series, creating a binning (empirical distribution) $(i, c(i))$, the performing a log-linear fit by transforming $c(i) \rightarrow \ln(1 + c(i))$ and applying linear least-squares regression to calculate α and β . Statistical models with simpler assumptions stemming from a "memoryless" assumption were attempted but did not see any feasible agreement with observed activity data (Fig. A2 B).

Histopathology

After euthanasia, samples of liver, spleen, ileum, cecum, and colon from each mouse were collected and fixed in 10% neutral buffered formalin at room temperature for 24 hours and stored in 70% ethanol before embedding in paraffin, sectioning at 5 μm and staining with hematoxylin and eosin (H&E). Histologic sections of all tissues were evaluated in a blinded manner by brightfield microscopy and scored on a scale from 0 to 4 for tissue damage by a board-certified veterinary pathologist (Table A1 and Fig. A1). The combined scores of spleen and liver from individual mice were used to calculate the median and interquartile range for each group. Whole slide images of liver and spleen

H&E-stained sections were captured as digital files by scanning at 40x using a 3DHistech Panoramic SCAN II FL™ scanner (EpreDia, Kalamazoo, MI). Digital files were processed by Aiforia Hub™ (Aiforia, Cambridge, MA) software for generating the images with 100 μm scale bars.

Complete Blood Count

Whole blood was collected by cheek bleed for complete blood count (CBC) one week prior to surgery for the pre-infection sample to determine each mouse's baseline. Infected terminal blood was collected at necropsy by cardiac puncture. Additional blood was collected from uninfected control animals by cardiac puncture after euthanasia and median values were used as the baseline for mice that were not their own pre-infection control. All blood was collected into EDTA tubes and analyzed on an Abaxis VetScan HM5.

Cytokine and Chemokine Analysis

Serum was stored at -80°C and thawed on ice immediately prior to cytokine assays. Serum cytokine levels were evaluated using an Invitrogen ProcartaPlex Cytokine/Chemokine Convenience Panel 1A 36 plex kit as per manufacturer instructions (ThermoFisher). Briefly, magnetic beads were added to each well of the 96-well plate and washed on the Bio-Plex Pro Wash Station. 25uL of samples and standards were then added to the plate along with 25uL of universal assay buffer. Plates were then shaken at room temperature for 1 hour and washed. 25uL of detection antibody was added and incubated for 30 minutes and washed away, followed by 50uL of SAPE for 30 minutes and washed away. 120uL of reading buffer was added and plates were evaluated using a

Bio-Plex 200 (BioRad). Samples and standards were run in duplicate, and samples were diluted as needed to get 25ul of serum per duplicate. The kit screens for the following 36 cytokines and chemokines: IFN gamma; IL-12p70; IL-13; IL-1 beta; IL-2; IL-4; IL-5; IL-6; TNF alpha; GM-CSF; IL-18; IL-10; IL-17A; IL-22; IL-23; IL-27; IL-9; GRO alpha; IP-10; MCP-1; MCP-3; MIP-1 alpha; MIP-1 beta; MIP-2; RANTES; Eotaxin; IFN alpha; IL-15/IL-15R; IL-28; IL-31; IL-1 alpha; IL-3; G-CSF; LIF; ENA-78/CXCL5; M-CSF. Median values of uninfected animals for each line were used as the baseline for that line.

QTL analysis

gQTL, an online resource designed specifically to run CC QTLs, was used to identify putative QTLs (90). Briefly, median values of each line for various parameters were uploaded to the website and QTLs were run using 1000 permutations with “automatic” transformation. Automatic picks either log or square root transformations, whichever normalizes the data best.

Transcriptomic analysis

Tissues were snap frozen in liquid nitrogen and stored in the -80°C freezer until ribonucleic acid (RNA) sequencing could be performed. Spleens were used for host gene expression analysis. All molecular work was performed in the Molecular Genomics Core of the Texas A&M Institute for Genome Sciences and Society (TIGSS). The following protocol is adapted from the Molecular Genomics Core, and TIGSS personnel aided in data acquisition and plot generation. Spleens were homogenized in Trizol and an aliquot taken for analysis. RNA samples were quantified with a Qubit Fluorometer (Life

Technologies) with a broad range RNA assay and concentrations were normalized for library preparation. RNA quality from the spleens were verified on an Agilent TapeStation with a broad range RNA ScreenTape. Total RNA sequencing libraries were prepared using the Illumina TruSeq Stranded mRNA-seq preparation kit. Barcoded libraries were pooled at equimolar concentrations and sequenced on an Illumina NovaSeq 6000 2x150 S4 flow cell. RNA-seq libraries were trimmed to remove adapter sequences and low-quality bases using TrimGalore version 0.6.6, with Cutadapt version 3.0 and FastQC version 0.11.9. Trimmed reads were mapped with Tophat2 version 2.1.1 to the appropriate pseudogenomes from UNC. Coordinate alignments were converted to the mm10 genome using Lapels version 1.1.1. Differential expression was conducted in R using the DESeq2 package. The resulting gene expression values were uploaded to Ingenuity Pathways (QIAGEN, enlo, Netherlands; www.ingenuity.com Application Build 261899, Content Version 18030641) for biological pathway analysis.

CHAPTER III

ELUCIDATING TOLERANCE MECHANISMS TO *SALMONELLA* TYPHIMURIUM ACROSS LONG-TERM INFECTIONS USING THE COLLABORATIVE CROSS

Overview

Salmonella is a world-wide health concern with rising incidences of antibiotic resistance. Better understanding of the molecular mechanisms underlying natural disease resistance or tolerance to a given pathogen may present the opportunity to develop novel interventions. Resistance is defined as the absence of clinical disease with low (or no) pathogen burden, while tolerance is minimal clinical disease in the face of high pathogen burden. We studied 18 lines of the collaborative cross mice that survive acute STm infections while maintaining a bacterial load. We orally infected these lines and monitored them for three weeks post-infection. 5 lines cleared STm by the end of the experiment and were classified as resistant, while 6 lines that maintained a bacterial load and survived to the end of the experiment and were classified as tolerant. The remaining 7 lines survived longer than 7 days but succumbed to infection before the end of the study period and were called delayed susceptible to differentiate them from the susceptible lines that do not survive to day 7. The tolerant lines maintained bacterial burdens in Peyer's patches, mesenteric lymph node, as well as in spleen and liver, while resistant significantly reduced bacterial colonization. Tolerant lines had lower pre-infection temperatures than both delayed susceptible and resistant lines and had disrupted circadian patterns sooner than resistant lines. Tolerant lines also had higher

circulating total white blood cells, driven by increased numbers of neutrophils, than resistant lines. Tolerant lines also had higher circulating levels of IFN-gamma and MCP-1, and lower levels of ENA-78 than resistant lines. Resistant lines had reduced tissue damage in spleen and liver while tolerant lines had more severe tissue damage. QTLs revealed 1 significant association and 6 suggestive associations, which require further validation to identify underlying genes associated with tolerance.

Introduction

Salmonella enterica are Gram negative bacteria that cause a range of disease phenotypes including gastroenteritis, sepsis, and typhoid fever in various mammalian and avian hosts (8, 10). 93.8 million cases Non-typhoidal *Salmonella* (NTS) occur world-wide every year in humans, resulting in 155,000 deaths (1). The severity of NTS infections depends on several factors including host age, health, and genetics, as well as *Salmonella* serotype causing the infection (3–5). *Salmonella enterica* serotype Typhimurium (STm) causes gastroenteritis in humans and can cause serious bacteremia. In mice, this serotype causes a fatal systemic infection in susceptible mouse strains that models invasive infections in humans (10, 21).

Strains of inbred mice respond to STm infection differently. C57BL/6J and BALB/cJ have mutations in Solute Carrier Family 11 Member 1 (*Slc11a1*) and are highly susceptible to fatal STm bacteremia (23, 25, 26). Other strains including 129SvJ, CBA/J, and A/J, are wild type at the *Slc11a1* locus and do not develop severe systemic salmonellosis. Other genes, including Neutrophil Cytosolic Factor 2 (*Ncf2*), Toll-like

Receptor 4 (*Tlr4*), Interferon gamma (*Ifng*), and Histocompatibility complex (H2) haplotypes have also been linked to survival after STm infections in mice (10, 27, 30–32). Our recent work with Collaborative Cross (CC) mice suggests that while these genes influence survival after STm infection, they are not the only genes that influence susceptibility to STm infection (1w paper). Studies using this genetically diverse population of mice suggested that the disease outcomes after STm infection in mice are much more complex than a binary susceptible and resistant classification (1W paper).

Host response to infections has been categorized as susceptible and resistant, based on the host's ability to clear the infection; either the host is able to kill the invading pathogen and survive, or the host is unable to fight off the infection and dies (10, 67). Beyond resistant and susceptible, a third response called tolerance has been acknowledged in plant systems and is now being applied to other systems including drosophila and mice (47, 49, 68–72). In tolerance, the host tolerate high pathogen burden yet has minimal signs of infection (72–74).

Since previous STm infection studies have used primarily traditionally inbred mouse strains, most of the genetic diversity in the mouse has not been explored. The Collaborative Cross (CC) mouse population is a panel of recombinant inbred lines that recapitulate the genetic diversity found in human populations (38–40, 101). The CC founders capture 90% of the genetic diversity found in the mouse genome and represents a wider range of phenotypes, including immune phenotypes, than traditional inbred lines (36, 44, 45). For example, lines with high viral titers after experiment infection with

influenza virus or Ebola virus and good health status have been identified in the CC (41, 56, 102).

To differentiate tolerance from resistance to *Salmonella* infections, 18 lines of the CC that were not susceptible to acute infection were orally infected with STm for up to three weeks. Our experiments revealed STm tolerant lines that maintained a significantly higher bacterial burden in PP, MLN, spleen, and liver than resistant lines. Tolerant lines also lost more weight than resistant lines despite surviving infection. Not surprisingly, resistant lines had significantly reduced tissue damage in spleen and liver relative to tolerant lines. Whole blood and serum were also collected at necropsy, and tolerant lines had more circulating total white blood cells, driven by higher circulating neutrophils, and higher serum Interferon-gamma (IFN-gamma), and Monocyte Chemoattractant Protein-1 (MCP-1) than resistant lines. Resistant lines had significantly more circulating Epithelial Neutrophil-Activating Protein 78 (ENA-78) than tolerant lines. Using quantitative trait loci (QTL) analysis, one significant association, Scq1, and six suggestive associations were identified.

Results

Three-week *Salmonella* infections distinguish tolerant and resistant lines and reveal another phenotype: delayed susceptibility.

Based on survival of acute STm infections (7 days), 18 CC mouse lines were chosen to undergo a three-week infection with STm ATCC14028 to differentiate between tolerant and resistant phenotypes. Tolerance was defined as lines that had at

least 4/6 mice survive to day 7 during one-week infections (1W paper), at least 4/ 6 mice survive to day 21 during three-week infections, and had a median colonization of at least 10^3 CFU/g in liver and 10^4 CFU/g in spleen (Fig. 18A-D). Resistant lines had the same or better survival as tolerant mice but had reduced bacterial burden with a median of $<10^3$ CFU/g in liver and $<10^4$ CFU/g in spleen (Fig.18A-D).

Of the 18 lines analyzed, six were categorized as tolerant (CC002, CC017, CC038, CC043, CC072, CC078) and five were resistant (CC015, CC024, CC051, CC057, CC058). The remaining seven lines did not fit into either the tolerant or resistant category because 3/ 6 or fewer mice survived the three-week study period, despite having at least 4/ 6 mice survive our earlier acute study. We categorized these lines as “delayed susceptible” since they survive longer than susceptible lines.

Delayed susceptible lines had a mean survival time of at least 7 but less than 16 days (Fig. 18A). Tolerant lines had a mean survival time between 16 days and 18 days (Fig. 18A). Four of the five resistant lines had all 6 mice survive to day 21. The remaining resistant line, CC058, 4/6 mice survive to day 21 with a mean survival of 16.83 days (Fig. 18A). In general, both delayed susceptible and tolerant lines lost weight, while resistant lines gained weight. Delayed susceptible lines lost between 0.93% - 15.67% of their starting weights while tolerant lines lost between 1.02% - 5.97% (Fig. 18B). Resistant lines gained between 2.05% - 8.17% of their starting weight, excluding CC058 which lost 5.51% (Fig. 18B).

We defined tolerance and resistance by a line’s ability to control the systemic phase of infection and focused on bacterial burden in spleen and liver. Resistant lines

ranged in median colonization from 3.9×10^1 - 7.53×10^2 CFU/g in liver and 1.88×10^2 - 7.48×10^3 CFU/g in spleen (Fig. 18C, D). Tolerant lines ranged in median colonization from 1.74×10^3 - 2.78×10^4 CFU/g in liver and 4.5×10^4 - 2.13×10^5 CFU/g in spleen (Fig. 18C, D). Delayed susceptible lines overlapped with the tolerant median colonization ranges for both organs, ranging from 2.07×10^3 - 9.44×10^4 CFU/g in liver and 6.5×10^4 - 7.5×10^5 CFU/g in spleen (Fig. 18C, D). The overlapping ranges of tolerant and delayed susceptible lines show that the tolerant lines are able to survive a bacterial burden that is fatal for other CC lines. One tolerant line, CC072, had the highest colonization of all tolerant lines in both spleen and liver, while another, CC043, was more poorly colonized in both organs, illustrating that there is a broad spectrum of bacterial colonization that is tolerated across host genetics.

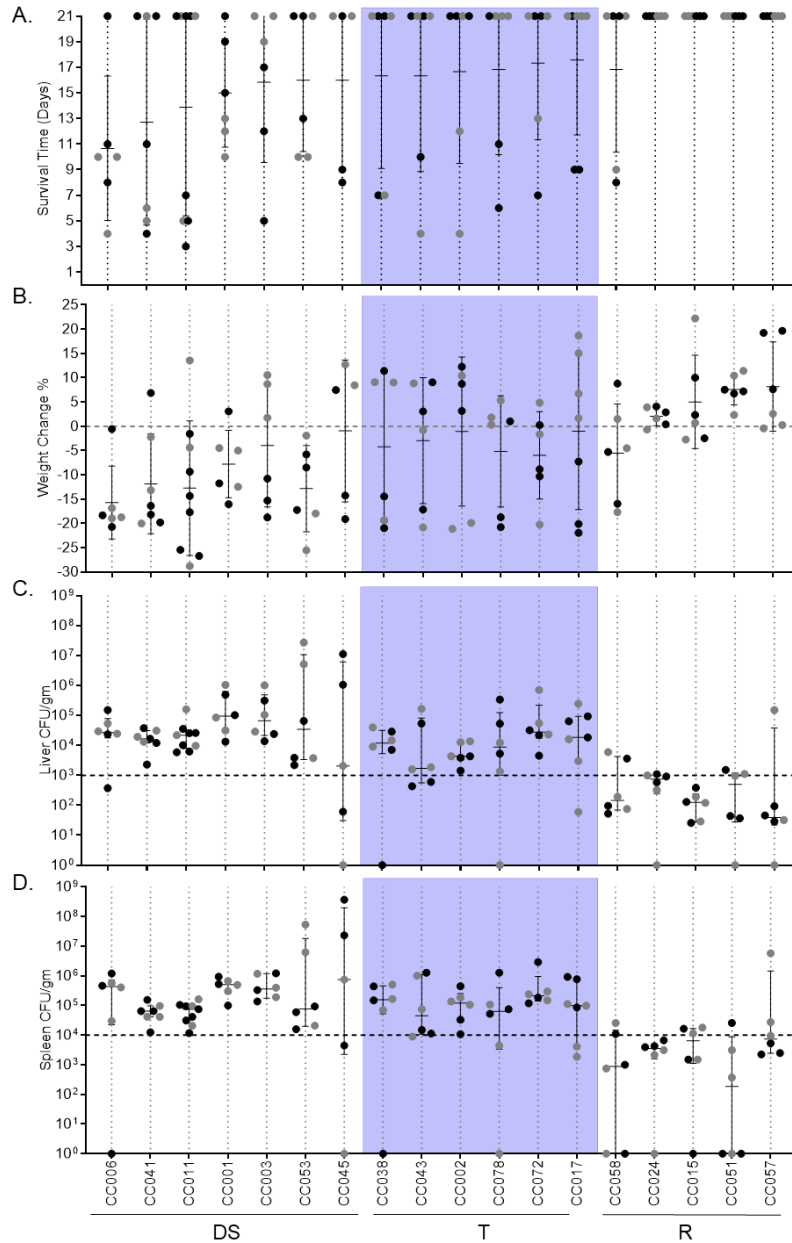


Figure 18: Delayed susceptible, tolerant, and resistant lines show distinct responses to STm infections.

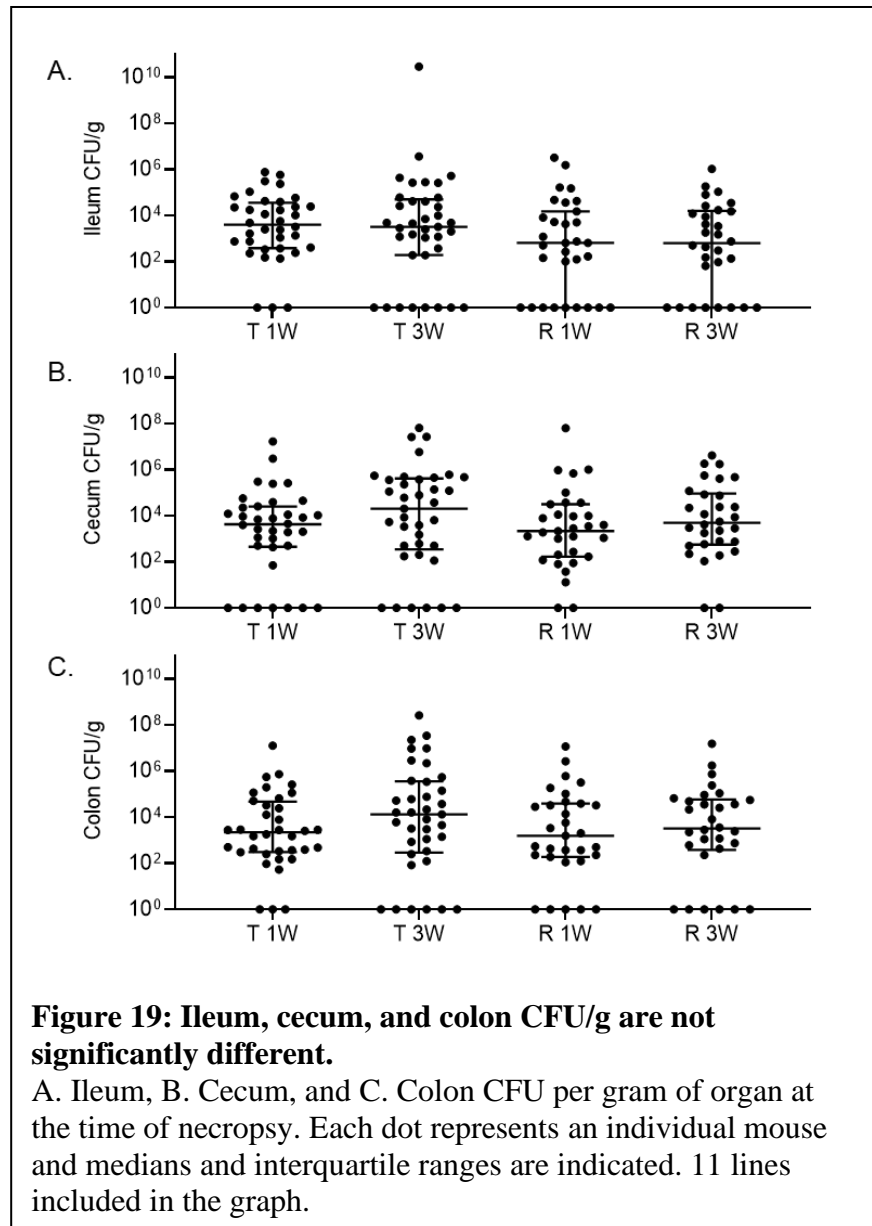
A. Survival time and B. percent weight change after infection with STm. Lines are shown in ascending order of survival and weight change if survival was equal between lines. Mean and standard deviation are shown. C. Liver and D. Spleen CFU per gram of organ at time of necropsy. Median and interquartile range shown. Dots represent individual mice and black dots represent males and grey dots represent females. 18 CC lines are represented. (DS = delayed susceptible, T = tolerant, R = resistant).

Tolerant lines maintain a higher bacterial load than resistant lines in Peyer's Patches and mesenteric lymph nodes.

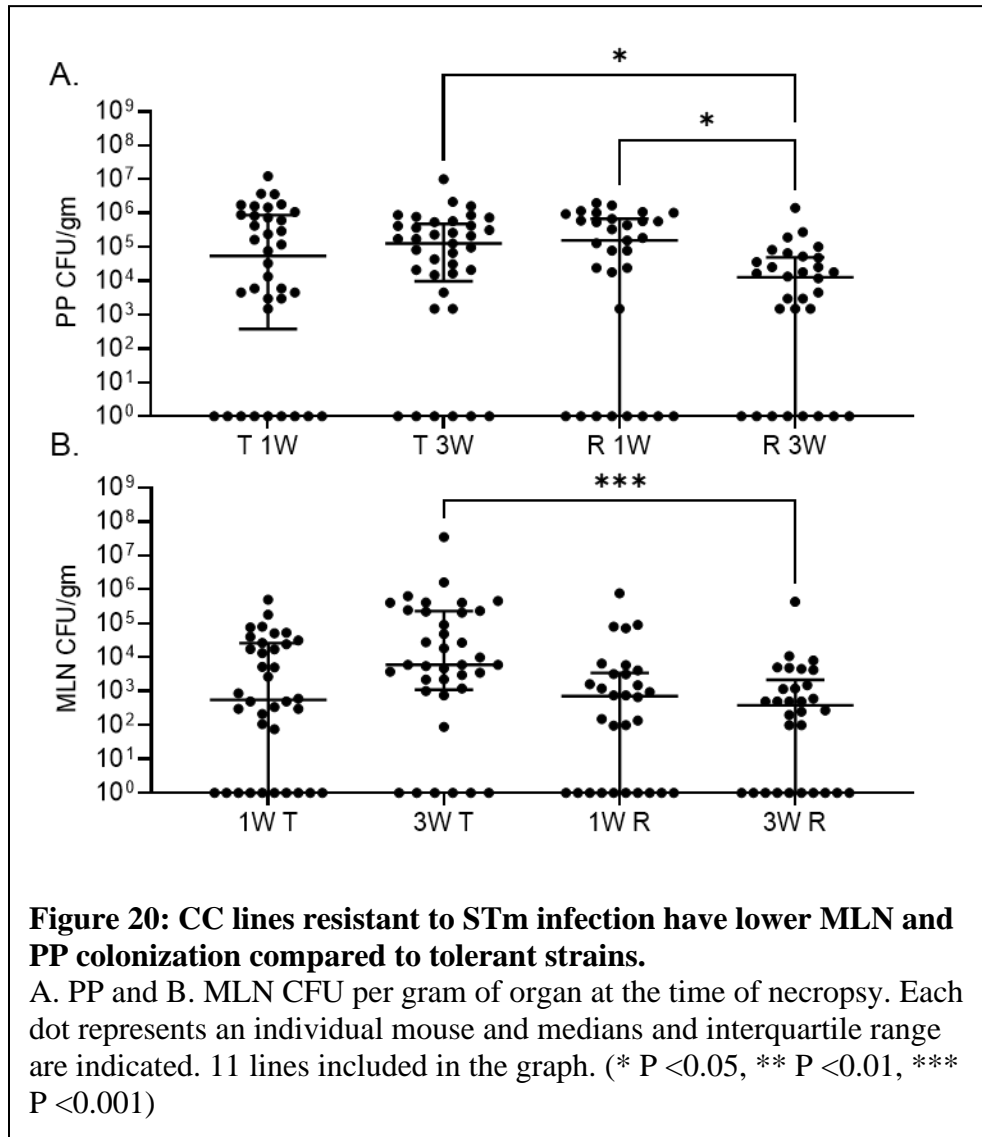
While the focus for defining tolerance was on spleen and liver, ileum, cecum, colon, MLN, and PP were also examined for bacterial load after STm infection.

Bacterial burden in ileum, cecum, and colon was not significantly different between tolerant or

resistant lines at one- or three-weeks post-infection (Fig. 19, $P = 0.5600$, >0.9999 , and >0.9999). Tolerant and resistant lines were colonized similarly in their PP and MLN during one-week infections in previous experiments (Fig. 20A, B, $P =$



>0.9999). Resistant lines were able to reduce their PP colonization significantly between one- and three-weeks post-infection (Figure 20A, 1.56×10^5 CFU/g and 1.28×10^4 CFU/g, $P = 0.0451$), while colonization of the MLN in these lines remained stable. Tolerant lines were stably colonized in PP and MLN between one- and three-weeks post-infection (Fig. 20A, B). Finally, after three weeks of infection with STm, resistant lines limit STm colonization of the MLN while tolerant lines do not (Fig. 20B, 3.87×10^2 CFU/g and 6.00×10^3 CFU/g, $P = 0.0008$).



Resistant lines had higher baseline body temperatures than tolerant lines and stayed on circadian pattern longer.

Mice were implanted with telemetry devices that tracked temperature and activity continuously. Baseline measurements were taken for one week pre-infection and for up to three weeks post-infection. The median minimum, median, and median maximum pre-infection temperatures were significantly different across resistant, tolerant, and delayed susceptible lines. The temperature minimum corresponds to the “rest period” of the mouse, the maximum corresponds to the “active period,” and the median describes a 24-hour period.

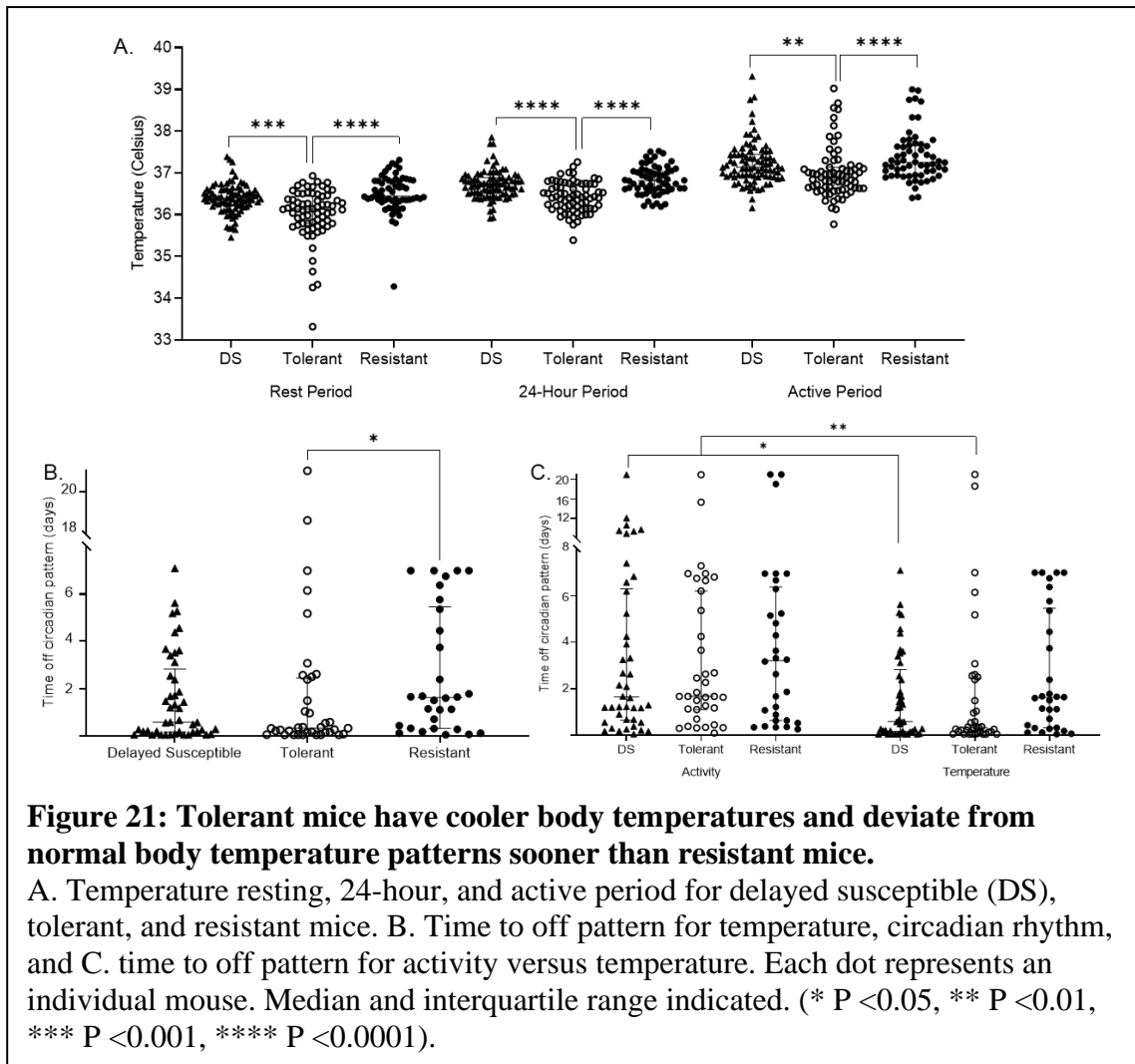
Tolerant lines had a lower baseline median body temperature pre-infection than resistant or delayed susceptible lines (Fig. 21A). This difference was apparent during the rest period, the active period, and over a full 24-hour interval (Fig. 21A, Table 9). As body temperature can be altered by differences in activity, activity levels were also analyzed for the fraction of time the mouse was active throughout a 24-hour period. The fraction of time the mouse was active for their rest period, active period, and overall 24-hour period was no significantly different between these groups (Fig. 22A).

Time to circadian pattern disruption after infection was also determined for temperature and activity patterns. For body temperature, resistant mice maintained their circadian pattern the longest, with a median of 2,324.5 minutes (1.61 days) (Fig. 21B). Delayed susceptible lines deviated from their normal pattern of body temperature significantly earlier (835 minutes, ~13 hours) and tolerant lines deviated from their normal circadian pattern of body temperature very quickly after STm infection (463

minutes, 7.7 hours) (Fig. 21B, $P = 0.0458$). All groups maintained their circadian patterns for a similar amount of time for activity level (Fig. 22B). When activity and temperature time to “off-pattern” were compared for each group, both delayed susceptible and tolerant mice had disrupted temperature circadian pattern sooner than their activity circadian patterns, illustrating that one does not influence the other (Fig. 21C). Delayed susceptible mice got off their temperature pattern a median of 1,523.5 minutes (1.06 days) earlier than their activity pattern (Fig 21C, $P = 0.0351$), while tolerant mice got off their temperature pattern a median of 1,940 minutes (1.34 days) earlier (Fig. 21C, $P = 0.0031$). Disrupted circadian pattern of temperature and activity occurred approximately the same timing in resistant mice (Fig. 21C, $P = >0.9999$). For delayed susceptible and tolerant mice, changes in temperature pattern signaled earlier changes in health than changes in activity level, consistent with previous reports (1W paper).

Table 9: Median values of temperature for rest period, 24-hour period, and active period.

	DS	Tolerant	Resistant
Rest period	36.39	36.13	36.445
24-hour period	36.73	36.42	36.815
Active period	37.13	36.9	37.25



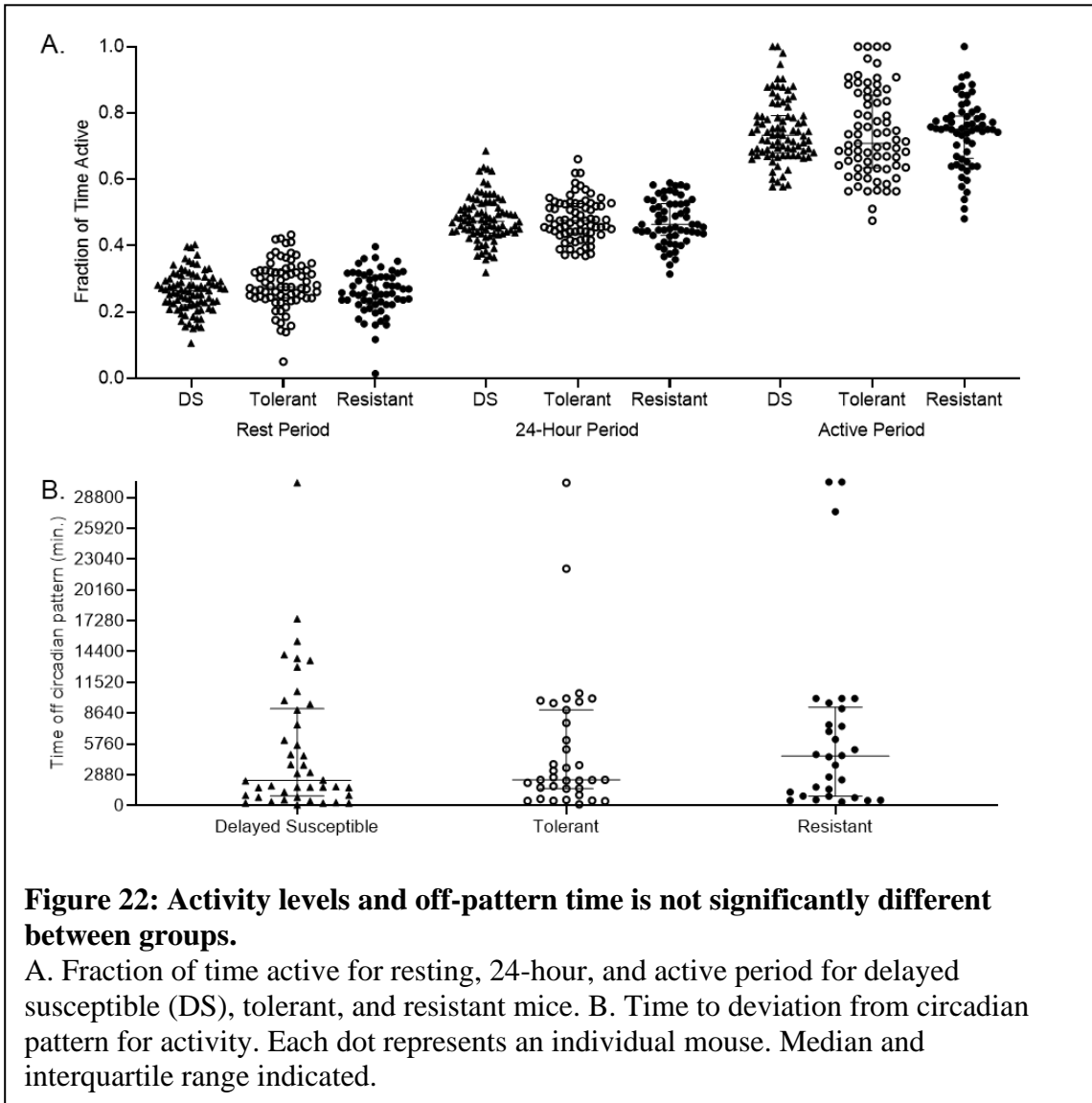


Figure 22: Activity levels and off-pattern time is not significantly different between groups.

A. Fraction of time active for resting, 24-hour, and active period for delayed susceptible (DS), tolerant, and resistant mice. B. Time to deviation from circadian pattern for activity. Each dot represents an individual mouse. Median and interquartile range indicated.

Resistant lines have reduced total white blood cell counts, driven by circulating neutrophils counts, compared to tolerant lines at three-weeks post-infection.

Complete blood counts (CBC) were performed pre-infection and at the time of necropsy for one- and three- week infections. The differences between the post-infection and pre-infection CBC components were calculated to determine the response of CBC components to STm infection (Table 10). We excluded delayed susceptible lines, because they were euthanized at earlier time points than tolerant and resistant lines. At three-weeks post-infection, resistant mice had significantly fewer circulating white blood cells (WBC) at $2.61 \times 10^9/L$ compared to tolerant mice who had $5.29 \times 10^9/L$ (Fig. 23A, $P = 0.0396$). The differential count suggested that circulating neutrophils (NEU) were significantly reduced in resistant mice than tolerant mice at three-weeks post-infection with $2.16 \times 10^9/L$ of blood compared to $5.58 \times 10^9/L$ of blood (Fig. 23B, $P = 0.0029$). Circulating monocyte (MON) and lymphocyte (LYM) numbers were similar between resistant and tolerant mice (Fig. 23C, D, $P = 0.2278, >0.9999$). Our findings suggest that circulating neutrophils in tolerant mice remain elevated for the duration of the study period.

Table 10: Infected Complete Blood Counts taken at necropsy time minus uninfected mean for respective line.

Includes 18 CC lines. Mean and standard deviation shown.

CBC Parameter	CC001		CC002		CC003		CC006		CC011		CC015		CC017		CC024		CC038	
	Mean	SD	Mean	SD	Mean	SD	Mean	SD	Mean	SD	Mean	SD	Mean	SD	Mean	SD	Mean	SD
WBC 10 ⁹ /l	5.72	2.49	11.65	3.74	11.70	8.57	2.78	8.78	13.77	11.91	1.68	2.88	6.05	7.56	2.53	4.21	5.58	4.02
LYM 10 ⁹ /l	-3.87	2.25	2.32	2.76	-0.16	2.90	-3.42	5.60	-1.91	2.50	0.35	1.68	0.13	4.49	0.52	3.72	0.39	1.53
MON 10 ⁹ /l	0.62	0.22	0.49	0.48	0.99	1.34	0.46	0.73	1.64	1.42	0.11	0.30	0.41	0.47	-0.01	0.30	0.45	0.27
NEU 10 ⁹ /l	8.98	0.93	8.86	3.57	10.87	8.44	5.74	3.75	14.07	9.67	1.22	1.03	5.51	3.56	2.02	2.44	4.74	2.54
LYM% %	-67.75	8.25	-43.68	17.29	-60.66	16.62	-42.07	18.25	-58.29	10.95	-21.16	14.07	-35.27	22.32	-15.93	17.65	-40.88	15.59
MON% %	4.20	2.34	-0.17	4.06	3.68	5.41	2.52	2.97	5.49	3.97	-0.48	3.77	1.34	2.53	-0.73	2.89	3.50	2.85
NEU% %	63.57	7.49	43.83	17.71	56.98	12.50	39.53	16.69	52.77	8.60	21.62	12.54	33.86	21.57	16.63	20.15	37.35	17.27
RBC 10 ¹² /l	-2.47	1.21	0.17	1.92	-1.69	4.37	-2.73	3.14	-1.77	2.69	-0.62	3.81	0.18	3.82	-1.09	1.51	-0.92	2.05
HGB g/dl	-4.68	1.86	-0.97	3.03	-4.14	5.97	-4.87	5.44	-4.23	4.70	-0.48	5.69	-0.43	6.30	-1.93	2.83	-2.03	2.49
HCT %	-16.47	5.96	-2.63	10.70	-14.94	23.25	-17.88	16.96	-15.19	15.80	-3.60	15.53	-1.43	19.51	-6.76	7.71	-7.59	7.78
MCV fl	-5.83	2.56	-3.67	1.21	-6.00	5.48	-3.50	0.84	-7.00	4.12	-2.40	4.28	-3.43	3.46	-1.33	0.58	-2.83	4.96
MCH pg	-1.72	0.83	-1.25	0.72	-1.74	1.44	-1.12	1.55	-2.06	0.88	0.16	0.96	-0.97	1.42	-0.43	0.76	-0.83	1.27
MCHC g/dl	-0.23	0.91	-0.35	1.43	0.10	1.47	-0.17	2.81	-0.39	2.02	1.44	3.86	0.04	3.30	-0.20	1.39	-0.07	2.64
RDWs fl	-3.12	3.03	-9.52	4.11	3.44	3.68	-2.98	1.52	0.47	4.79	-9.56	5.29	-4.36	4.87	-3.90	3.15	-2.48	4.92
RDWc %	1.25	2.38	-3.42	2.11	3.72	2.93	-0.08	0.61	2.72	2.46	-4.06	3.32	-0.80	2.06	-1.40	1.45	-0.07	1.59
PLT 10 ⁹ /l	-139.33	264.92	-53.17	343.36	-170.40	222.21	-64.67	292.16	35.00	331.63	-25.20	83.86	11.86	307.54	-26.00	248.59	44.00	128.75
PCT %	-0.07	0.20	0.05	0.25	-0.19	0.22	-0.01	0.23	0.05	0.26	0.00	0.06	0.01	0.22	-0.02	0.16	0.04	0.08
MPV fl	0.60	0.87	2.47	4.10	-0.74	2.91	0.98	0.57	0.77	0.71	0.68	0.69	0.01	0.52	-0.07	0.38	0.47	0.66
PDWs fl	3.20	1.01	2.50	2.60	-5.50	6.10	2.50	3.42	2.84	2.28	1.68	0.62	-0.56	2.77	-0.90	1.08	0.40	1.18
PDWc %	5.00	1.05	0.08	7.11	-4.84	4.39	2.48	4.17	4.39	3.45	1.70	1.00	-0.66	3.82	-1.40	1.64	0.72	1.91

CBC Parameter	CC041		CC043		CC045		CC051		CC053		CC057		CC058		CC072		CC078	
	Mean	SD	Mean	SD	Mean	SD	Mean	SD	Mean	SD	Mean	SD	Mean	SD	Mean	SD	Mean	SD
WBC 10 ⁹ /l	8.94	6.22	0.52	3.76	12.79	12.31	1.38	5.80	2.38	2.82	2.53	3.59	4.13	6.20	10.34	5.33	3.30	7.00
LYM 10 ⁹ /l	-0.91	2.03	-0.77	3.46	1.66	2.78	-1.59	4.86	-2.11	3.00	0.87	3.36	-0.86	6.31	-0.94	1.79	-2.63	4.45
MON 10 ⁹ /l	0.57	0.36	0.07	0.08	1.75	2.07	0.29	0.42	0.36	0.58	0.14	0.18	0.23	0.42	0.59	0.54	0.48	0.92
NEU 10 ⁹ /l	9.29	4.32	1.22	0.73	9.37	12.17	2.69	2.51	4.18	2.91	1.51	1.21	4.76	2.53	10.69	4.68	5.45	6.21
LYM% %	-62.19	10.39	-30.03	21.83	-33.24	38.97	-21.75	17.32	-54.50	26.14	-17.83	18.98	-34.19	22.77	-54.55	7.40	-30.77	28.09
MON% %	2.91	2.50	1.38	1.77	5.90	6.49	1.87	2.60	3.53	5.56	1.67	3.09	1.11	3.13	1.13	3.31	1.67	4.70
NEU% %	59.29	9.91	28.65	21.25	27.38	33.69	19.92	15.79	51.27	26.50	16.18	16.12	33.07	20.02	53.37	7.09	29.07	23.90
RBC 10 ¹² /l	-0.43	2.28	-2.10	0.50	-1.38	3.39	-0.60	0.89	-2.31	2.87	0.26	2.44	1.57	2.12	2.11	3.72	-1.79	1.47
HGB g/dl	-2.09	3.60	-4.08	0.84	-2.74	4.94	-1.77	1.20	-4.30	3.83	-0.33	4.06	0.86	3.83	2.23	6.43	-3.83	2.20
HCT %	-6.53	9.54	-11.32	2.58	-8.38	17.00	-7.44	4.18	-15.50	13.52	-2.01	12.43	3.80	10.21	7.11	19.37	-10.48	6.52
MCV fl	-4.71	2.14	-3.33	2.16	-2.20	1.79	-4.00	1.26	-3.50	2.59	-4.33	1.75	-4.00	1.67	-4.17	1.72	-2.50	1.87
MCH pg	-1.56	0.89	-1.75	0.94	-0.72	0.48	-0.88	0.48	-1.30	0.55	-0.95	1.20	-1.16	1.06	-0.92	1.08	-1.20	0.64
MCHC g/dl	-0.06	1.66	-1.77	2.87	-0.38	0.68	0.53	0.72	-0.62	1.77	0.30	2.72	-0.13	2.65	0.48	2.12	-1.07	2.06
RDWs fl	-3.16	1.56	-2.98	3.54	-0.30	1.63	-3.88	1.89	-4.32	4.77	-6.37	2.81	-3.16	5.39	-6.23	6.02	1.97	6.15
RDWc %	0.44	1.25	-0.05	1.47	0.36	1.19	-0.37	1.02	-0.57	2.57	-1.43	0.64	0.09	2.17	-1.68	3.53	1.70	2.93
PLT 10 ⁹ /l	-175.00	169.11	31.17	170.96	57.20	208.30	9.83	214.28	-1.17	240.28	48.17	####	318.56	193.26	78.83	167.03	104.33	327.55
PCT %	-0.14	0.11	0.03	0.09	0.06	0.11	0.02	0.15	0.00	0.15	0.03	0.08	0.21	0.13	0.06	0.13	0.08	0.22
MPV fl	-0.26	1.32	0.13	0.63	0.76	0.66	0.38	0.44	0.17	0.37	0.02	0.52	-0.12	0.36	0.17	0.59	0.28	0.57
PDWs fl	-2.29	2.65	0.18	1.78	1.74	3.04	1.20	2.09	0.32	2.01	-1.07	2.09	-2.00	2.02	0.60	3.13	0.70	2.72
PDWc %	-3.07	2.87	-0.30	2.61	2.42	4.50	1.58	2.94	0.37	3.44	-1.75	3.75	-2.58	2.44	0.78	3.85	1.08	4.02

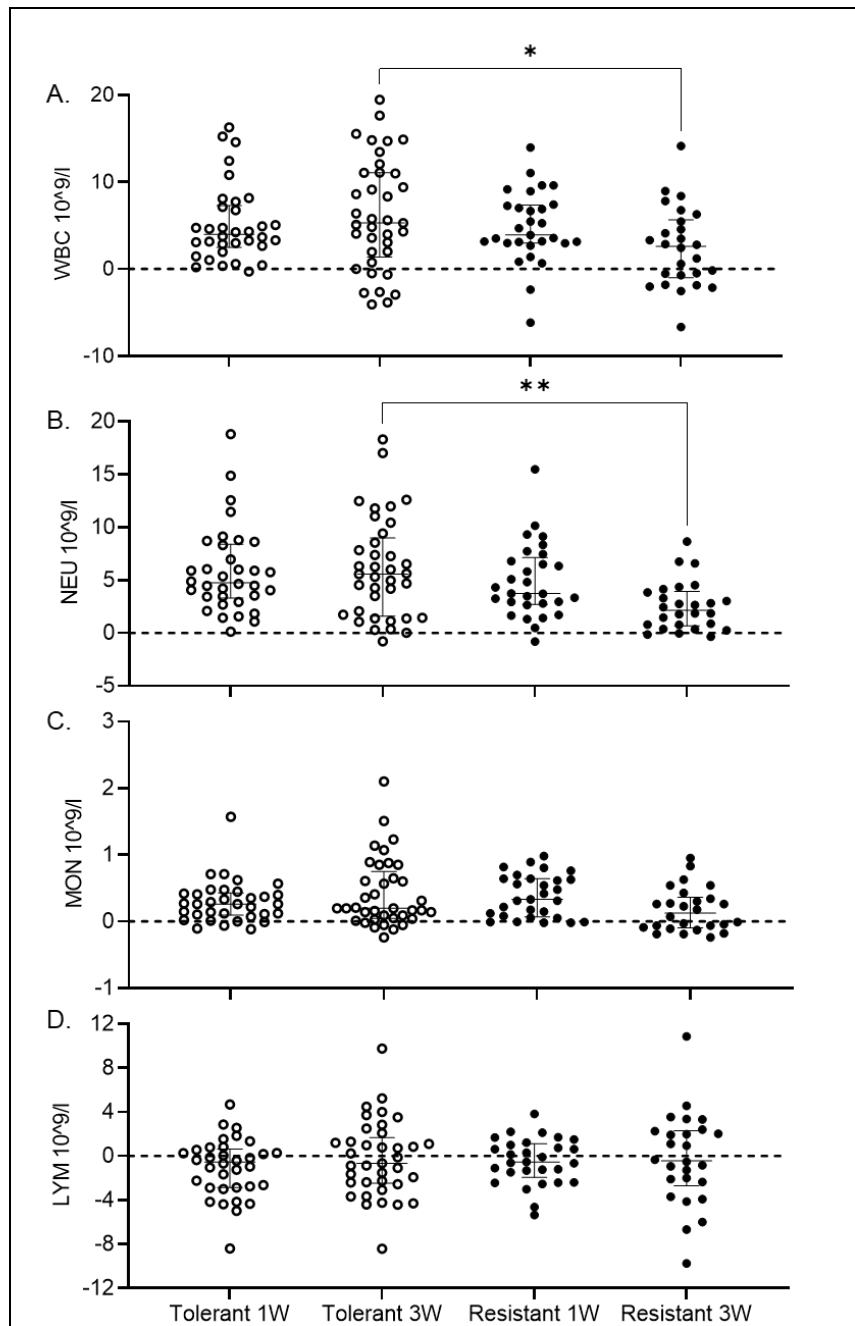


Figure 23: Tolerant mice have higher WBC and higher NEU than resistant mice.

Differences between infected and uninfected for A. White Blood cells, B. neutrophils, C. monocytes, D. lymphocytes. Each dot represents an individual mouse and lines represent medians and interquartile ranges. (* $P < 0.05$, ** $P < 0.01$).

At three-weeks post-infection, resistant lines have reduced IFN-gamma and MCP-1 levels and increased ENA-78 levels compared to tolerant lines.

The levels of 36 cytokines/chemokines in serum from uninfected, one, and three week infected animals were determined. The changes in circulating cytokine/chemokine levels between uninfected animals and infected animals were calculated (Table 11). Delayed susceptible lines were excluded from this analysis because their serum was collected at earlier time points post-infection. Changes in the levels of only three cytokines were significantly different between tolerant and resistant mice at three-weeks post-infection: IFN- γ , MCP-1, and ENA-78.

IFN- γ is vital for controlling intracellular replication of STm. At three-weeks post-infection, resistant lines had a median increase of 25.99 pg/ml compared to a median increase of 200.04 pg/ml of circulating IFN- γ in tolerant lines (Fig. 24A, $P = 0.0001$). MCP-1 is a chemoattractant for monocytes. Over the course of infection, resistant mice had significantly reduced circulating levels of MCP-1 from a median increase of 123.57 pg/ml at one-week post-infection to a median increase of 9.27 pg/ml at three-weeks post-infection (Fig. 24B, $P = <0.0001$). At three-weeks post-infection, resistant mice have significantly lower levels of circulating MCP-1 in response to infection than tolerant mice with a median increase of 9.27 pg/ml compared to a median increase of 117.54 pg/ml (Fig. 24B, $P = 0.0005$). ENA-78, also known as CXCL5, is a chemoattractant for neutrophils and has a greater increase at three-weeks in resistant lines than in tolerant lines. Resistant lines had increased ENA-78 levels by a median of 37.91 pg/ml, while tolerant lines had decreased ENA-78 levels by a median of 87.90

pg/ml (Fig. 24C, $P = <0.0001$). Resistant lines also significantly increased their ENA-78 levels from one-week to three-weeks post infection from - 42.11 pg/ml to 37.91 pg/ml (Fig. 24C, $P = 0.0016$).

(Fig. 24C, $P = 0.0016$).

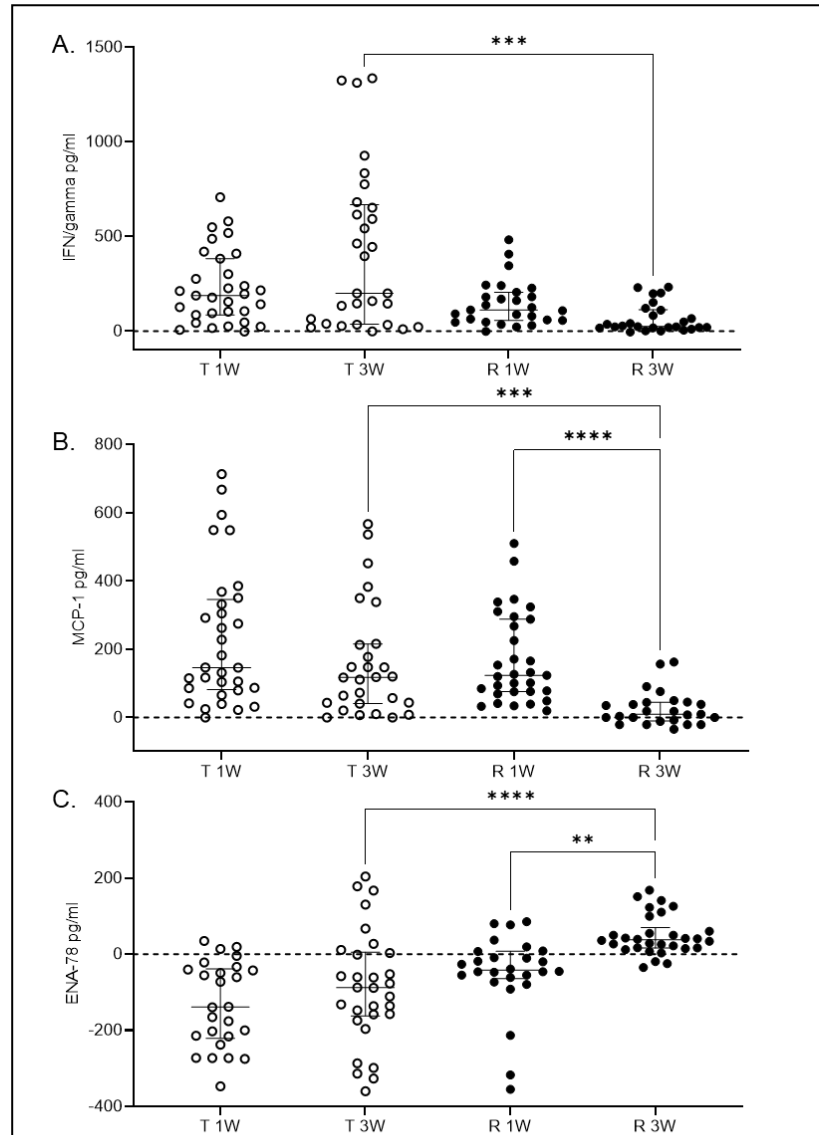


Figure 24: Tolerant lines have more IFN- γ and MCP-1, but less ENA-78 at 3 weeks post-infection than resistant lines.

The differences between infected and uninfected levels of A. IFN- γ , B. MCP-1, C. ENA-78 in tolerant and resistant lines. Dots represent individual mice and lines represent medians and interquartile ranges. Outliers were removed. (* $P < 0.05$, ** $P < 0.01$, *** $P < 0.001$, **** $P < 0.0001$).

Table 11: 36 Infected Cytokines taken at necropsy time minus uninfected mean for respective line.
Includes 18 CC lines. Mean and standard deviation shown.

Cytokine	CC001		CC002		CC003		CC006		CC011		CC015		CC017		CC024		CC038	
	Mean	SD	Mean	SD	Mean	SD	Mean	SD	Mean	SD	Mean	SD	Mean	SD	Mean	SD	Mean	SD
ENA-78(LUX)	703.14	894.17	62.42	376.53	-26.46	82.40	-835.05	79.06	66.05	233.61	-7.31	6.47	-141.42	45.90	17.90	46.82	82.66	78.48
Eotaxin	-429.80	132.55	1992.77	3140.69	-836.91	250.86	-364.91	347.13	-157.88	264.74	27.86	274.92	-406.18	206.44	-225.24	240.01	2777.71	1089.23
G-CSF/CSF-3	900.70	1425.15	155.21	76.14	263.68	971.85	66.12	65.95	173.57	284.04	-3.95	9.39	56.46	65.40	175.99	383.00	47.29	57.94
GM-CSF	5.29	4.16	14.42	20.85	16.83	5.73	3.54	5.51	1.29	1.66	0.00	0.00	1.01	1.68	19.33	41.93	-0.02	0.00
Gro-alpha/KC	16.45	15.30	76.95	78.92	73.50	61.74	37.72	34.73	-7.27	8.03	2.75	13.75	29.85	23.68	101.84	235.08	47.80	40.59
IFN-alpha	0.00	0.00	0.00	0.00	0.00	0.00	0.00	0.00	0.00	0.00	0.00	0.00	0.00	0.00	13.21	32.37	0.00	0.00
IFN-gamma	357.82	404.33	1091.99	1267.60	719.78	643.72	520.67	753.94	210.96	281.48	18.68	9.40	431.98	352.49	535.45	1058.64	463.37	656.13
IL-1alpha	302.04	319.72	9.37	4.31	29.63	5.74	14.87	16.34	25.70	44.54	1.16	1.92	3.90	3.82	8.06	4.27	2.87	5.63
IL-1beta	6.88	9.87	20.13	22.71	21.86	13.24	6.30	5.13	1.91	1.70	0.05	0.69	5.09	2.26	9.67	19.35	15.08	18.49
IL-10	41.14	37.05	145.13	225.06	81.75	89.97	17.28	42.32	34.31	55.36	0.00	0.00	1.34	3.55	780.88	1902.57	0.00	0.00
IL-12p70	0.54	1.13	3.22	2.89	5.08	3.10	1.09	4.31	-1.17	0.20	0.00	0.00	0.35	0.69	96.25	231.61	-0.45	0.00
IL-13	0.78	1.14	-0.24	0.12	5.51	3.29	1.30	2.90	0.00	0.00	0.00	0.00	0.03	0.07	0.86	1.64	0.00	0.00
IL-15/IL-15R	71.05	60.18	27.22	23.65	39.18	12.64	17.34	24.64	14.29	16.26	0.00	0.00	4.71	4.91	91.23	205.19	9.40	13.29
IL-17A	5.55	10.02	51.04	76.86	14.17	7.13	4.82	5.62	1.24	2.39	1.34	3.29	3.14	1.77	13.78	24.25	57.81	56.94
IL-18	869.73	1312.55	4410.18	4993.27	2159.03	509.21	956.05	980.38	343.78	472.12	95.78	147.87	1083.56	472.67	1832.44	3444.17	4428.08	3057.75
IL-2	4.66	5.99	11.73	11.04	11.61	4.77	2.28	2.48	0.43	1.30	0.00	0.00	1.06	1.98	28.77	66.29	0.00	0.00
IL-22	42.22	31.23	506.50	574.20	1157.32	2132.19	114.82	114.79	36.09	28.43	6.23	16.92	38.34	26.08	2681.52	6357.50	474.29	473.07
IL-23	24.09	37.25	180.45	197.91	109.13	87.17	73.51	64.97	17.28	26.07	0.41	22.00	4.62	20.09	5998.00	14559.21	92.75	89.72
IL-27	19.90	13.25	36.08	44.28	53.58	29.93	12.61	15.82	11.50	11.62	4.23	6.66	21.64	14.67	13.43	10.22	24.87	50.54
IL-28	3550.05	3229.69	590.24	418.13	510.02	195.45	130.64	176.40	217.13	365.26	3.16	44.59	-36.85	43.47	813.05	1714.27	149.39	297.11
IL-3	93.63	108.74	13.45	8.28	20.63	15.33	10.71	10.28	7.59	9.95	-0.92	2.51	2.94	2.25	179.73	427.10	-0.65	4.41
IL-31	551.02	515.09	31.51	45.26	102.46	45.01	23.32	31.04	17.11	31.59	5.22	5.85	4.49	5.36	70.26	126.58	9.72	17.21
IL-4	1.21	1.23	6.63	11.30	3.75	1.41	1.53	1.10	0.30	0.76	0.23	0.68	1.18	0.60	0.74	0.68	3.17	4.41
IL-5	-7.67	5.03	6.02	30.66	10.46	9.61	9.96	8.54	-14.84	14.52	-1.11	6.47	9.39	4.56	38.82	102.01	4.95	13.05
IL-6	164.42	125.94	370.16	349.49	1124.19	1482.20	188.19	323.42	67.37	54.00	4.73	8.42	141.92	104.59	748.09	1650.35	144.63	167.78
IL-9	51.19	120.94	275.97	298.62	258.65	176.55	18.77	65.30	32.42	54.96	13.27	33.22	143.81	50.94	128.74	121.92	186.88	319.33
IP-10	125.33	122.04	342.83	347.63	193.80	146.44	75.30	99.37	34.03	19.54	33.06	42.71	124.96	85.60	68.08	74.66	888.06	1195.15
LIF	4.81	21.11	0.07	4.51	30.52	17.92	11.13	18.96	-0.31	2.99	-4.56	0.00	0.72	1.65	9.88	8.30	-10.51	0.00
MCP-1	46.11	79.34	227.74	246.10	255.40	538.34	45.52	75.79	26.70	85.87	19.37	45.68	314.92	227.45	32.23	63.27	152.63	239.42
MCP-3	114.30	165.83	1431.62	1764.22	237.38	230.15	93.95	189.21	48.05	132.68	2.44	69.27	268.29	151.45	-37.60	111.05	249.94	219.90
M-CSF	0.70	0.53	0.08	0.12	0.54	0.37	0.14	0.24	0.04	0.09	0.00	0.00	0.16	0.19	0.07	0.17	0.00	0.00
MIP-1alpha	1.08	0.86	5.36	5.14	11.58	16.28	0.27	1.88	0.28	0.44	0.00	0.00	1.05	0.66	1.38	1.15	5.88	8.31
MIP-1beta	3.28	2.70	17.97	17.16	50.80	94.30	5.86	5.57	2.97	2.41	1.44	0.90	12.48	7.58	18.69	36.74	57.98	32.13
MIP-2	2.42	11.22	6.67	19.66	10.70	18.06	2.51	5.75	-8.39	3.68	4.32	3.87	10.18	6.33	29.69	6.42	14.05	24.36
RANTES	174.98	68.97	52.95	57.84	214.04	182.02	44.69	84.94	14.95	21.87	4.93	13.54	51.37	43.73	12.92	19.36	142.46	201.85
TNF-alpha	90.89	104.68	158.64	120.40	265.89	175.60	120.62	159.75	18.87	18.40	2.08	3.49	80.73	50.48	57.13	87.20	155.58	195.53

Cytokine	CC041		CC043		CC051		CC053		CC057		CC058		CC072		CC078	
	Mean	SD	Mean	SD	Mean	SD	Mean	SD	Mean	SD	Mean	SD	Mean	SD	Mean	SD
ENA-78(LUX)	-117.75	83.30	-86.83	112.08	-40.27	62.37	-176.54	38.21	22.24	48.73	83.23	69.42	-221.40	184.43	186.06	622.06
Eotaxin	862.10	2635.35	-370.33	344.41	2101.11	3000.02	-329.78	177.18	31.55	530.20	#####	#####	34.65	445.31	4928.28	1784.57
G-CSF/CSF-3	232.39	256.29	36.30	92.02	110.89	62.67	85.48	206.53	61.89	109.54	91.37	65.43	31.82	15.86	124.56	132.29
GM-CSF	12.47	19.46	0.07	1.76	11.57	13.00	2.35	2.68	1.13	2.78	1.71	2.65	7.78	7.06	38.83	53.19
Gro-alpha/KC	41.73	64.67	-4.92	13.55	104.09	121.91	6.17	21.95	15.69	26.60	43.70	34.75	18.29	7.40	193.18	121.49
IFN-alpha	0.00	0.00	0.00	0.00	2.12	5.19	0.00	0.00	0.00	0.00	0.00	0.00	0.00	0.00	0.00	0.00
IFN-gamma	-75.27	646.28	52.08	48.88	220.55	389.09	93.70	94.15	163.78	349.03	200.63	189.15	918.27	476.85	785.67	1162.79
IL-1alpha	7.52	2.94	1.92	3.50	10.73	7.30	4.64	6.48	7.40	7.05	5.47	5.06	12.31	9.41	6.01	5.24
IL-1beta	16.67	20.76	-0.84	0.68	16.28	10.36	2.67	3.99	1.16	2.60	12.80	11.88	10.87	7.40	19.09	15.37
IL-10	13.30	46.19	24.11	40.61	7.14	21.02	132.78	325.25	27.92	68.38	0.00	0.00	59.11	61.52	129.97	273.39
IL-12p70	4.38	9.42	-1.41	0.68	-0.76	5.14	0.10	0.25	-0.70	0.44	0.39	0.95	2.54	2.88	0.00	0.00
IL-13	-0.57	2.76	0.00	0.00	6.04	14.10	0.00	0.00	0.00	0.00	0.00	0.00	0.98	1.28	5.23	7.59
IL-15/IL-15R	11.66	17.12	5.55	6.24	17.16	15.72	9.16	10.68	10.53	24.91	5.02	6.68	26.73	8.56	18.33	24.67
IL-17A	37.67	59.11	-2.80	1.11	34.83	32.45	-0.35	3.11	1.90	3.02	35.17	32.96	10.24	4.10	85.50	54.61
IL-18	3437.57	4363.21	-284.22	262.96	4215.84	2924.68	353.98	722.95	415.63	445.82	#####	#####	2099.13	766.24	6001.05	3122.37
IL-2	4.47	7.03	-0.19	0.12	-0.66	5.88	1.77	2.94	-0.03	0.88	0.07	0.16	5.74	3.82	7.99	17.87
IL-22	531.13	639.44	14.36	30.96	450.38	366.53	18.87	29.89	20.45	40.17	495.40	434.08	157.28	45.63	753.57	573.86
IL-23	116.01	85.73	4.28	28.77	240.26	167.40	0.24	44.44	5.28	38.78	112.25	78.76	52.33	52.82	91.98	62.00
IL-27	29.44	28.06	11.82	14.23	95.92	195.43	23.55	16.18	-1.15	29.47	49.81	68.84	21.69	12.30	50.21	32.29
IL-28	362.94	259.88	23.95	59.46	524.11	319.12	-16.07	132.25	131.05	203.60	272.73	235.10	194.05	212.95	133.06	217.82
IL-3	18.98	13.05	2.26	3.73	18.31	15.76	2.38	4.52	8.48	11.06	8.96	7.94	7.66			

Tissue damage is more severe in tolerant lines than in resistant lines.

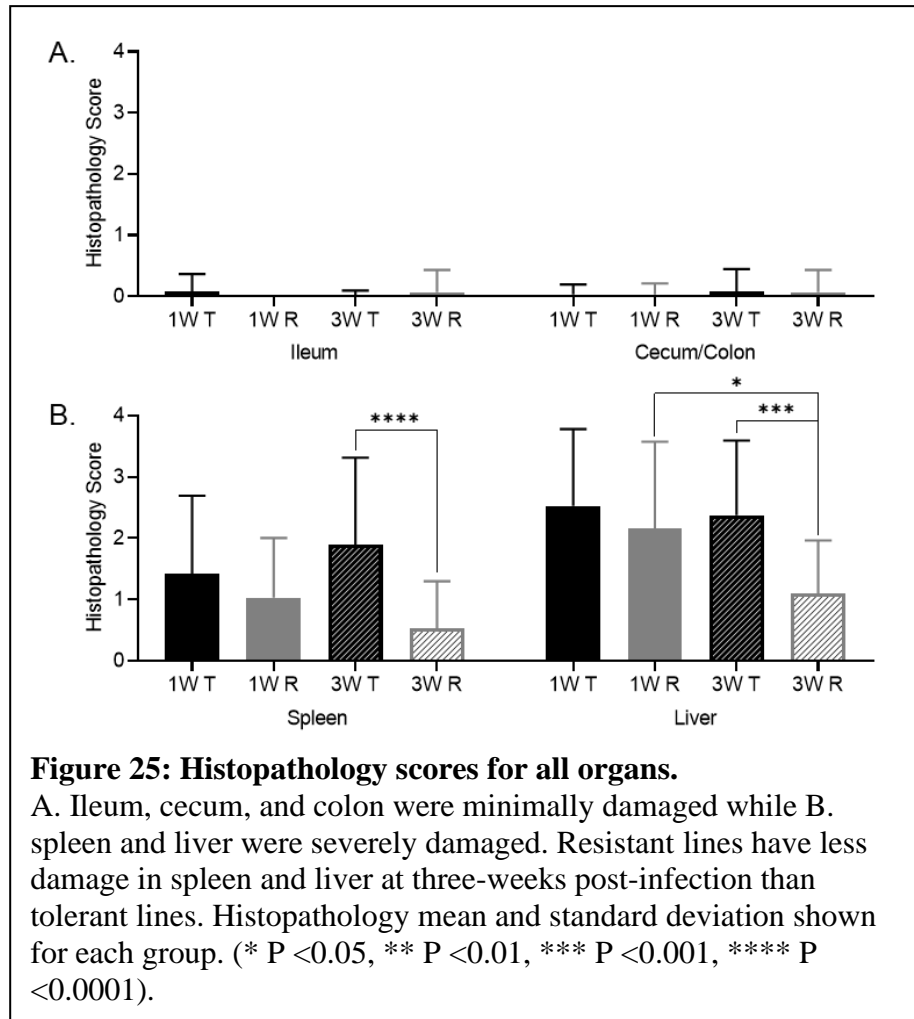
Sections of ileum, cecum, colon, spleen, and liver were stained with H&E and scored by a board-certified pathologist blindly using a scale of 0 to 4 (0 = normal, 4 = severe damage, Table A1 and Fig. A1). Intestinal organs had minimal damage (scores 0-

1) and were excluded from further analysis (Fig. 25A).

Spleen and liver had a

range of damage and were examined further at one and three weeks

post-infection in tolerant and resistant lines only.



When mice were grouped by response to infection, there was no significant difference between tolerant and resistant at one-week for either spleen or liver damage, however at three-weeks post-infection, significant differences were apparent. Tolerant

lines had a mean of 1.89 (\pm 1.43) while resistant lines had a mean of 0.53 (\pm 0.77) for spleen (Fig. 25B, $P = <0.0001$). At three weeks post-infection, damage in the liver was more pronounced in tolerant lines with a mean of 2.38 (\pm 1.22) and a mean of 1.10 (\pm 0.87) for resistant (Fig. 25B, $P = 0.0005$). Liver damage decreased between one and three weeks post-infection in resistant from a mean of 2.15 (\pm 1.42) to 1.10 (\pm 0.87) (Fig. 25B, $P = 0.011$).

Significant and suggestive genetic associations were identified across various phenotypes for three-week STm infections

All 18 CC lines that were infected for three-weeks with STm were included in a quantitative trait association of relevant phenotypes. A significant association was identified for spleen colonization on Chr 3 (*Scq1*), while a suggestive association was identified for liver colonization on Chr 13 (Fig. 26 and Table 12). *Scq1* contains 533 genes, but there were no clear haplotype differences due to the small number of lines in our analysis (Fig 26A, B). The association for liver colonization on Chr 13 contains 20 genes, and NZO has a high haplotype effect and B6 has a low haplotype effect (Fig 26C, D). A haplotype effect means that having a certain haplotype at region is associated with either a positive (high) or negative (low) effect on the phenotype. However, none of the 20 genes in this region had SNP differences across any of the founding CC strains.

To overcome the limitations of small line numbers while exploring what genes distinguish tolerant and resistant lines, all 32 CC lines whose response to infection with STm is known were included in a binary QTL analysis. Resistant lines (CC015, CC024,

CC051, CC057, CC058) were assigned a value of one while the remaining tolerant, delayed susceptible, and susceptible lines were assigned a value of zero. No significant associations were identified, but three suggestive associations were identified on Chr 3, 13, and 17 (Fig. 27 and Table 12). The association on Chr 3 contains 212 genes and had a high haplotype effect (more resistant) for NZO, 129, and WSB (Fig. 27A, B). There were no genes with SNP differences between NZO, 129, and WSB and the remaining CC founder strains. The association on Chr 13 contained 29 genes and had a high haplotype effect (more resistant) for PWK and B6 (Fig. 27A, C). There were no genes that had SNP differences that followed the haplotype effects. The association on Chr 17 contained 64 genes and had a high haplotype effect (more resistant) for PWK, NZO, and CAST (Fig. 27A, D). Only one gene had a SNP difference that corresponded to the haplotype effects.

Tolerance to STm infection was also examined by assigning tolerant lines (CC002, CC017, CC038, CC043, CC072, CC078) a score of one and susceptible and delayed susceptible lines a score of zero. A total of 27 CC lines were included in this analysis because resistant lines were excluded. No significant associations were found, but suggestive associations were found on Chr 2 and Chr 6 (Fig. 28 and Table 12). The association on Chr 2 contained 618 genes and NOD and NZO had a high haplotype effect. Thus, lines that had a NOD or NZO allele at this location were more likely to be tolerant to STm infections (Fig. 28A, B). There were no genes in the Chr 2 region that had SNP differences corresponding to haplotype effects. The association on Chr 6 had 751 genes, but no haplotype effects were identified (Fig. 28A, C). While the experiments

examining spleen and liver bacterial burdens did not contain enough lines to identify significant associations, the binary categorizations did not capture enough phenotypic diversity to be significant.

Table 12: QTLs for resistance and tolerance categorization and spleen/liver CFU after STm infections.

18 CC lines were included in spleen and liver colonization QTL, 32 CC lines were in the resistance QTL, and 27 CC lines were in the tolerance QTL. Ran using gQTL.

QTL name	Phenotype	SNP ID	Chr	LOD	P-value	Proximal (Mb)	Max (Mb)	Distal (Mb)	Haplotype Effect
	Resistance	UNC5787203	3	8.440316676	2.07E-06	95.337641	95.941154	100.13873	high: NZO, 129, WSB
	Resistance	UNC22954569	13	9.372510013	3.10E-07	81.534966	81.874475	83.810408	high: B6, PWK
	Resistance	UNC28565037	17	6.85483751	4.88E-05	86.907259	88.969496	90.806468	high: PWK, NZO, CAST
	Tolerance	JAX00511029	2	7.896238979	6.19E-06	159.046383	168.267076	181.435941	high NOD, NZO
	Tolerance	UNC12344672	6	6.53383592	9.14E-05	114.366484	147.330979	147.373575	
Scq1	Spleen Colonization	UNC5768062	3	9.643123956	1.78E-07	79.587437	93.367756	95.953161	
	Liver Colonization	JAX00364751	13	7.279721297	2.11E-05	81.827562	83.661598	83.796286	high: NZO, low: B6

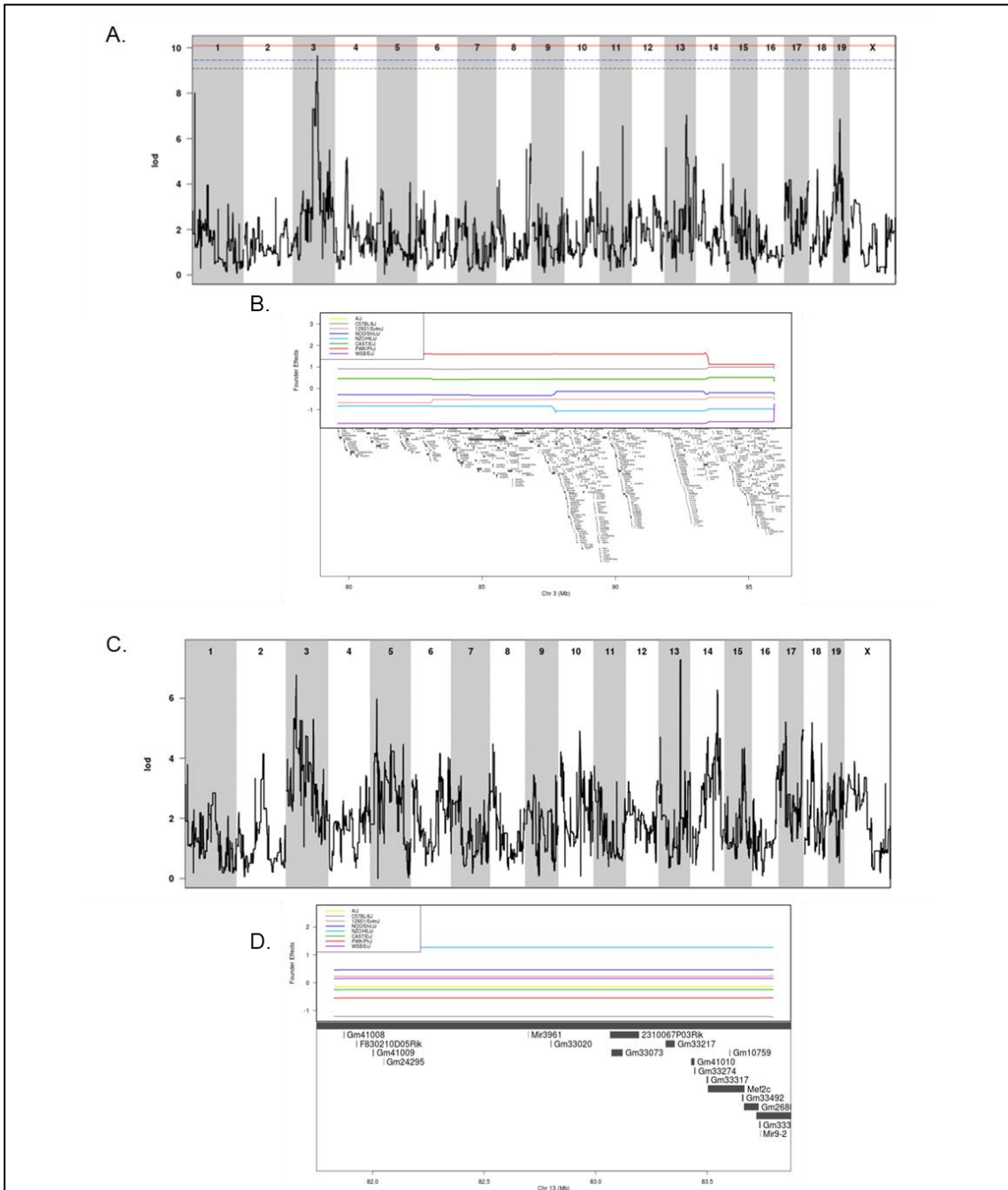


Figure 26: QTLs for CFU for 18 CC lines.

A. QTL of spleen CFU at three weeks post-infection and B. allele effect plots zoomed in on Chr 3. C. QTL of liver CFU at three weeks post-infection and D. allele effect plots zoomed in on Chr 13. Green line is 85% significant, blue line is 90% significant, red line is 95% significant. Results obtained from gQTL.

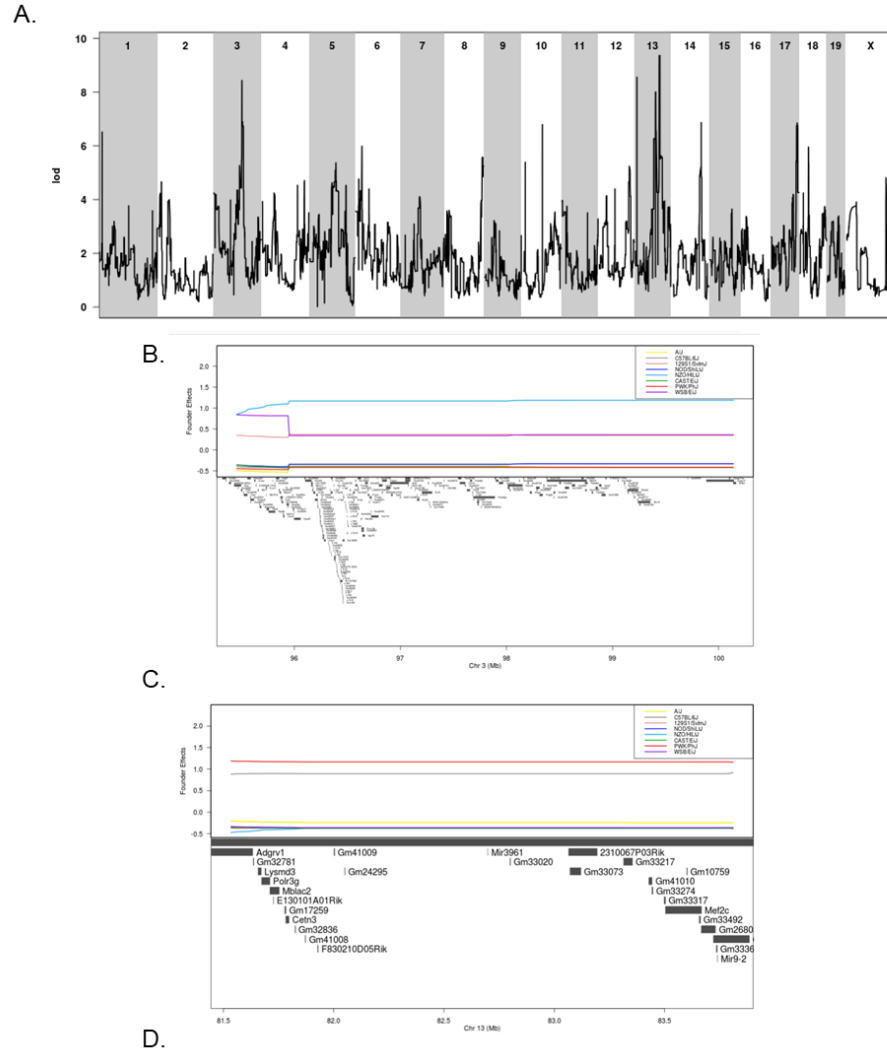
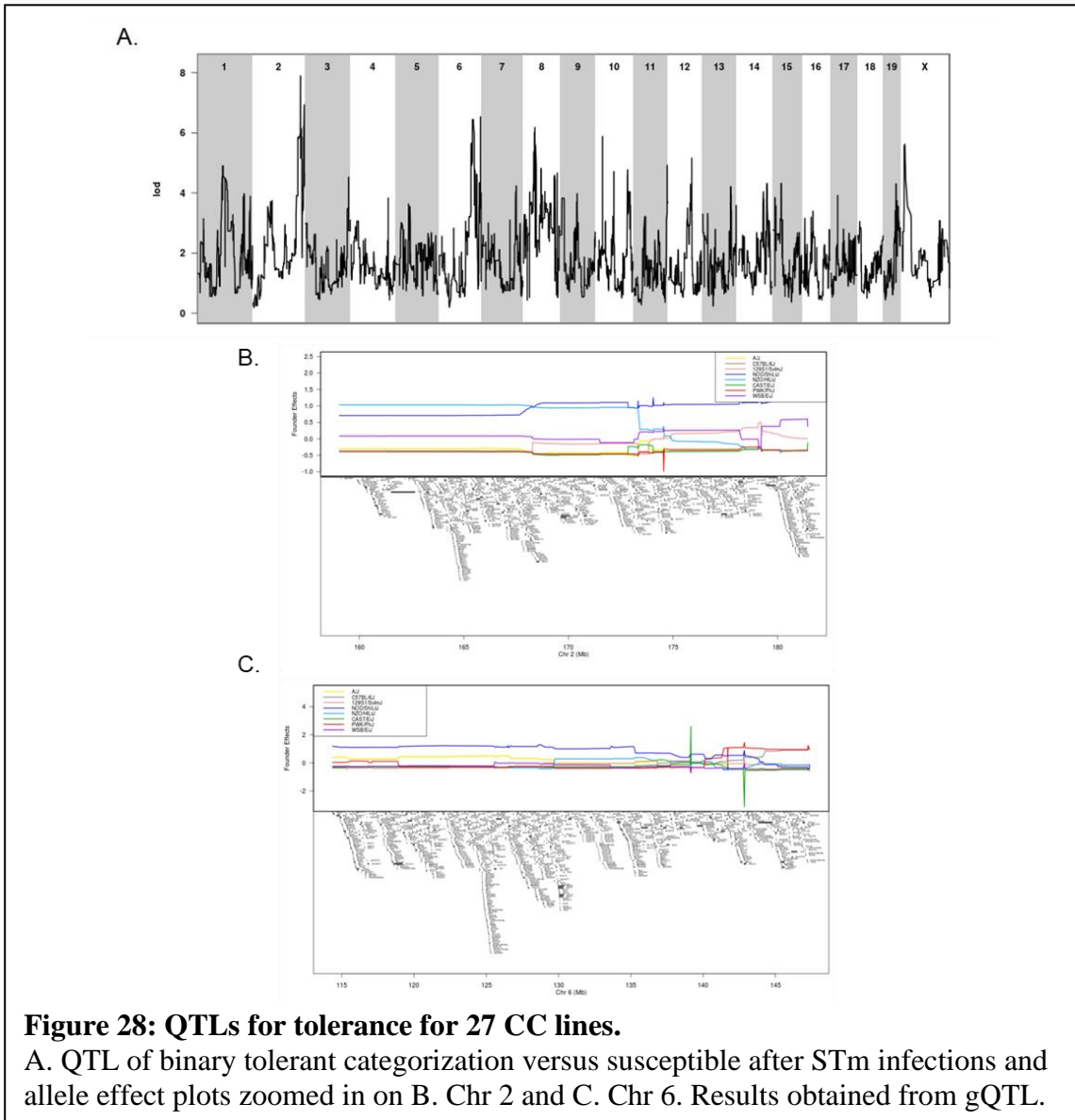


Figure 27: QTLs for resistances for 32 CC lines.

A. QTL of binary resistant categorization versus everything after STm infections and allele effect plots zoomed in on B. Chr 3, C. Chr 13, and D. Chr 17. Results obtained from gQTL.

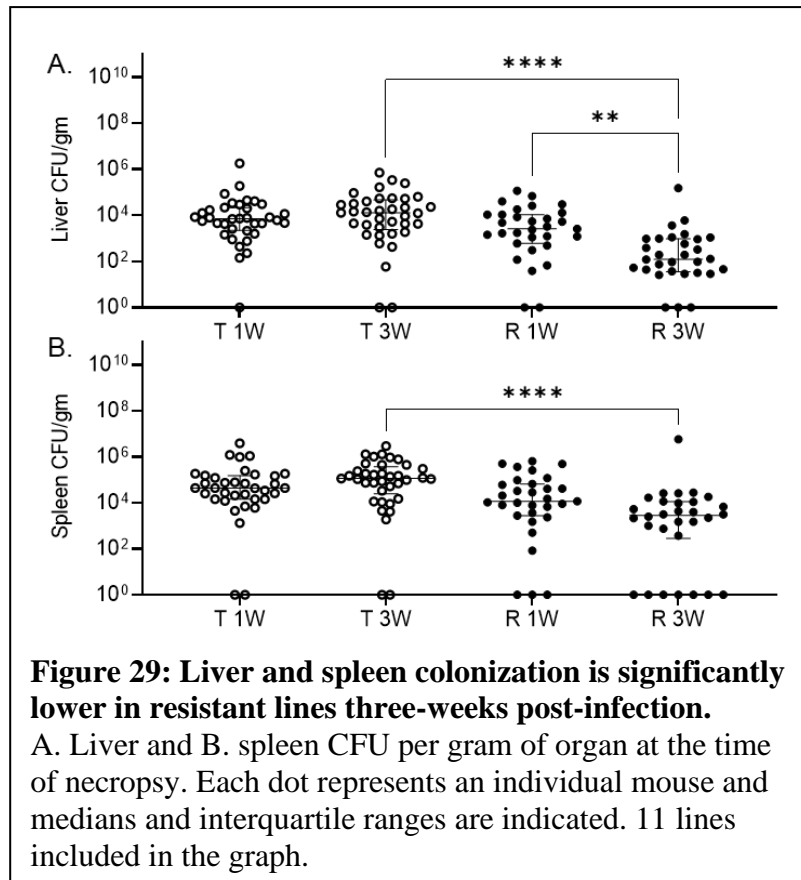


Discussion

To differentiate host disease phenotypes more finely after STm infection and identify potential mechanisms, we infected 18 lines of CC mice that survive acute infection for a longer three-week infection. Bacterial burden was indistinguishable between these lines at one-week post-infection, so differentiating tolerant and resistant phenotypes required a longer infection period (47, 72).

We found that seven of these 18 lines that survived acute infections did not survive the three-week infections and thus had a survival phenotype we termed “delayed susceptible”. Six of the remaining lines fit the criteria for tolerance, because they survived infection at a bacterial burden that caused serious systemic infection in delayed susceptible lines.

Resistant lines were colonized in both liver and spleen, at very low levels compared to their tolerant counterparts, suggesting that they are clearing the infection. When all resistant lines were grouped, they had a median of 1.26×10^2 CFU/g in liver and 2.82



$\times 10^3$ CFU/g in spleen at three weeks, significantly less than tolerant lines that had a median of 1.29×10^4 CFU/g in liver and 1.13×10^5 CFU/g in spleen (Fig. 29, both $P = <0.0001$).

While infection of spleen and liver are hallmarks of the systemic phase of STm infection, STm initially passes through the intestine and reticuloendothelial (RE) system including PP and MLN. While the bacterial load in the intestinal organs was not significantly different between the groups, we found that PP and MLN colonization were different. Long-term STm colonization in mice is linked to the persistence of infection in the RE system, particularly in the MLN (103). Tolerant lines, defined by persistently higher bacterial load, had significantly more STm in their MLN, spleen, and liver than resistant lines, supporting a role for the RE system in long-term colonization.

Pre-infection body temperatures differ between surviving lines and susceptible lines in acute (one week) STm infections. Surviving lines had cooler pre-infection baseline temperature by ~ 0.3 °C across their resting period, active period, and full 24-hour period. In our current work, tolerant lines had the lowest body temperatures across all three time periods compared to resistant and delayed susceptible lines. Tolerant lines also had cooler body temperatures when compared to susceptible lines from acute infections by ~ 0.5 °C. Since tolerance is focused on minimizing damage done by both the pathogen and the host's own immune response, this lower baseline temperature may be protective from damage caused by high fevers post-infection (93). Resistant mice and delayed susceptible mice appear to be better positioned to mount a full fever response that helps resistant mice survive but may contribute to the delayed susceptible mice

succumbing to disease. Baseline body temperature differences are independent of activity level.

Time to disrupted circadian patterns for body temperature were different between resistant and tolerant lines. Resistant lines maintained body temperature circadian patterns for > one day longer than tolerant lines, yet both groups survived equally. Thus, tolerant lines survive despite showing disease symptoms (104). Detection of circadian pattern disruption was also compared between temperature and activity for each phenotypic group. Disruption of temperature patterns was a more sensitive predictor of disease onset for tolerant and delayed susceptible lines, but not for resistant lines. Both groups maintained activity patterns over a day longer than temperature pattern, showing that changes in temperature patterns are more sensitive measure of illness than activity.

Immune differences were also apparent between tolerant and resistant lines. Tolerant lines had a larger rise in white blood cell count driven by a significantly higher increase in neutrophils than resistant lines after infection with STm. Neutrophils are part of the innate immune system and are vital to early control of infections (25). Since resistant lines appear to have started clearing the infection, the lower bacterial count may decrease the need for large numbers of neutrophils, or resistant mice may have more efficiently infiltrated tissues with neutrophils, thus lowering their circulating number. Histopathology showed a large number of polymorphonuclear infiltrates, which include neutrophils, in both spleen and liver, supporting this.

Cytokines are another component of the immune system that we explored. We discovered 3 cytokines that were significantly different between tolerant and resistant

lines. IFN- γ was increased in both resistant and tolerant lines, but tolerant lines had a much larger increase after infection. IFN- γ keeps STm at a manageable level for the host, and neutralizing IFN- γ causes STm to replicate more rapidly resulting in severe infection (103). Since tolerant lines have such a high level of IFN- γ , this likely contributes to controlling their bacterial burden and perhaps their disease symptoms. MCP-1 was also reduced in resistant mice relative to their tolerant counterparts. Since STm resides and replicates in monocytes, high levels of MCP-1 may not be protective (105). High levels of MCP-1 have been linked to more severe organ damage/failure, higher levels of septic shock, and higher mortality (106, 107). Finally, ENA-78, which was increased in resistant mice and decreased in tolerant mice, is a neutrophil chemoattractant (34). Tolerant lines have a significantly higher number of circulating neutrophils than resistant lines, despite having less circulating ENA-78. Hepatocytes secrete ENA-78 in response to bacterial invasion or tissue damage (108). Hepatocytes in resistant lines could be attempting to recruit more neutrophils in order to clear residual STm in the liver (108). Alternatively, tolerant lines could be manipulating their immune response to limit neutrophil mediated tissue damage. Further experiments are required to distinguish between these and other possibilities.

Tissue damage in spleen and liver was also reduced in resistant mice at three-weeks post-infection relative to one week post-infection. Tolerant mice did not repair tissue damage between one- and three-weeks post-infection. Resistant mice appeared able to repair tissue damage by three weeks post-infection. Interestingly, tissue repair has been linked to tolerance for other pathogens, yet we did not observe this (48, 75).

However, tolerant mice appeared to have similar tissue damage at one week versus three weeks post-infection, suggesting that these mice may be actively preventing worsening tissue damage. Alternatively, tolerance to STm infections could rely more on modulating the immune system through cytokine and WBC changes instead of tissue damage repair, since we see changes in these parameters (71, 75).

QTL analysis was also used to examine resistance, tolerance, and spleen and liver STm colonization. While one significant and six suggestive associations were found, the small number of CC lines used and the lack of normal distribution of data did not yet allow us to identify the individual genes responsible for these associations (109). In future work, RNA seq gene expression data will be used to pinpoint candidate genes underlying the QTL associations we have identified.

Materials/Methods

Bacterial strains and media

The *Salmonella enterica* ser. Typhimurium strain (HA420) used for this study was derived from ATCC14028. HA420 is a fully virulent, spontaneous nalidixic acid resistant derivative of ATCC14028 (100). Strains were routinely cultured in Luria-Bertani (LB) broth and plates, supplemented with antibiotics when needed at 50 mg/L nalidixic acid (Nal).

For murine infections, strains were grown aerobically at 37°C to stationary phase in LB broth with nalidixic acid and diluted to generate an inoculum of $2-5 \times 10^7$

organisms in 100 microliters. Bacterial cultures used as inoculum were serially diluted and plated to enumerate colony forming units (CFU) to determine the exact titer.

Murine Strains

Collaborative cross (CC) mice were used in these experiments. Most animals were bred and maintained (on 2919 chow or 4% based on strain requirements) in the Division of Comparative Medicine at Texas A&M University. CC045 mice were obtained from UNC Collaborative Cross Core. Our experiments utilized 18 lines of CC mice, 3 females and 3 males per line for a total of 112 mice (CC045 only had 2 females due to an experimental complication) (Table 13). All animal experiments were conducted in accordance with the Guide for the Care and Use of Laboratory Animals, and with the TAMU IACUC (AUP# 2018-0488 D and 2015-0315 D).

Table 13: Number of mice used and facility origin for 18 CC lines.

Strain	Male	Female	Origin
CC001	3	3	TAMU
CC002	3	3	TAMU
CC003	3	3	TAMU
CC006	3	3	TAMU
CC011	6	3	TAMU
CC015	3	3	TAMU
CC017	3	4	TAMU
CC024	3	3	TAMU
CC038	3	3	TAMU
CC041	4	3	TAMU
CC043	3	3	TAMU
CC045	3	2	UNC
CC051	3	3	TAMU
CC053	3	3	TAMU
CC057	3	3	TAMU
CC058	3	3	TAMU
CC072	3	3	TAMU
CC078	3	3	TAMU

Placement of Telemetry Devices

5 to 9-week-old mice (CC) were anesthetized with isoflurane anesthesia. The abdomen was opened with a midline abdominal incision (up to 2 cm). Starr life science G2 E-mitter devices were loosely sutured to the ventral abdominal wall. The abdominal

muscle layer was closed with 5-0 vicryl, and the skin layer was closed using stainless steel wound clips (FST 9mm). Animals were given an intraperitoneal injection of Buprenorphine (0.0001 mg/g) for pain prior to recovery from anesthesia, and every 8 hours thereafter as necessary for pain control. After recovery from anesthesia, implanted mice were group-housed and monitored twice daily for pain and wound closure for 7 days post-surgery, when the clips were removed. Any animals found to have serious complications after surgery were humanely euthanized.

Infection with *Salmonella* Typhimurium

After 7 days of acclimation in the BSL-2 facility, 8 to 12-week-old implanted CC mice were weighed and infected by gavage with a dose of $2-5 \times 10^7$ CFU of *S. Typhimurium* HA420 in 100 microliters of LB broth. Infected mice were monitored twice daily for signs of disease and activity by visual inspection. When telemetry data and health condition data suggested the development of clinical disease from infection, mice were humanely euthanized. If animals remained clinically healthy throughout the duration of the experiment, they were humanely euthanized at 21 days post-infection.

Bacterial load determination

Mice were humanely euthanized, and the spleen, liver, ileum, cecum, colon, Peyer's patches, and mesenteric lymph nodes were collected. A third of each organ was collected in 3 mL of ice-cold PBS, weighed, homogenized, serially diluted in 1X PBS, and plated on Nal plates for enumeration of *S. Typhimurium* in each organ. Peyer's patches and mesenteric lymph nodes were collected whole. Data are expressed as CFU/g of tissue.

Telemetry Monitoring

Prior to placing implanted mice on telemetry platforms, mice were moved into individual cages and provided with a cardboard hut and bedding material. Individual cages containing implanted, uninfected mice were placed onto ER4000 receiver platforms, and the collection of body temperature (once per minute), and gross motor activity (continuous measurement summed each minute) data was initiated. Body temperature and gross motor activity data was collected for 7 days from uninfected mice. Mice were removed briefly from the receiver platforms for infection and then were placed back on the platforms and data collection was resumed. Infected animals were continuously monitored by telemetry in addition to twice daily visual monitoring.

Identification of deviation from circadian pattern of body temperature

Additional clinical information, such as the time of inoculation relative to the start of the experiment (denoted T), was used in centering time series for comparison between mice (typically, seven days after the beginning of monitoring). Quantitative detection of deviation from the baseline “off-pattern,” using temperature data was calculated on an individual basis. A temperature time series was filtered, a definition of healthy variation was defined, then the time of first “off-pattern” was calculated using that definition on post-inoculation data.

Each mouse time series was pre-processed using a moving median filter with a one-day window. For a specific minute t , the median collection of temperature values from $[t-720, t+720]$ was used in calculating a median for the value t . After this processing, healthy variation was defined as any temperature falling within the range of

minimum to maximum values during the pre-inoculation phase [T-5760,T] (5760 minutes=4 days. This choice allowed for enough data to account for natural inter-day variation due to potential factors such as inter-line variation, epigenetic differences, and sex differences, while avoiding bias due to observed acclimation time after transfer to a new facility in some mice in the first few days of observation (Fig. A2 A).

Identifying post-inoculation off-pattern behavior was done by identifying temperature values that fall outside the interval of healthy variation. The post-inoculation interval ranges from [T+60,T+10080] (7 days), where the one-hour gap was used to avoid false positive detection due to the physical disturbance associated with inoculation (Fig. A2 A).

Detection of deviation from circadian pattern of activity

While activity data does exhibit circadian patterns, this data necessitated a different approach to preprocessing because activity values are inherently non-negative and have a modal value of zero. Hence, we approached the analysis of activity data from the perspective of determining the parameters of a stochastic process. For a time interval t , we worked from the assumption that the number of activity values observed to be i obey the following distribution:

$$\ln(p(A(t) = i)) = \alpha + \beta i$$

where the coefficient β , expected to be negative, corresponds to the modeling assumption that the relative drop in observed activity counts ought to decay (note $0 < e^{\beta} < 1$ if β is negative). For instance, if the value of $\beta = -0.693$, so that $e^{\beta} \approx 1/2$, this would represent the assumption that there are half as many activity values observed to be

1 (one movement per minute) than 2 (two movements per minute). In actuality, this decay coefficient is typically observed as $\beta \approx -0.025$ to $\beta \approx -0.015$, representing that observed activity values decay by half around every 27-46 values.

This theory is implemented in practice by windowing a mouse's activity time series, creating a binning (empirical distribution) $(i, c(i))$, the performing a log-linear fit by transforming $c(i) \rightarrow \ln(1 + c(i))$ and applying linear least-squares regression to calculate α and β . Statistical models with simpler assumptions stemming from a "memoryless" assumption were attempted but did not see any feasible agreement with observed activity data (Fig. A2 B).

Histopathology

After euthanasia, samples of liver, spleen, ileum, cecum, and colon from each mouse were collected and fixed in 10% neutral buffered formalin at room temperature for 24 hours, stored in 70% ethanol before embedding in paraffin, sectioning at 5 μm , and staining with hematoxylin and eosin (H&E). Histologic sections of all tissues were evaluated in a blinded manner by bright field microscopy and scored on a scale from 0 to 4 for tissue damage by a board-certified veterinary pathologist (Table A1 and Fig. A1). The combined scores of spleens and liver from individual mice were used to calculate the median and interquartile range for each group. Whole slide images of liver and spleen H&E-stained sections were captured as digital files by scanning at 40x using a 3DHistech Panoramic SCAN II FL™ scanner (EpreDia, Kalamazoo, MI). Digital files were processed by Aiforia Hub™ (Aiforia, Cambridge, MA) software for generating the images with 100 μm scale bars.

Complete Blood Count

Whole blood was collected by cheek bleed for complete blood count (CBC) one week prior to surgery for the pre-infection sample. Blood from infected animals was collected at necropsy by cardiac puncture. Blood was collected from additional uninfected control animals by cardiac puncture and median values were used as the baseline for mice that did not serve as their own pre-infection control. All blood was collected into EDTA tubes and analyzed on an Abaxis VetScan HM5.

Cytokine and Chemokine Analysis

Serum was stored at -80°C and thawed on ice immediately prior to cytokine assays. Serum cytokine levels were evaluated using an Invitrogen ProcartaPlex Cytokine/Chemokine Convenience Panel 1A 36 plex kit as per manufacturer instructions (ThermoFisher). Briefly, magnetic beads were added to each well of the 96-well plate and washed on the Bio-Plex Pro Wash Station. 25uL of samples and standards were then added to the plate along with 25uL of universal assay buffer. Plates were shaken at room temperature for 1 hour and washed. 25uL of detection antibody was added and incubated for 30 minutes and washed away, followed by 50uL of SAPE for 30 minutes and washed away. 120uL of reading buffer was added and plates were evaluated using a Bio-Plex 200 (BioRad). Samples and standards were assayed in duplicate, and samples were diluted as needed to get 25ul of serum per duplicate. The kit screens for the following 36 cytokines and chemokines: IFN gamma; IL-12p70; IL-13; IL-1 beta; IL-2; IL-4; IL-5; IL-6; TNF alpha; GM-CSF; IL-18; IL-10; IL-17A; IL-22; IL-23; IL-27; IL-9; GRO alpha; IP-10; MCP-1; MCP-3; MIP-1 alpha; MIP-1 beta; MIP-2; RANTES; Eotaxin;

IFN alpha; IL-15/IL-15R; IL-28; IL-31; IL-1 alpha; IL-3; G-CSF; LIF; ENA-78/CXCL5; M-CSF. Median values of uninfected animals for each line were used as the baseline for that line.

QTL analysis

gQTL, an online resource designed specifically to identify CC QTLs, was used to find putative QTL associations (90). Briefly, median values of each line for various parameters were uploaded to the website and QTL analysis was performed using 1000 permutations with “automatic” transformation. Automatic transformation picks either log or square root transformations, whichever best normalizes the data.

Transcriptomic analysis

Tissues were snap frozen in liquid nitrogen and stored in -80°C freezer until ribonucleic acid (RNA) sequencing could be performed. Spleens were used for host gene expression analysis. All molecular work was performed in the Molecular Genomics Core of the Texas A&M Institute for Genome Sciences and Society (TIGSS). The following protocol is adapted from the Molecular Genomics Core, and TIGSS personnel aided in data acquisition and plot generation. Spleens were homogenized in Trizol and an aliquot was taken for analysis. RNA samples were quantified with a Qubit Fluorometer (Life Technologies) with a broad range RNA assay and concentrations were normalized for library preparation. RNA quality from the spleens was verified on an Agilent TapeStation with a broad range RNA ScreenTape. Total RNA sequencing libraries were prepared using the Illumina TruSeq Stranded mRNA-seq preparation kit. Barcoded libraries were pooled at equimolar concentrations and sequenced on an Illumina

NovaSeq 6000 2x150 S4 flow cell. RNA-seq libraries were trimmed to remove adapter sequences and low-quality bases using TrimGalore version 0.6.6, with Cutadapt version 3.0 and FastQC version 0.11.9. Trimmed reads were mapped with Tophat2 version 2.1.1 to the appropriate pseudogenomes from UNC. Coordinate alignments were converted to the mm10 genome using Lapels version 1.1.1. Differential expression was conducted in R using the DESeq2 package. The resulting gene expression values were uploaded to Ingenuity Pathways (QIAGEN, enlo, Netherlands; www.ingenuity.com Application Build 261899, Content Version 18030641) for biological pathway analysis.

CHAPTER IV

CC045 SURVIVES *SALMONELLA* TYPHIMURIUM INFECTION DESPITE

CARRYING THE SUSCEPTIBLE MUTATION IN *SLC11A1*

Overview

Susceptibility to deadly *Salmonella* Typhimurium (STm) infections has been linked to numerous genes in mice. A mutation in one gene, *Slc11a1* renders mice unable to survive STm infection. However, a Collaborative Cross line, CC045, survives 7 days post-infection despite carrying this *Slc11a1* mutation. To determine how this line survives STm infections, we generated an F2 population with another CC line that carries the *Slc11a1* mutation (CC061) and is susceptible to deadly STm infection. CC061xCC045 F1 mice were infected with STm to determine if the survival phenotype was dominant or recessive. The F1s all survived STm infection, suggesting a dominant mode of inheritance. A majority of the F2s survived infection as well, supporting the hypothesis that the survival phenotype is linked to a dominant allele. The F2s also maintained a high bacterial burden in spleen and liver while maintaining their body weight better than CC061, the parental line. Tail snips were genotyped on miniMUGA and R/qt12 was used to find QTLs using the survival data. Since weight change was a criterion for euthanasia, it was analyzed as a covariate. Four significant associations were found on Chromosomes (Chr) 8, 12, 15, and 19 and a significant allele interaction was identified between Chr 12 and 15.

Introduction

Salmonellae are a group of foodborne pathogens that cause limited to severe disease, depending on the serotype (3, 8, 12). The serotypes are primarily split into typhoidal serotypes that cause typhoid fever and nontyphoidal serotypes that cause either self-limiting gastroenteritis or bacteremia (5, 25). Non-typhoidal serotypes, such as Typhimurium, cause an estimated 93.8 million cases world-wide per year with 155,000 deaths (1, 110). The severity of disease is influenced by several factors including host genetics, health status, co-infections, age, and infecting serotype (2, 4).

Salmonella enterica serotype Typhimurium (STm) causes murine typhoid that models human bacteremia. Some inbred mouse strains survive this systemic infection, while others do not, primarily based on mutations in a single gene: Solute Carrier Family 11 Member 1 (*Slc11a1*, formerly known as natural resistance associated macrophage protein 1 (*Nramp1*)) (20, 111). Mutations in other genes, including neutrophil cytosolic factor 2 (*Ncf2*) and toll-like receptor 4 (*Tlr4*), have also been linked to poor survival outcomes to STm infections, but the *Slc11a1* mutation is the most detrimental to survival (27, 32). *Slc11a1* encodes a metal ion transporter expressed on the surface of macrophages phagosomes. This molecule pumps divalent ions including iron and manganese out of the phagosome, limiting intracellular growth (28). There are two known alleles: the wild type form (*Slc11a1^r*), conferring resistance to systemic STm infection, and a mutant form (*Slc11a1^s*) characterized by a single SNP change that results in an aspartic acid replacing glycine at amino acid position 169 that renders the

protein non-functional, conferring susceptibility to systemic infection with STm (29, 103, 112).

While *Slc11a1* genotype predicts survival after STm infection in traditional inbred mouse strains, we discovered that the CC045 collaborative cross (CC) mouse line survives acute STm infection despite having this mutation (1W paper). The CC are a panel of recombinant inbred lines whose founders capture 90% of genetic diversity in the mouse and recapitulate the diversity found in a human population (37, 40). Of the eight founder strains used to generate this population, only one strain (C57BL/6J) carries the *Slc11a1* mutation and only five CC lines (CC021, CC031, CC042, CC045, CC061) carry this mutation. One of these lines, CC042, is especially susceptible to STm infection due to an additional de novo mutation in the *Itgal* gene that results in extremely high bacterial burden in spleen and liver (65, 66).

CC045 mice survive to day 7 post STm infection with similar bacterial burden in spleen and liver compared to other *Slc11a1* mutant mice, while the other *Slc11a1* mutant mice did not (1w paper). To further understand this phenotype, we characterized bacterial burden, weight change, and baseline and infected white blood cell counts across all five *Slc11a1* CC mutant lines and C57BL/6J mice in one-week infections with STm. We generated a F1 and F2 populations from a cross of CC061 with CC045 (*Slc11a1^s*, but susceptible) to identify genes that reduce susceptibility to STm infection in CC045. F1 offspring survived to day 7 post-infection, lost less weight than CC061, but were colonized to a lower degree in spleen and liver than CC045. These findings suggest that the genetic component responsible for CC045 survival after STm is

dominant. When F2s were infected, we found that most survived day 7 but those surviving mice were more poorly colonized in spleen and liver. Bacterial burden in spleen and liver were weakly correlated with survival time. When R/qt12 was used to analyze the survival time, associations were identified on Chr 8, 12, 15, and 19. Several promising candidate genes were found in these regions that require further investigation to determine their validity.

Results

CC045 survives longer and maintains body weight better than other CC lines carrying the *Slc11a1* mutant allele, despite having similar bacterial burden in spleen and liver.

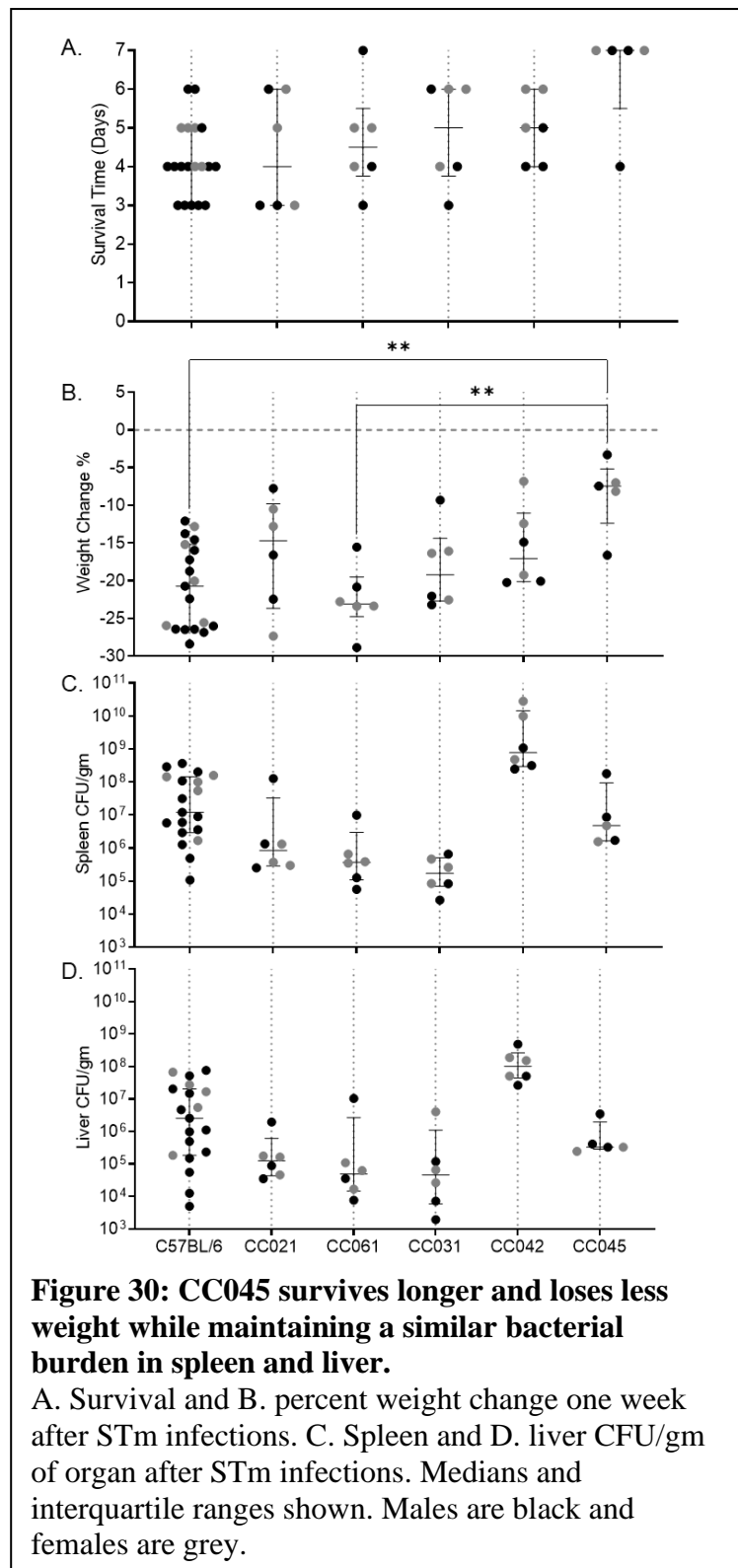
C57BL/6 (B6) and 5 CC lines (CC021, CC031, CC042, CC045, CC061) carry the *Slc11a1* mutant allele. These lines were infected with *S. Typhimurium* (STm) ATCC14028 and monitored over one-week post-infection. B6 survived a median of 4 days, CC021 a median of 4 days, CC031 a median of 5 days, CC042 a median of 5 days, CC061 a median of 4.5 days (Fig. 30A). CC045 was the only line to carry the mutant allele that survived the whole experiment with a median survival of 7 days (Fig. 30A).

Percent weight change during STm infection was also determined. While all lines lost weight, CC045 lost significantly less than B6 and CC061. CC045 lost a median of 7.44%, while B6 lost 20.73%, and CC061 lost 23.08% (Fig. 30B $P = 0.0084$ and 0.0073 , respectively). While CC021, CC031, and CC042 did not lose significantly more

than CC045, all lost a higher median percent (Fig. 30B, 14.70%, 19.21%, 17.08%, $P = 0.5608, 0.2064, >0.9999$).

Since *Slc11a1*

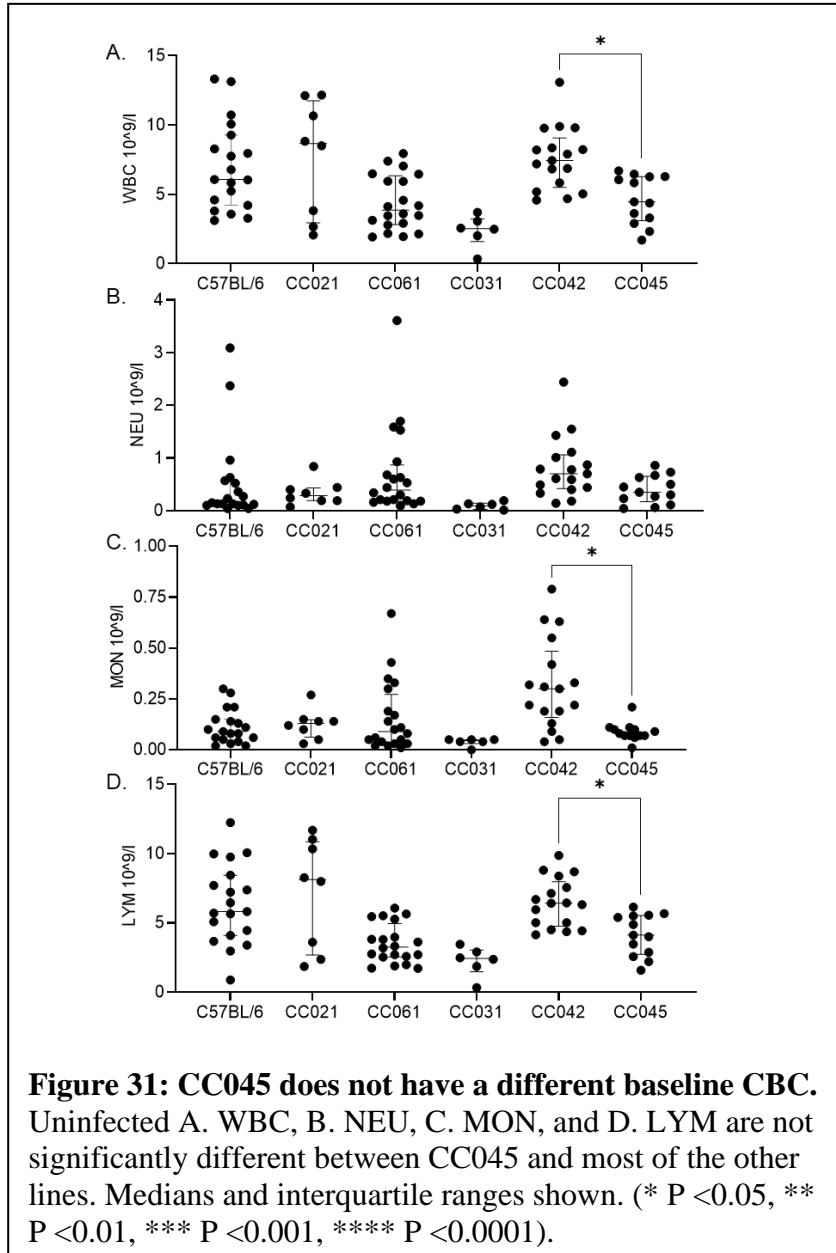
mutations allow uncontrolled intracellular replication of STm, bacterial burden in both spleen and liver was enumerated. In the spleen, B6 had a median CFU of 1.22×10^7 , CC021 had 8.48×10^5 , CC031 had 1.73×10^5 , CC042 had 7.80×10^8 , CC045 had 4.83×10^6 , and CC061 had 3.70×10^5 (Fig. 30C). For liver, B6 had a median CFU of 2.56×10^6 , CC021 had 1.27×10^5 , CC031 had 4.64×10^4 , CC042 had 1.02×10^8 , and CC045 had 3.31×10^5 , and



CC061 had 4.96×10^4 (Fig. 30D). CC045 was not significantly different than any of the other CC lines for bacterial burden in spleen or liver.

Baseline complete blood counts for CC045 do not account for its longer survival time.

Complete blood counts (CBC) were determined on whole blood collected from the submandibular vein of uninfected mice. We focused on total white blood cells (WBC) and the differential counts for neutrophils (NEU), monocytes (MON), and lymphocytes (LYM). All CC lines were compared to CC045 to identify



baseline differences in circulating numbers of these cell types.

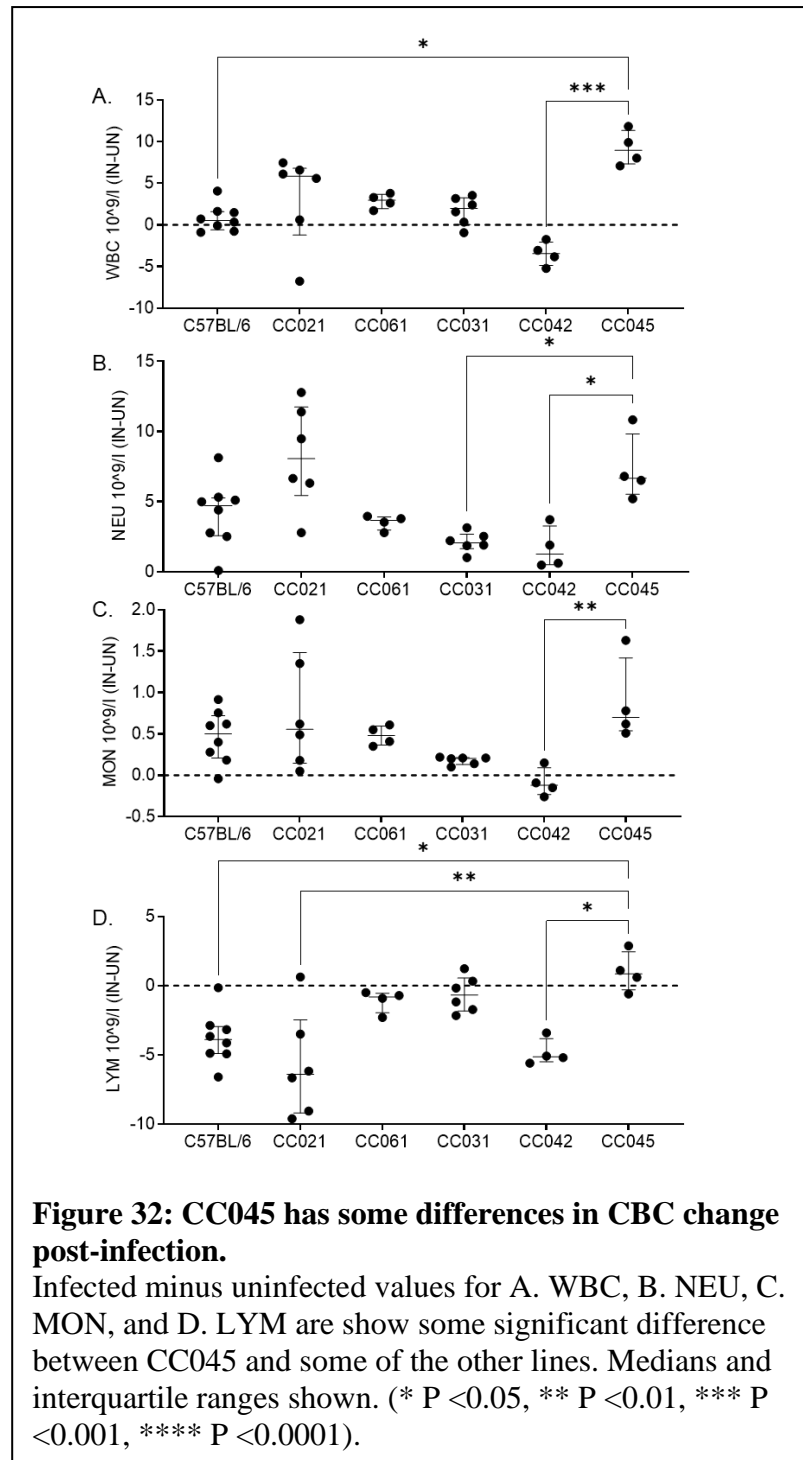
Total circulating WBCs were significantly different between uninfected CC045 and CC042. CC045 mice had a median total WBC count of $4.46 \times 10^9/L$, while CC042 had $7.45 \times 10^9/L$ versus (Fig. 31A, $P = 0.0205$). There were no significant differences between CC045 and any of the other CC lines in circulating neutrophil numbers (Fig. 31B). CC045 mice had significantly fewer circulating monocytes than CC042 with a median of $8.0 \times 10^7/L$ versus $3.0 \times 10^8/L$ (Fig. 31C, $P = 0.0121$), and significantly fewer circulating lymphocytes (a median of $4.12 \times 10^9/L$ versus $6.41 \times 10^9/L$ (Fig. 31D, $P = 0.0467$)). While there were baseline differences between CC045 and CC042, this did not apply to the other *Slc11a1* mutant lines we tested.

Post-infection Complete Blood Counts are different between CC045 and various other *Slc11a1* mutants, but these differences do not explain its survival.

At the time of necropsy, whole blood was collected from a cardiac puncture and the CBC was performed. The difference between post-infection values and pre-infection values was calculated to see how white blood cell counts changed after STm infection. All values were compared to CC045 values to identify significant differences.

The change in circulating WBC was significantly different between B6 and CC042 compared to CC045. B6 increased circulating WBC by $5.3 \times 10^8/L$ and CC042 reduced WBC by $3.44 \times 10^9/L$, while CC045 increased WBC by $8.98 \times 10^9/L$ in response to infection with STm (Fig. 32A, $P = 0.0116$ and 0.0003). Furthermore, CC045 had a

more robust change in circulating neutrophil numbers than CC031 and CC042 (Fig. 32B, $6.67 \times 10^9/L$ versus $2.07 \times 10^9/L$ and $1.27 \times 10^9/L$, $P = 0.0141$ and 0.0197). The number of circulating monocytes was only significantly different between CC045 and CC042. CC045 increased circulating monocyte numbers by a median of $7.0 \times 10^8/L$ while CC042 reduced circulating monocytes numbers by a median of $1.2 \times 10^8/L$ in response to STm



infection (Fig. 32C, $P = 0.0034$). Circulating lymphocyte numbers were significantly different between B6, CC021, and CC042 compared to CC045 in response to infection.

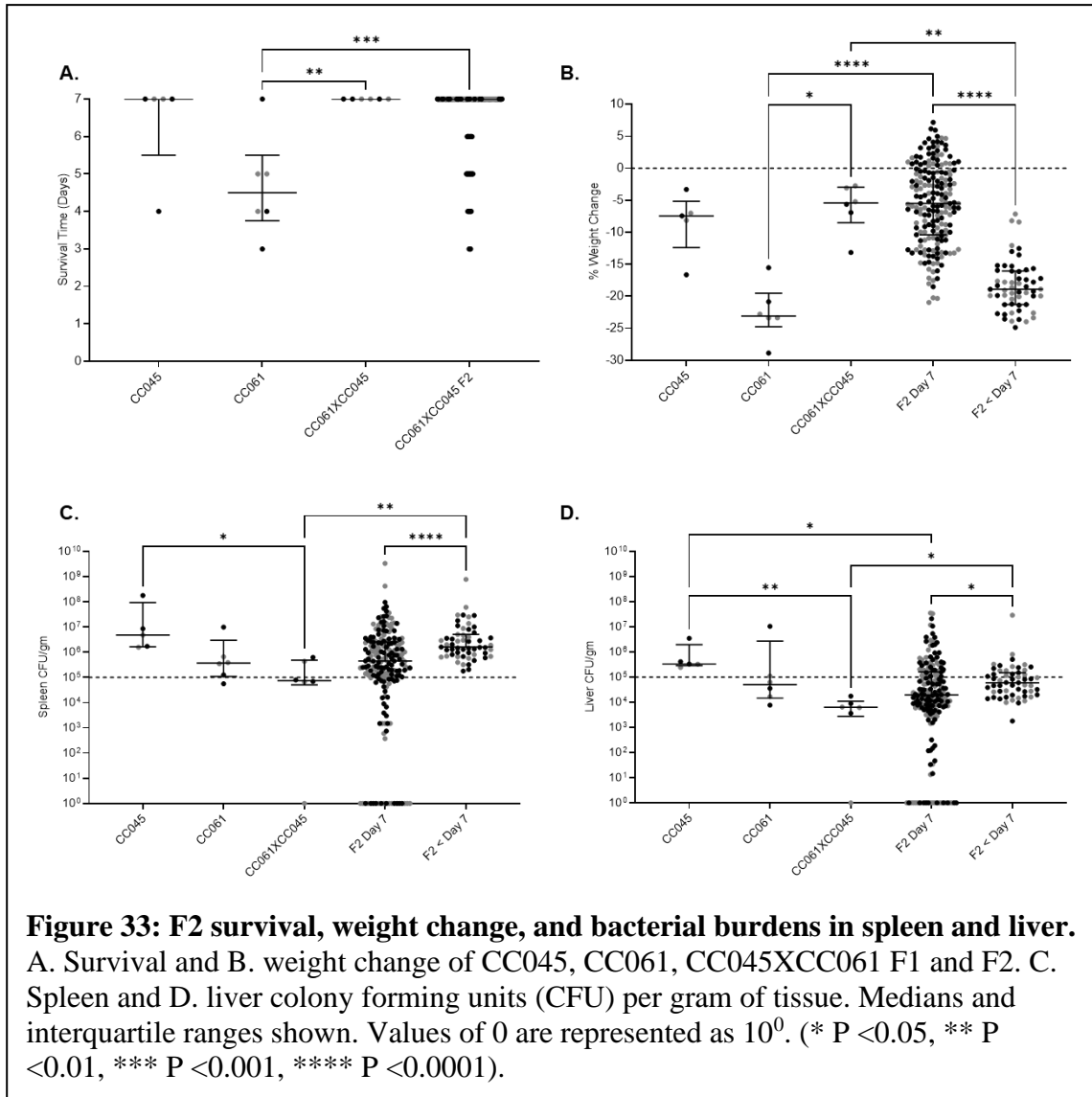
Only CC045 increased circulating lymphocytes numbers by a median of $8.6 \times 10^8/L$, while B6, CC021, and CC042 reduced circulating lymphocytes by medians of $3.89 \times 10^9/L$, $6.41 \times 10^9/L$, and $5.14 \times 10^9/L$, respectively (Fig. 32D, $P = 0.0372$, 0.0067 , and 0.0164). Thus, CC045 had bigger changes in total white blood cell count, neutrophils, monocytes, and lymphocytes than some other *Slc11a1^s* CC lines. However, these changes were not consistent across all *Slc11a1^s* lines tested.

CC061xCC045 F1s are colonized like susceptible CC061 but have longer survival like CC045.

Although bacterial burden in spleen and liver in both CC045 and CC061 was similar (Fig. 30C, D and Fig. 33C, D), CC061xCC045 F1s were less colonized with STm in spleen and liver than the CC045 parental line (Fig. 33C, D, $P = 0.0061$ and 0.0007). The F1s were colonized similar to the CC061s in spleen and liver (Fig. 33C, D, $P = >0.9999$ and 0.2144).

The biggest differences between the parental lines CC045 and CC061 were survival time and weight loss during STm infection. CC045 mice survive a median of 7 days post-infection with STm and only lose a median of 7.44% of their body weight, while CC061 survive a median of 4.5 days and lose a median of 23.08% of their body weight (Fig. 33A, B). F1s resulting from a cross of CC061 and CC045 survived a median of 7 days and lost only 5.42% of their body weight, which is significantly different from CC061 parents ($P = 0.0041$ and 0.0063), but not CC045 parents ($P =$

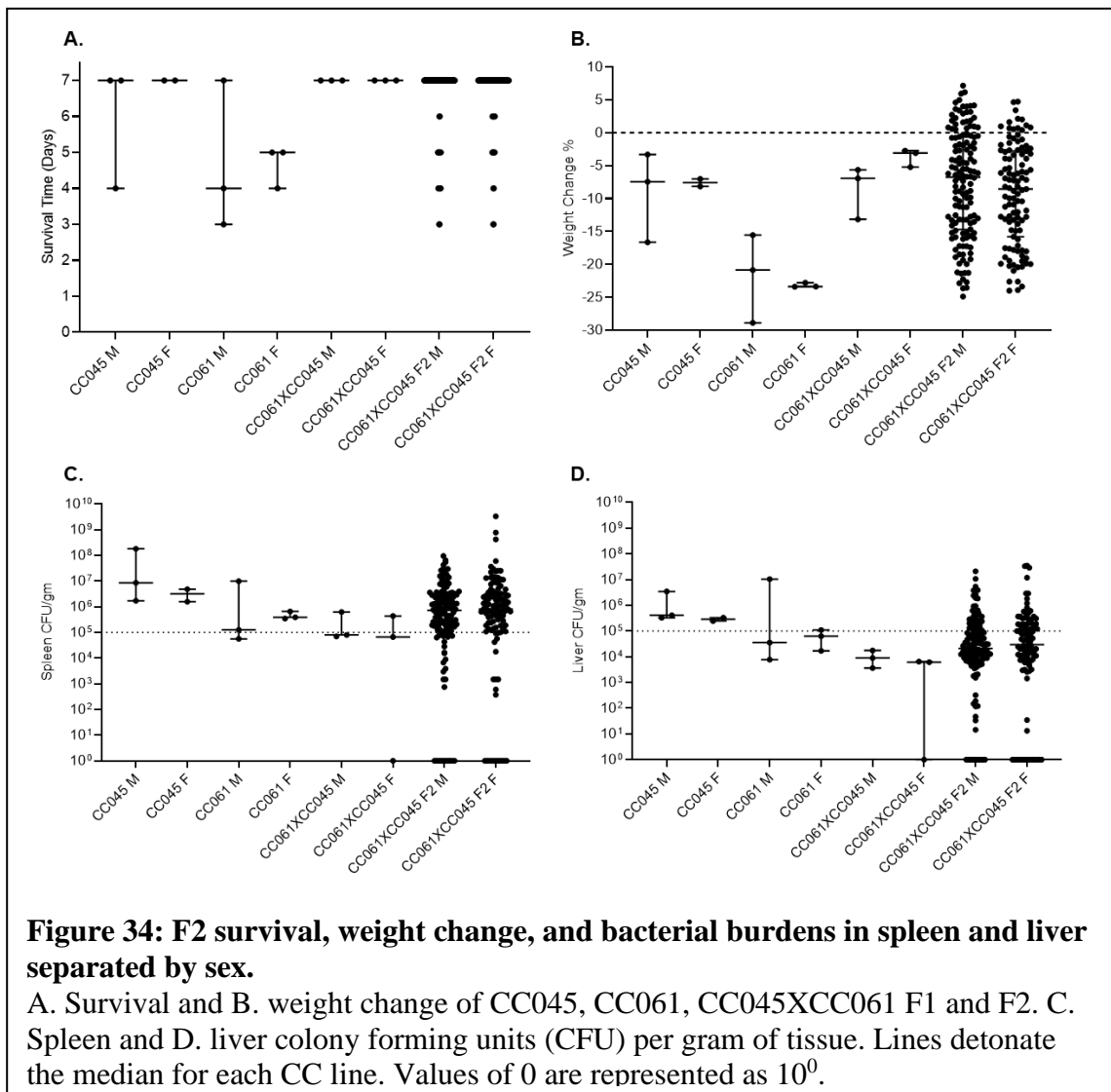
>0.9999 both) (Fig. 33A, B). The F1s survive longer and maintain their body weight similar to CC045 parents but are colonized more poorly than CC045.



CC061xCC045 F2s have two distinct phenotypic groups.

When all F2s are combined, the median survival of the group is 7 days post STm infection. However, 190 F2s survived to day 7 (surviving) and 55 succumbed before day

7 (susceptible), representing two subgroups (Fig. 33A). When the groups are separated by surviving and susceptible, the median survival time for the susceptible group is 5 days, significantly less than the median for surviving mice surviving mice ($P = <0.0001$). The overall median weight loss for all F2s is 9.11%, but the surviving mice lost less weight (median loss of 5.50%) than susceptible mice that have a median loss of 18.91% (Fig. 33B, $P = <0.0001$). Weight loss was also correlated with survival for the



F2s (Fig. 35, $R = 0.65$, $P = <0.0001$). For both survival time and weight loss, there was no sex difference found in any of the groups (Fig. 34A, B)

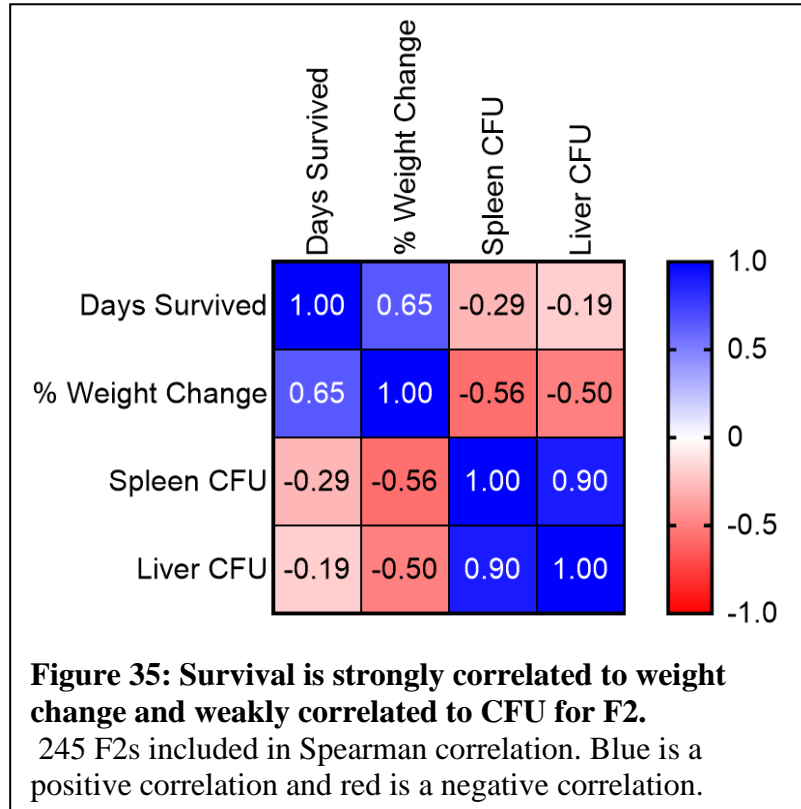
Bacterial burden in spleen and liver are lower in surviving F2 mice than in susceptible mice with a median of 4.50×10^5 compared to 1.62×10^6 for spleen ($P = <0.0001$) and a median of 1.96×10^4 and 6.00×10^4 for liver ($P = 0.0237$) (Fig. 33C, D).

Surviving mice still

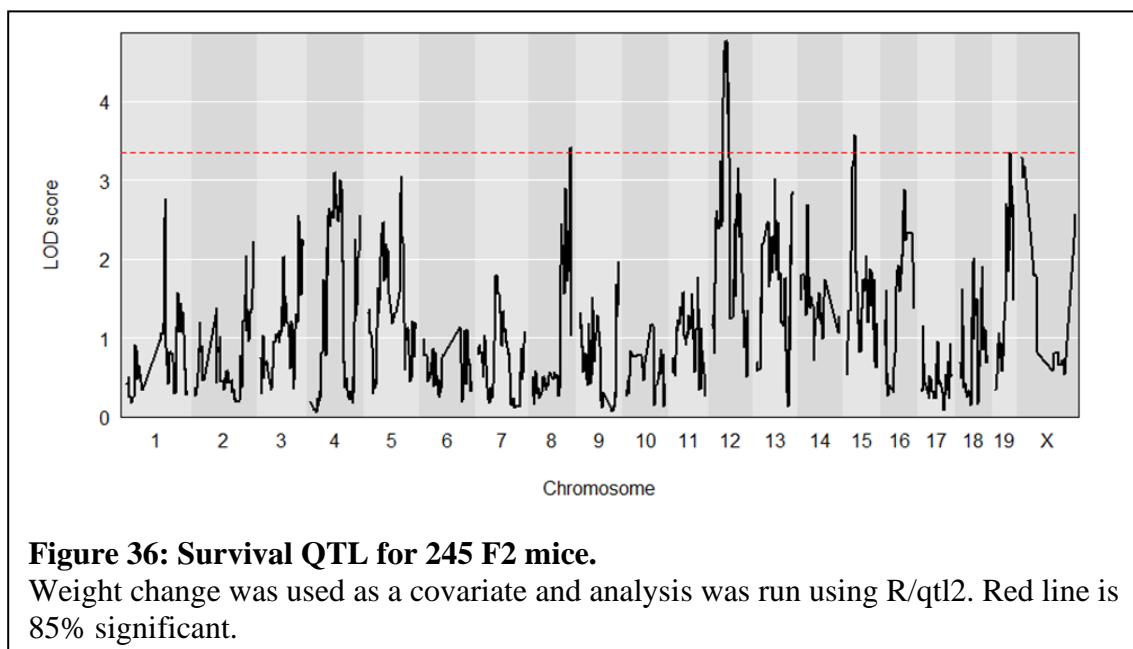
maintain a high bacterial burden. Both spleen and liver colonization were weakly negatively correlated with survival time (Fig. 35, $R = -0.29$, $P = <0.0001$, $R = -0.19$, $P = 0.0024$). For spleen and liver colonization, there was no sex difference found in any of the groups (Fig. 34C, D).

QTL analysis revealed significant associations on Chromosome 8, 12, 15, and 19.

245 F2 mice were infected with STm, of which 190 survived to day 7. Since weight change was highly correlated with survival time and was in fact a cutoff point, it



was included as a covariate. Since we are interested in understanding how some mice are able to survive such high bacterial burdens, 26 mice that did not have any bacterial burden in the spleen or liver were excluded from the analysis. Using R/qt12 (22), survival time with weight as a covariate revealed significant associations on Chromosome (Chr) 8, 12, 15, and 19 (Fig. 36). The association on Chr 12 was the most highly significant. We named the associations in numerical order as *45Stmsq 1*, 2, 3, and 4 (CC045 *Salmonella* Typhimurium survival QTL) (Table 14). For haplotypes, AA corresponded to two CC045 alleles, BB corresponded to two CC061 alleles, and H corresponded to a heterozygous individual with one CC045 and one CC061 allele.



45Stmsq1 is on Chr 8 and contains a total of 3,247 genes and 291 protein coding genes. The most significant SNP is at 123.946966 Mb, where the AA haplotype (CC045) was associated with the highest survival time post-infection (Table 14 and Fig. 37A). *45Stmsq2* is on Chr 12 and contains 531 genes, 27 of which are protein coding. The most

significant SNP is at 43.339731 Mb, where the AB haplotype (heterozygous) was associated with the highest survival time post-infection (Table 14 and Fig. 37B). This data suggests that having one allele at this locus from each parent was better for survival than having two alleles from either parent. *45Stmsq3* is on Chr 15 and contains 444 genes, and of these 22 are protein coding. The most significant SNP is at 33.531940 Mb, with the AB (heterozygous) haplotype associated with the highest survival time post-infection, similar to *45Stmsq2* (Table 14 and Fig. 37C). *45Stmsq4* is on Chr 19 and contains 2,523 genes and 174 are protein coding genes. The most significant SNP is at 48.483409 Mb, where the AA (CC045) haplotype was associated with the best survival time post-infection (Table 14 and Fig. 37D).

Table 14: Significant survival QTL associations for CC061xCC045 F2 mice.

QTL name	Chr	lod	Proximal (Mb)	Max (Mb)	Distal (Mb)	Haplotype Effect
<i>45Stmsq 1</i>	8	3.407321	95.66071	123.947	124.1749	high: AA (CC045)
<i>45Stmsq 2</i>	12	4.772857	37.490793	43.3397	51.84914	high: AB (CC045xCC061)
<i>45Stmsq 3</i>	15	3.573585	26.623276	33.5319	33.65468	high: AB (CC045xCC061)
<i>45Stmsq 4</i>	19	3.357829	38.223373	48.4834	55.39187	high: AA (CC045)

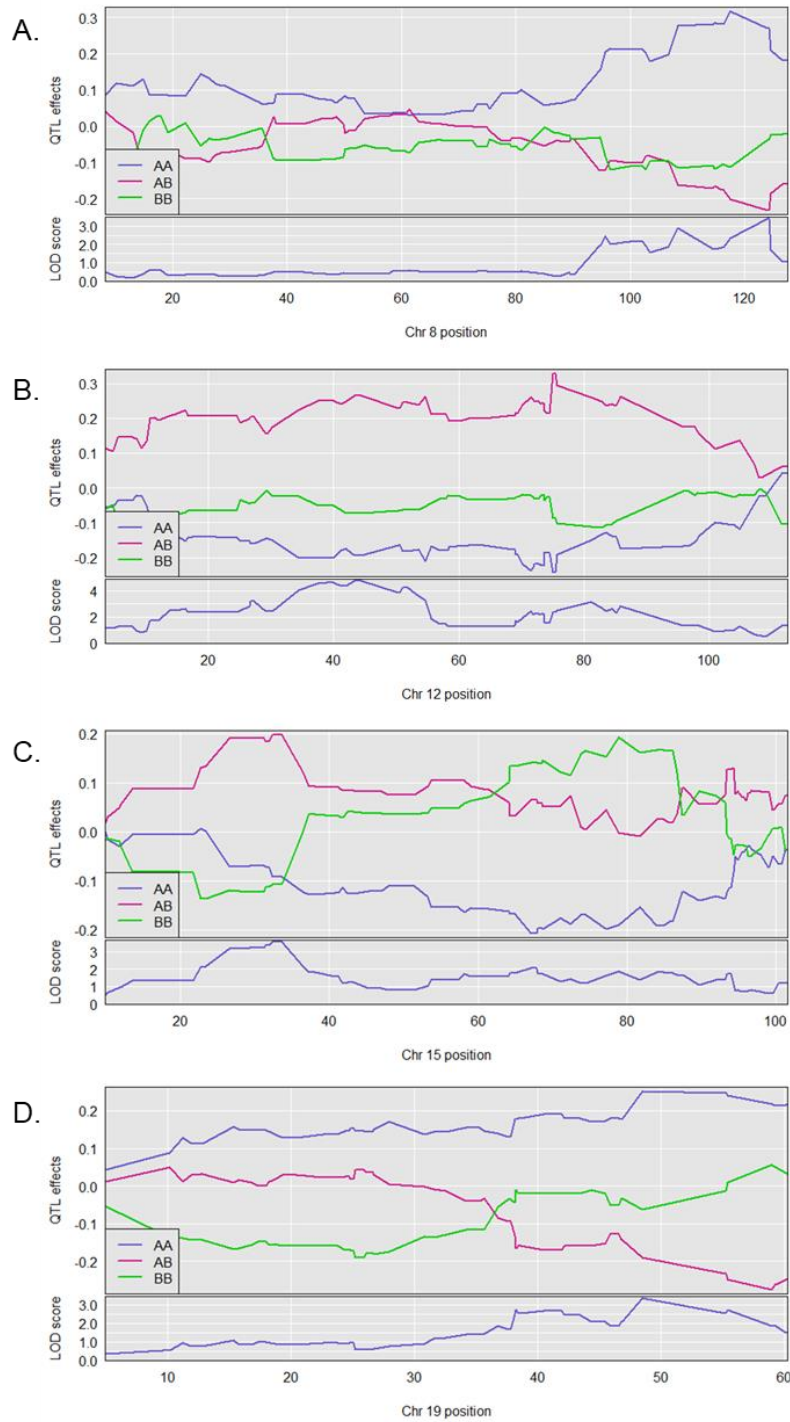


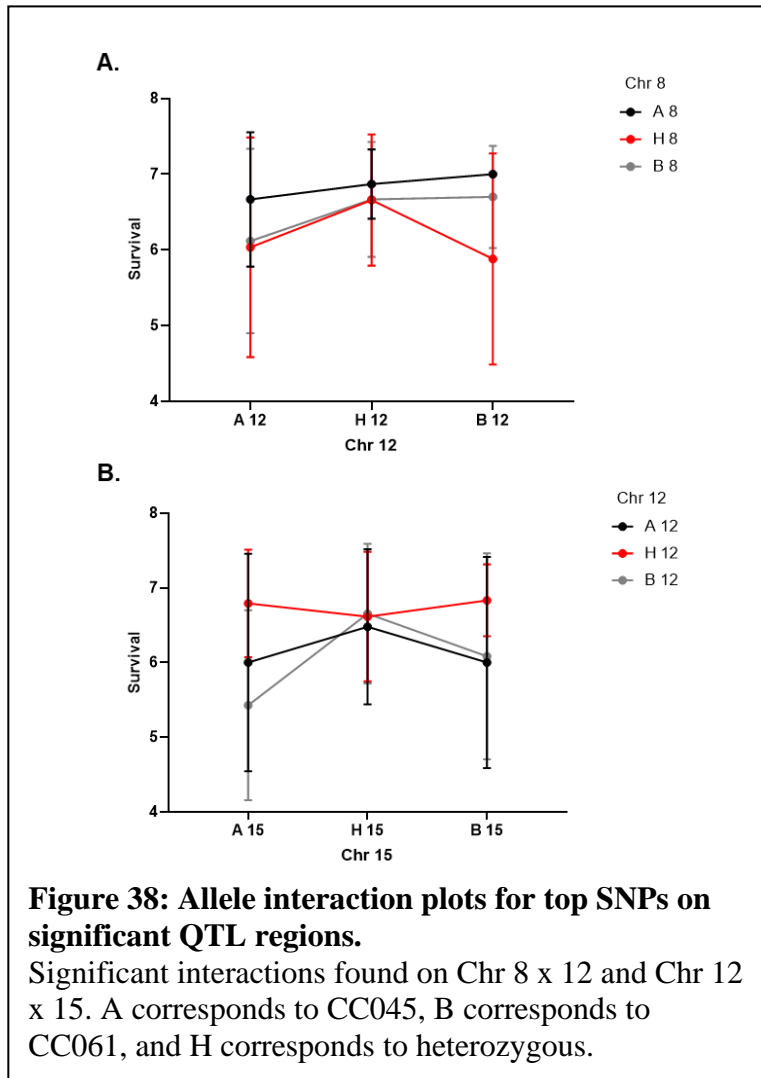
Figure 37: Allele effect plots for significant QTL regions.
 Chr A. 8, B. 12, C. 15, and D. 19. AA corresponds to CC045, BB corresponds to CC061, and AB corresponds to a heterozygous allele.

Allele interactions for significant QTL SNPs.

In order to identify interactions between the significant associations found in the survival QTL, the top SNP for each association was examined for all chromosome

combinations (8x12, 8x15, 8x19, 12x15, 12x19, and 15x19) for survival time for each allele. Only two interactions showed significant differences between the different haplotype groups: 8x12 and 12x15 (Fig. 38).

Chr 8 and Chr 12 had one significantly different interaction that was AH by HB ($P = 0.0382$). In this case, if a mouse had a CC045 allele



on Chr 8 and was heterozygous on Chr 12, they survived significantly longer post-infection than a mouse that was heterozygous on Chr 8 and had a CC061 allele on Chr 12 (Fig. 38A, 6.87 vs 5.88 days). However, since all alleles are different, this appears to

simply illustrate the haplotype association of heterozygous individuals at Chr 8 with shorter survival time than other haplotypes.

Chr 12 and 15 had two significantly different interactions that were BA by HA and BA by HB (Fig. 38B, $P = 0.0242, 0.0370$). If a mouse had a CC061 allele on Chr 12 and a CC045 allele on Chr 15, they survived a shorter time post-infection than a mouse that was heterozygous on Chr 12 and had a CC045 allele on Chr 15 (Fig. 38B, 5.43 vs 6.79 days). It appears that having a CC045 allele on Chr 15 is modified for worse survival time by being heterozygous on Chr 12. The next interaction identified was for a CC061 allele on Chr 12 and a CC045 allele on Chr 15, which survived shorter post-infection than mice that were heterozygous on Chr 12 and had a CC061 allele on Chr 15 (Fig. 38B, 5.43 vs 6.83 days). However, since there were no commonalities in alleles between the two groups, this may not be a true allele interaction.

Discussion

Mutation in *Slc11a1* (*Slc11a1^s*) has long been linked to an inability of mice to survive after STm infections (28). However, we recently determined that line CC045, a member of the CC mouse reference collection of lines, survived STm infection despite carrying an *Slc11a1* mutation which normally confers susceptibility to STm infection. In addition to a difference in survival time, the CC045 line lost significantly less weight than several other *Slc11a1^s* lines studied. The goal of our work here was to resolve this apparent paradox and identify new genetic determinants that seem to override the *Slc11a1* mutation.

First, we determined whether CC045 mice were clearing the STm and thus surviving longer. We compared spleen and liver bacterial burden of CC045 mice with B6 mice and four other CC lines known to carry the *Slc11a1* mutation and found that CC045 has similar bacterial load to these other lines. Thus, the longer survival time and lower body weight loss of CC045 is not simply due to lower bacterial colonization.

Because white blood cells are a primary effector of innate and adaptive immunity (44), we determined the baseline levels of circulating white blood cells in uninfected animals. CC045 may simply be primed to survive infection better due to a higher circulating WBC count. In uninfected mice, CC045 had comparable circulating WBC numbers to all lines except for CC042 that actually had higher numbers, contrary to previous reports (66). Thus, CC045 does not have a difference in baseline WBC levels, and its survival after STm infection must be due to another mechanism.

Another potential explanation for the survival phenotype of CC045 is that they may be able to better mobilize neutrophils, monocytes, and lymphocytes post-infection than other CC lines tested. This did not appear to be the case as CC045 did not have a consistently greater change in circulating WBC than other *Slc11a1^s* CC lines. CC045 had significantly higher change in circulating neutrophils after STm infection than both CC031 and CC042, but not for the other three lines and had significantly higher change in circulating monocytes than CC042. CC045 had significantly higher levels of circulating lymphocytes than B6, CC021, and CC042 after STm infections. CC045 mice do have a greater change in circulating lymphocytes than other lines, however this may

reflect the beginning of an adaptive immune response facilitated by longer survival time (35).

To further explore CC045 survival after STm infection in the face of the *Slc11a1* mutation, we generated an F2 population with a STm susceptible CC line bearing the *Slc11a1* mutation, CC061. We infected CC061xCC045 F1s and they survived to day 7, lost less weight than their CC061 parent, and were less colonized in spleen and liver than their CC045 parent. Since all F1s survived, the alleles allowing CC045 to overcome their *Slc11a1* mutation appear to be dominant. Reduced STm burden in the F1s was unexpected but was restored in the F2s.

We infected 245 F2s with STm and monitored them for 7 days post-infection. 190 F2 mice survived to day 7, a roughly 3:1 ratio expected in a Mendelian dominant/recessive inheritance pattern. The group of surviving F2 lost significantly less weight than both the CC061 and the non-surviving F2s, but similar amounts to the CC045 and the F1s. The surviving F2s were colonized to a similar level as both parental lines and F1s in the spleen but were colonized significantly less than CC045 in the liver. This lower liver colonization could be due to the discrepancy in sample size between the CC045 and F2s. The surviving F2s had significantly lower bacterial burden in both spleen and liver than the non-surviving F2s, but this is likely due in part to the subset of surviving mice with no bacterial burden in these organs. Of the 190 mice that survived, 26 had no bacteria in either their spleen or liver, an unexpected result, but a high enough number that it is unlikely to be due to an infection error.

We used Spearman's correlation on the F2 results and identified a positive correlation between survival and weight change, as well as between spleen CFU/g and liver CFU/g. There was also a slight negative correlation between survival time and spleen and liver CFU/g. Thus, mice that were more highly colonized were more likely to die early. However, this correlation was not strong, due to a high number of highly colonized mice surviving to day 7.

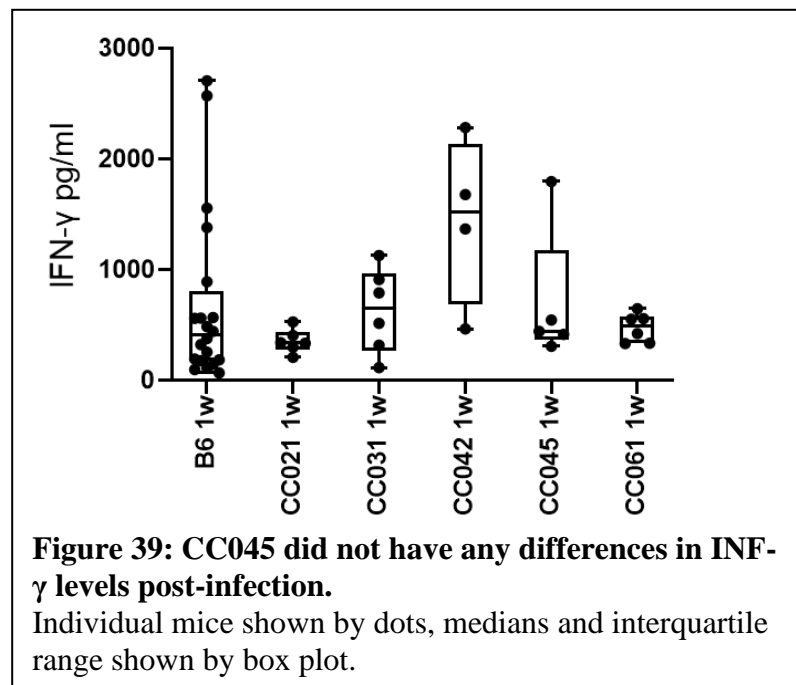
Next, QTL was performed on survival time. Since there was such a high correlation between survival and weight change, weight change was used as a covariate. The 26 uncolonized mice were also excluded because our interest is how CC045 survives high colonization levels. The QTL gave four significant associations: *45Stmsq1*, 2, 3, and 4 on Chr 8, 12, 15, and 19, respectively.

Allele interactions between the top SNP for each association were explored to determine if there were any interactions. Interactions were found between Chr 8 and 12 and Chr 12 and 15. Only one of the interactions between Chr 12 and 15 was likely a true interaction of alleles. When a mouse had an A allele on Chr 15, a B allele on Chr 12 made the mouse survive more poorly than if it was heterozygous at the Chr 12 locus. The A allele on Chr 12 appeared to be intermediate.

Significant regions were also explored to identify genes that would be good candidates for survival of STm infection. First, on Chr 8, there were two candidate genes: interleukin 17C (*Il17c*) and interleukin 34 (*Il34*). *Il17c* is a cytokine produced by epithelial cells, including those in the intestine, that has similar properties to *Il17a* (113). The role of *Il17c* is still largely unknown, but its family member *Il17a* is required to help

mount a sufficient immune response to STm infections (114). *Il34* is recently discovered cytokine that causes proliferation, activation, and survival of monocytes/macrophages, a vital innate immune cell type to combat STm infection (34, 115). On Chr 12, the DnaJ heat shock protein family (Hsp40) member B9 (*Dnajb9*) was a candidate gene. *Dnajb9* is a chaperone protein that stabilizes proteins when a cell is under stress, such as an infection, and is reported to be involved in B-cell maturation (116). Finally, on Chr 15, death-associated protein 1 (*Dap*), which is activated by IFN- γ and causes cell death, was a candidate gene (117, 118). IFN- γ is upregulated in *Salmonella* infections (119), so it is possible that CC045 control their IFN-gamma production to prevent excessive cell death. However, we did not find any significant differences in IFN- γ production at the time of necropsy in our mice (Fig. 39). Because necropsy times differed across lines, it is possible that this timing issue obscured our ability to detect differences in INF- γ levels in the current infection paradigm. In order to confirm the putative roles of these genes in

survival after STm infection survival, further analysis is needed.



Materials/Methods

Bacterial strains and media

The *Salmonella enterica* ser. Typhimurium strain (HA420) used for this study was derived from ATCC14028. HA420 is a fully virulent, spontaneous nalidixic acid resistant derivative of ATCC14028 (100). Strains were routinely cultured in Luria-Bertani (LB) broth and plates, supplemented with antibiotics when needed at 50 mg/L nalidixic acid (Nal).

For murine infections strains were grown aerobically at 37°C to stationary phase in LB broth with nalidixic acid and diluted to generate an inoculum of 2-5 x10⁸/ml.. Bacterial cultures used as inoculum were serially diluted and plated to enumerate colony forming units (CFU) to determine the exact titer.

Murine Strains

Both conventional mice (B6), collaborative cross (CC), F1s (CC061xCC045) and outbred F2 (CC061xCC045) mice were utilized in these experiments. Most animals were bred and maintained in the Division of Comparative

Table 15: Number of mice used for infections and facility of origin.

Strain	Male	Female	Origin
B6	14	5	TAMU
CC021	3	3	UNC
CC031	3	3	UNC
CC042	3	3	TAMU
CC045	3	2	UNC
CC061	3	3	TAMU
CC061XCC045 F1	3	3	UNC
CC061XCC045 F2	138	107	TAMU

Medicine at Texas A&M University. The CC045 and CC061xCC045 F1s were obtained from the UNC Collaborative Cross Core. Our experiments used both male and females

of 5 lines of CC mice in addition to B6, CC061xCC045 F1s, and F2s (Table 15). All animal experiments were conducted in accordance with the Guide for the Care and Use of Laboratory Animals, and with the TAMU IACUC (AUP# 2018-0488 D, 2015-0315 D, and 2019-0411).

Infection with *Salmonella* Typhimurium

Mice were separated into individual cages and given a paper hut when transferred from the breeding facility to the BSL-2 facility. After 2 days of acclimation in the BSL-2 facility, 8 to 12-week-old B6, CC, F1, or F2 mice were weighed and infected by gavage with a dose of $2-5 \times 10^7$ CFU of *S. Typhimurium* HA420 in 100 microliters of LB broth. Infected mice were monitored twice daily for signs of disease by visual inspection. When health conditions suggested the development of clinical disease from infection, mice were humanely euthanized. If animals remained clinically healthy throughout the duration of the experiment, they were humanely euthanized at 7 days post-infection. 3 male and 3 female mice of each CC line were used (CC045 only had 2 females due to an experimental complication) and each control for a total of 48 inbred mice, 6 F1s, and 245 F2s.

Bacterial load determination

Mice were humanely euthanized, and the spleen and liver were collected. Half of each organ was collected in 3 mL of ice-cold PBS, weighed, homogenized, serially diluted in 1X PBS, and plated on Nal plates for enumeration of *S. Typhimurium* in each organ. Data are expressed as CFU/g of tissue.

Complete Blood Count

For B6 and CC mice, whole blood was collected by puncture of the submandibular vein (cheek bleed) for complete blood count (CBC) one week prior to infection for pre-infection sample to determine the baseline for each mouse. Blood from infected mice was collected at necropsy by cardiac puncture. All blood was collected into EDTA tubes and analyzed on an Abaxis VetScan HM5 machine.

F2 breeding/Genotyping

CC061 females were bred with CC045 males to generate CC061xCC045 F1 mice by the UNC Collaborative Cross Core. The F1 mice were shipped to the Division of Comparative Medicine at Texas A&M University. The mice were then bred in trios (2 females and 1 male) and offspring were weaned at 3 weeks of age. The resulting F2 mice were grouped housed until they were 8-12 weeks old. Tail snips were taken at weaning from F2 mice and were genotyped using miniMUGA at Neogen. The miniMUGA has 11,125 markers (120).

QTL analysis

219 F2 mice were included in the QTL analysis. Mice with no bacterial burden in the spleen and liver were excluded. The analysis was run using the R/qlt2 program and 999 permutations (121). Survival time with weight change as a covariate was used as the input. CC045 was called the AA parent and CC061 was called the BB parent.

CHAPTER V

CONCLUSIONS AND FUTURE DIRECTIONS

Salmonella is a serious global human health concern that causes extensive morbidity and mortality. *Salmonella* also have an increasing incidence of antibiotic resistance, limiting treatment options for severe or recurrent cases (19). 2% of human cases are colonized long-term by *Salmonella* with 65% of these patients having recurrent diarrheal disease (122). The recurrent diarrheal disease is a distinct phenotype from asymptomatic carriage and perhaps represents tolerance (123). The majority (93%) of the long-term colonization cases were in individuals who were immunocompetent (122, 123). Discovering why some hosts are able to survive STm infections, even in the face of long-term colonization, was the goal of this project. Since most studies performed on STm have been on traditional inbred mouse strains, they have not captures the effect of host genetic diversity on disease outcome. We used the Collaborative Cross, which is as diverse as a human population, to achieve this goal (37).

We orally infected 32 CC lines with STm and monitored them initially for one week. We identified 14 lines that were susceptible to STm infection as they did not survive to day seven post-infection. Eighteen lines survived the full study period. The range of median CC line survival was four to seven days, similar to that observed in B6 and CBA mice. This similar range of survival may be due to the technical parameters of our experiment: seven days may not be a long enough window to capture variable survival at the higher end, and four days may be the quickest a mouse can succumb to

STm using the current infection paradigm. Weight change in the CC lines was more variable than the control strains B6 and CBA. Bacterial burden in spleen and liver were also much more variable than the control strains, demonstrating that the CC models more diversity than inbred strains. One drawback of this study was that all of the 18 surviving lines did not have significantly different bacterial burdens in spleen and liver, so tolerance and resistance could not be differentiated at one-week post-infection.

To further identify tolerant versus resistant lines, lines that survived acute infection were orally infected for three-weeks. Surprisingly, we found a subset of these lines (seven) that survived acute infection but could not survive the three-week infections and had high bacterial burdens. We defined these lines as having a “delayed susceptible” phenotype. We classified six of the remaining lines as tolerant. These lines survived STm infections and maintained a bacterial burden of at least 10^3 CFU/g in their liver and 10^4 CFU/g in their spleen. This bacterial burden was similar to that of delayed susceptible lines, but was fatal for delayed susceptible. Resistant lines were colonized at very low levels in both liver and spleen, suggesting that they are clearing the infection.

At one-week post-infection, there was no significant differences in bacterial burden between tolerant and resistant lines in any organs. Furthermore, there was no significant difference between bacterial burdens in tolerant and resistant lines in ileum, cecum or colon at three-weeks post-infection. However, the bacterial burdens in PP and MLN were significantly different at three-weeks post-infection. When a host ingests STm contaminated food or water, the bacteria enter the gut epithelium through the PP (124). Long-term colonization of hosts by STm can result from persistence of organisms

in MLN (103). Tolerant lines, which are defined by maintenance of bacterial load, had significantly more STm in their MLN than resistant lines. However, neither group significantly increased nor decreased their bacterial burden at three-weeks post-infection when compared to one-week levels, suggesting tolerance is more complex than persistence in MLN alone.

Telemetry provides unique insight into each mouse's minute-by-minute temperature and activity. This minute-by-minute reading allowed us to establish each mouse's unique circadian pattern of body temperature and activity and to pinpoint the exact minute that each mouse started to develop disease, before symptoms were visible. Interestingly, mice that survived acute infections had a lower uninfected baseline body temperature during rest periods, during active periods, and overall. Because fever is generally thought to be disease fighting (78, 93–95), we expected mice with higher baseline temperatures to mount a quicker fever response since it would require a smaller change in temperature, but this did not appear to be the case. During three-week infections, we found that tolerant lines had the lowest temperatures across all three time periods when compared to resistant, delayed susceptible, and susceptible lines. Since tolerance is focused on minimizing damage done by both the pathogen and the host's own immune response, this lower baseline temperature may be protective from damage caused by high fevers post-infection (78, 93, 125). While resistant and delayed susceptible mice were warmer than tolerant mice, they were still cooler than susceptible mice.

One of the first explanations for temperature differences could be activity differences since activity raises body temperature (125, 126). When evaluating pre-infection baseline activity for one-week infections, surviving mice spent more time at rest during periods of the day when mice were the most active than susceptible mice. The increased time at rest in surviving lines is probably not the cause of lower body temperature in these lines, as even during periods when susceptible and surviving mice spent equal time at rest, surviving lines maintained a lower body temperature. Similar to what was found in acute infections, pre-infection activity levels did not differ across the groups during three-week infections, meaning the temperature differences are independent of activity level.

Circadian pattern disruption was also measured using the telemetry data for both one- and three- week infections. During one-week infections, there was no significant difference in how rapidly surviving and susceptible infected mice deviated from their normal circadian pattern of temperature or activity after infection. During three-week infections, resistant lines maintained temperature circadian rhythm for over a day longer than tolerant lines, yet both groups survived equally long, showing that tolerant lines survive despite showing disease symptoms (104). Circadian pattern disruption detection was also compared between temperature and activity for each phenotypic group and temperature was shown to be a more sensitive predictor of disease onset for susceptible, tolerant, and delayed susceptible lines, but not resistant lines. This data suggests that temperature, not activity levels, may be the first indicator of a developing disease.

CBC and cytokine levels were also assessed for one- and three- week infections but were not significantly different when comparing surviving and non-surviving lines at one-week post-infection. At this timepoint, differences originate from underlying line differences rather than from differential response to STm infection, highlighting the diversity of even baseline immune parameters in the CC (2, 44). However, at three-weeks post-infection, tolerant lines had a higher increase in overall WBC driven by a significantly higher increase in neutrophils than resistant lines. Since neutrophils are part of the initial immune response to infection, lower neutrophil counts of resistant lines may be due to clearance of enough bacteria, that their neutrophils are simply more efficient at reaching infection sites, or that they have switched to the adaptive immune response (127). However, since there were no differences in lymphocyte numbers, which include T and B cells and are a key part of the adaptive immune system, it is more likely due either bacterial burden or neutrophil efficiency.

At three-weeks post-infection, three cytokines were significantly different between tolerant and resistant lines. The first cytokine, IFN- γ , was increased in both resistant and tolerant lines, but tolerant lines had a much higher increase after infection. IFN- γ keeps STm levels at a manageable level, while keeping the host healthy, and neutralizing IFN- γ causes STm to reactivate and causes severe infection (103, 105). Since tolerant lines have such a high level of IFN- γ , this must be a contributing factor to controlling their high bacterial burden. Removing IFN- γ from tolerant mice may even cause them to become susceptible. The next cytokine that was significantly lower in resistant mice than tolerant mice was MCP-1, which attracts monocytes to the site of

infection. Since STm resides and replicates in monocytes, high levels of MCP-1 are not always protective (106). High levels of MCP-1 cause more severe organ damage/failure, higher levels of septic shock, and higher mortality (34, 106, 107). The last cytokine that was significantly different was ENA-78, which attracts neutrophils to infection sites. ENA-78 was increased in resistant mice and decreased in tolerant mice, contrary to what we would expect since tolerant lines have a significantly higher number of neutrophils than resistant lines (108). Resistant lines could be attempting to recruit more neutrophils to fight off the remaining STm since they are still colonized, or that tolerant lines could be trying to control their immune response by reducing neutrophil numbers. Controlling the cytokine response is important, because dysregulation can lead to sepsis and death (107, 128, 129).

Since the immune response can also cause organ damage (73, 75), histopathology scores were examined for ileum, cecum, colon, spleen, and liver. At one-week post-infection, tissue damage in spleen and liver had a small but significant correlation with survival time, while ileum, cecum, and colon were minimally damaged. Splenic damage drove the small correlation suggesting that liver damage, while more severe, is better tolerated than splenic damage. Interestingly, at one-week post-infection, there were some lines that exhibited quite severe damage in both organs yet survived (CC011, CC017, CC045, CC072, and CC078) and some lines that did not have as severe of damage and did not survive (CC005, CC025, and CC030). This supports that there is heterogeneity in infection response and suggests there is more than one way to survive an infection. Three-week post-infection tissue samples were also examined and compared to the one-

week tissue samples. Again, the ileum, cecum, and colon were minimally damaged and spleen and liver more severely damaged. Tissue damage in spleen and liver was reduced in resistant mice at three-weeks post-infection compared to one-week post-infection, while tolerant mice did not reduce tissue damage. Since tissue damage was present at one-week, it is likely that the resistant mice were able to reduce the damage by three-weeks by repairing the damage. Interestingly, tissue repair has been linked to tolerance to other pathogens, yet we do not see this in the tolerant mice in our experiment (48, 75, 130). However, the tolerant mice also did not have worsening tissue damage, so it is possible that they are controlling the damage without repair. Tolerant lines may be modulating their immune system to prevent further tissue damage instead of repairing the existing damage or that they are repairing the damage at the same rate as it is being generated, creating a homeostasis (71, 75).

While we have been able to define tolerance at a phenotypic level, we were interested in defining it at a genotypic level as well. In order to do this, we utilized QTL analysis to identify genetic regions that associated with the phenotypes. For one- and three-week infections, all of the collected parameters were analyzed to identify genes using gQTL. For one-week, several genomic intervals were associated with survival time. The two intervals found on Chr 1 corresponded to *Slc11a1* and *Ncf2*, previously known genes that have mutations linked to poor survival after STm infection (27, 112). Suggestive and significant intervals on Chr 2, 4, and 7 were also identified and two genes were identified as candidate genes based on SNP differences in haplotypes: *Bpifb2* and *Samhd1*. *Bpifb2* is a member of the lipid-transfer protein family and is predicted to

have bactericidal and permeability-increasing properties, making it a good candidate for further investigation (97). *Samhd1* is involved in regulating interferon pathways in response to viral infections, through NF-KB (98, 99). While *Samhd1* has been linked to the immune response, it has only been implicated in viral infections, but could have a previously unknown role in bacterial immunity. For three-week infections, suggestive and significant associations were identified for the phenotypes of resistance, tolerance, and spleen/liver STm colonization. While one significant and six suggestive associations were found, the small number of CC lines used and the lack of normal distribution of data did not allow for us to determine which genes were responsible for the associations alone (109). RNA sequencing data will allow us to narrow these regions into candidate genes.

While tolerance and resistance were not distinguishable at one-week post-infection, there were a few interesting phenotypes observed in some lines at this timepoint. One of these lines was CC051, which was colonized more poorly than CBA mice (resistant control) and gained weight. This data suggests that CC051 are more resistant to STm infection than previously studied inbred strains. This line was also the only line to show a reduced bacterial burden in spleen when compared to IV infections, suggesting a potentially unique intestinal phase of infection.

CC042 mice were significantly more highly colonized than the susceptible control B6 mice. This extreme susceptibility has been attributed to an additional mutation in the *Itgal* (65, 66). CC027 exhibited a stark sex difference with females surviving to day 7 and losing minimal weight while males succumbed to infection and

lost significantly more weight. Females were also significantly more poorly colonized in spleen and liver. This line offers a unique opportunity to explore how sex can influence outcome to disease, as it was the only line to exhibit completely opposite phenotypes between males and females (45, 86, 87). The final and most interesting line was CC045 which carries mutations in both *Slc11a1* and *Ncf2*, had bacterial loads in spleen and liver at similar levels as susceptible mice, and survived to day 7 with minimal weight loss (23–25, 27, 30). With a double mutation, we would have expected this line to be extremely susceptible to STm infections, so it must have some sort of compensatory mechanisms.

Since mutations in *Slc11a1* have long been established to cause susceptibility to intracellular pathogens such as STm (28), the survival of CC045 was unexpected and required further examination. First, we determined whether CC045 mice were clearing STm and thus surviving longer. CC045 was comparably colonized in spleen and liver compared to B6 and four other CC lines known to carry the *Slc11a1* mutation. In addition to a difference in survival time, the CC045 line lost significantly less weight than several other *Slc11a1* mutant lines studied. Thus, the longer survival time and lower body weight loss of CC045 is not due to lower bacterial colonization.

Because white blood cells are a primary effector of innate and adaptive immunity (44), we determined the baseline levels of circulating white blood cells (WBC). CC045 could be surviving STm infections due to being better primed to fight infection due to a higher circulating WBC count. CC045 had comparable circulating WBC numbers to all lines except for CC042 that had higher numbers than CC045, contrary to previous

reports (66). These findings show that CC045 survival after STm infection is not due to a higher baseline circulating WBC.

Another potential explanation for the survival phenotype of CC045 is that they may be able to better mobilize neutrophils, monocytes, and lymphocytes post-infection than other CC lines tested. This did not appear to be the case as CC045 did not have a consistently greater change in circulating WBC than other *Slc11a1* mutant CC lines. CC045 had significantly higher change in circulating neutrophils after STm infection than both CC031 and CC042, but not for the other three lines and had significantly higher change in circulating monocytes than CC042. CC045 had significantly higher levels of circulating lymphocytes than B6, CC021, and CC042 after STm infections. CC045 mice do have a greater change in circulating lymphocytes than other lines, however this is probably reflecting that the longer survival time allowed this line to begin to mount an adaptive immune response (35).

Because these obvious gross parameters did not explain CC045 survival after STm infection in the face of the *Slc11a1* mutation, we generated an F2 population with another CC line carrying the *Slc11a1* mutation, CC061. CC061xCC045 F1s survived to day 7 after STm infections, lost less weight than the CC061 parents, and were less colonized in spleen and liver than the CC045 parents. Since all F1s survived, the alleles enabling CC045 to overcome the *Slc11a1* mutation appear to be dominant. Reduced STm burden in the F1s was unexpected but was restored in the F2s.

We infected 245 F2s with STm and monitored them for a 7-days post-infection. 190 F2 mice survived to day 7, a roughly 3:1 ratio expected in a Mendelian

dominant/recessive inheritance pattern. The group of surviving F2 lost significantly less weight than both the CC061 parents and the non-surviving F2s, but similar amounts to the CC045 parents and the F1s. The surviving F2s were colonized to a similar level as both parental lines and F1s in the spleen. Surviving F2s were colonized more poorly in the liver compared to the CC045 parents, possibly due to the discrepancy in sample size between the CC045 and F2s. The surviving F2s had significantly lower bacterial burden in both spleen and liver than the non-surviving F2s, but this is likely due to the subset of surviving mice with no bacterial burden in these organs. Of the 190 mice that survived, 26 had no bacteria in either their spleen or liver, an unexpected result, but a high enough number that it is unlikely to be due to an infection error.

We used Spearman's correlation on the F2 results and identified a positive correlation between survival and weight change, as well as between spleen CFU/g and liver CFU/g. There was also a slight negative correlation between survival time and spleen and liver CFU/g. Thus, mice that were more highly colonized were more likely to die early. However, this correlation was not strong, due to a high number of highly colonized mice surviving to day 7.

Finally, QTL analysis was performed on survival time to determine why some of the F2s were able to survive bacterial burdens in their spleens and livers that killed other F2s. We found four significant associations: *45Stmsq1*, 2, 3, and 4 on Chr 8, 12, 15, and 19. These regions were explored to identify genes that would be good candidates for survival of STm infection. The region on Chr 8 contained two candidate genes: interleukin 17C (*Il17c*) and interleukin 34 (*Il34*). *Il17c* is a cytokine produced by

epithelial cells, including the intestine, that has similar properties to *I17a* (113). The role of *I17c* is still largely unknown, but it is predicted to act in a similar manner as its family member *I17a*, which is required to mount a sufficient immune response to invasive STm infections (114). *I134* is recently discovered cytokine that causes proliferation, activation, and survival of monocytes/macrophages, a vital cell type to combat STm infection (34, 115). The region on Chr 12 contained on candidate gene, DnaJ heat shock protein family (Hsp40) member B9 (*Dnajb9*). *Dnajb9* is a chaperone protein that stabilizes proteins when a cell is under stress, such as an infection, and is reported to be involved in B-cell maturation (116). Finally, on Chr 15, death-associated protein 1 (*Dap*), which causes cell death and is activated by IFN- γ , was a candidate gene (117, 118). IFN- γ is upregulated in *Salmonella* infections (119), so it is possible that CC045 are able to control their IFN- γ production to prevent excessive cell death after STm infection. However, we did not find any significant differences in IFN- γ production at the time of necropsy in our mice, but differences in necropsy times across lines could mask differences in INF- γ levels in the current infection paradigm. In order to confirm the candidacy of these genes in STm infection survival, further analysis is needed.

Overall, we were able to describe the phenotypes of the CC mice in response to STm infection over both acute and long-term infections. We were able to identify previously unknown genetic regions associated with survival time post-infection for both infections times and a significant association with spleen bacterial burden at three-weeks post-infection. To confirm and identify candidate genes found in the QTL regions found in one- and three-week infections, RNA-seq data is the next step. The tolerance and

resistance phenotypes were able to be defined at three-weeks post-infection. Telemetry data revealed that cooler baseline temperatures appeared to be more advantageous for STm infection survival, but the underlying cause was not explained and further experiments manipulating baseline temperatures would need to be performed to determine if it is a causative relationship. We also identified one line, CC045, that was able to survive one-week post-infection, despite carrying a previously not survivable mutation in *Slc11a1* through a novel mechanism that would require further genomic analysis to confirm.

REFERENCES

1. Majowicz SE, Musto J, Scallan E, Angulo FJ, Kirk M, O'Brien SJ, Jones TF, Fazil A, Hoekstra RM. 2010. The global burden of nontyphoidal salmonella gastroenteritis. *Clin Infect Dis* 50:882–889.
2. Collin R, Balmer L, Morahan G, Lesage S. 2019. Common Heritable Immunological Variations Revealed in Genetically Diverse Inbred Mouse Strains of the Collaborative Cross. *J Immunol* 202:777–786.
3. Gilchrist JJ, MacLennan C a., Hill AVS. 2015. Genetic susceptibility to invasive Salmonella disease. *Nat Rev Immunol* 15:452–463.
4. Stanaway JD, Parisi A, Sarkar K, Blacker BF, Reiner RC, Hay SI, Nixon MR, Dolecek C, James SL, Mokdad AH, Abebe G, Ahmadian E, Alahdab F, Alemnew BTT, Alipour V, Allah Bakeshei F, Animut MD, Ansari F, Arabloo J, Asfaw ET, Bagherzadeh M, Bassat Q, Belayneh YMM, Carvalho F, Daryani A, Demeke FM, Demis ABB, Dubey M, Duken EE, Dunachie SJ, Eftekhari A, Fernandes E, Fouladi Fard R, Gedefaw GA, Geta B, Gibney KB, Hasanzadeh A, Hoang CL, Kasaeian A, Khater A, Kidanemariam ZT, Lakew AM, Malekzadeh R, Melese A, Mengistu DT, Mestrovic T, Miazgowski B, Mohammad KA, Mohammadian M, Mohammadian-Hafshejani A, Nguyen CT, Nguyen LH, Nguyen SH, Nirayo YL, Olagunju AT, Olagunju TO, Pourjafar H, Qorbani M, Rabiee M, Rabiee N, Rafay A, Rezapour A, Samy AM, Sepanlou SG, Shaikh MA, Sharif M, Shigematsu M, Tessema B, Tran BX, Ullah I, Yimer EM, Zaidi Z, Murray CJL, Crump JA. 2019. The global burden of non-typhoidal salmonella invasive disease: a systematic

- analysis for the Global Burden of Disease Study 2017. *Lancet Infect Dis* 19:1312–1324.
5. Gordon MA. 2008. Salmonella infections in immunocompromised adults. *J Infect* 56:413–422.
 6. Fàbrega A, Vila J. 2013. Salmonella enterica serovar Typhimurium skills to succeed in the host: Virulence and regulation. *Clin Microbiol Rev* 26:308–341.
 7. Cianflone NFC. 2008. Salmonellosis and the GI Tract: More than Just Peanut Butter. *Curr Gastroenterol Rep* 10:424–431.
 8. Santos RL, Tükel Ç, Raffatellu M, Bäumlér AJ, Tsolis RM, Adams LG, Bevins CL. 2009. Life in the inflamed intestine, Salmonella style. *Trends Microbiol* 17:498–506.
 9. LaRock DL, Chaudhary A, Miller SI. 2015. Salmonellae interactions with host processes. *Nat Rev Microbiol* 13:191–205.
 10. Roy MF, Malo D. 2002. Genetic regulation of host responses to Salmonella infection in mice. *Genes Immun* 3:381–393.
 11. Haraga A, Ohlson MB, Miller SI. 2008. Salmonellae interplay with host cells. *Nat Rev Microbiol* 6:53–66.
 12. de Jong HK, Parry CM, van der Poll T, Wiersinga WJ. 2012. Host-Pathogen Interaction in Invasive Salmonellosis. *PLoS Pathog* 8:1–9.
 13. Corr SC, Gahan CCGM, Hill C. 2008. M-cells: Origin, morphology and role in mucosal immunity and microbial pathogenesis. *FEMS Immunol Med Microbiol* 52:2–12.

14. Ingram JP, Brodsky IE, Balachandran S. 2017. Interferon- γ in Salmonella Pathogenesis: New Tricks for an Old Dog. *Cytokine* 98:27–32.
15. CDC. 2019. Antibiotic resistance threats in the United States. *Centers Dis Control Prev* 1–113.
16. Martz SLE, McDonald JAK, Sun J, Zhang YG, Gloor GB, Noordhof C, He SM, Gerbaba TK, Blennerhassett M, Hurlbut DJ, Allen-Vercoe E, Claud EC, Petrof EO. 2015. Administration of defined microbiota is protective in a murine Salmonella infection model. *Sci Rep* 5:1–14.
17. Endt K, Stecher B, Chaffron S, Slack E, Tchitchek N, Benecke A, van Maele L, Sirard JC, Mueller AJ, Heikenwalder M, Macpherson AJ, Strugnell R, von Mering C, Hardt WD. 2010. The microbiota mediates pathogen clearance from the gut lumen after non-typhoidal salmonella diarrhea. *PLoS Pathog* 6.
18. Nathan C. 2004. Antibiotics at the crossroads. *Nature* 431:899–902.
19. Threlfall EJ. 2002. Antimicrobial drug resistance in Salmonella: problems and perspectives in food- and water-borne infections. *FEMS Microbiol Rev* Elsevier Sci 26:141–148.
20. Patin E, Hasan M, Bergstedt J, Rouilly V, Libri V, Urrutia A, Alanio C, Scepanovic P, Hammer C, Jönsson F, Beitz B, Quach H, Lim YW, Hunkapiller J, Zepeda M, Green C, Piasecka B, Leloup C, Rogge L, Huetz F, Peguillet I, Lantz O, Fontes M, Santo JP, Thomas S, Fellay J, Duffy D, Quintana-Murci L, Albert ML, Abel L, Alcover A, Astrom K, Bousso P, Bruhns P, Cumano A, Demangel C, Deriano L, Di Santo JP, Dromer F, Eberl G, Enninga J, Freitas A, Gelpi O,

- Boneca IG, Hercberg S, Leclerc C, Mouquet H, Pellegrini S, Pol S, Sakuntabhai A, Schwartz O, Schwikowski B, Shorte S, Soumelis V, Tangy F, Tartour E, Toubert A, Ungeheuer MN. 2018. Natural variation in the parameters of innate immune cells is preferentially driven by genetic factors resource. *Nat Immunol* 19:302–314.
21. Keestra-gounder AM, Tsolis RM, Bäumlér AJ. 2015. Now you see me , now you don't : the interaction of Salmonella with innate immune receptors. *Nat Rev Microbiol* 13:206–216.
22. Tsolis RM, Xavier MN, Santos RL, Bäumlér AJ. 2011. How to become a top model: Impact of animal experimentation on human Salmonella disease research. *Infect Immun* 79:1806–1814.
23. Lalmanach AC, Montagne A, Menanteau P, Lantier F. 2001. Effect of the mouse Nramp1 genotype on the expression of IFN- γ gene in early response to Salmonella infection. *Microbes Infect* 3:639–644.
24. Gopinath S, Hotson A, Johns J, Nolan G, Monack D. 2013. The Systemic Immune State of Super-shedder Mice Is Characterized by a Unique Neutrophil-dependent Blunting of TH1 Responses. *PLoS Pathog* 9.
25. Mastroeni P, Ugrinovic S, Chandra A, MacLennan C, Doffinger R, Kumararatne D. 2003. Resistance and susceptibility to Salmonella infections: Lessons from mice and patients with immunodeficiencies. *Rev Med Microbiol* 14:53–62.
26. Arpaia N, Godec J, Lau L, Sivick KE, McLaughlin LM, Jones MB, Dracheva T, Peterson SN, Monack DM, Barton GM. 2011. TLR signaling is required for

- salmonella typhimurium virulence. *Cell* 144:675–688.
27. Sancho-Shimizu V, Malo D. 2006. Sequencing, Expression, and Functional Analyses Support the Candidacy of *Ncf2* in Susceptibility to *Salmonella* Typhimurium Infection in Wild-Derived Mice. *J Immunol* 176:6954–6961.
 28. Fritsche G, Nairz M, Libby SJ, Fang FC, Weiss G. 2012. *Slc11a1* (*Nramp1*) impairs growth of *Salmonella enterica* serovar *typhimurium* in macrophages via stimulation of lipocalin-2 expression. *J Leukoc Biol* 92:353–359.
 29. Caron J, Larivière L, Nacache M, Tam M, Stevenson MM, McKerly C, Gros P, Malo D. 2006. Influence of *Slc11a1* on the outcome of *Salmonella enterica* serovar enteritidis infection in mice is associated with Th polarization. *Infect Immun* 74:2787–2802.
 30. Khan RT, Chevenon M, Yuki KE, Malo D. 2014. Genetic dissection of the *Ity3* locus identifies a role for *Ncf2* co-expression modules and suggests *Selp* as a candidate gene underlying the *Ity3.2* locus. *Front Immunol* 5:1–13.
 31. Li Q, Cherayil BJ. 2003. Role of toll-like receptor 4 in macrophage activation and tolerance during *Salmonella enterica* serovar Typhimurium infection. *Infect Immun* 71:4873–4882.
 32. Bihl F, Larivière L, Qureshi ST, Flaherty L, Malo D. 2001. LPS-hyporesponsiveness of *mnd* mice is associated with a mutation in Toll-like receptor 4. *Genes Immun* 2:56–59.
 33. Kang E, Crouse A, Chevallier L, Pontier SM, Alzahrani A, Silué N, Campbell-Valois FX, Montagutelli X, Gruenheid S, Malo D. 2018. Enterobacteria and host

- resistance to infection. *Mamm Genome* 29:558–576.
34. Eckmann L, Kagnoff MF. 2001. Cytokines in host defense against Salmonella. *Microbes Infect* 3:1191–1200.
 35. Loomis WP, Delaney MA, Johnson ML, Cookson BT. 2021. Failure of CD4 T cell-deficient hosts to control chronic nontyphoidal salmonella infection leads to exacerbated inflammation, chronic anemia, and altered myelopoiesis. *Infect Immun* 89:1–16.
 36. Smith CM, Sasseti CM. 2018. Modeling Diversity: Do Homogeneous Laboratory Strains Limit Discovery? *Trends Microbiol* 26:892–895.
 37. Threadgill DW, Churchill GA. 2012. Ten years of the collaborative cross. *Genetics* 190:291–294.
 38. Churchill G, Airey D, Allayee H, ... 2004. The Collaborative Cross , a community resource for the genetic analysis of complex traits. *Nat Rev Genet* 36:1133–1137.
 39. Aylor DL, Valdar W, Foulds-mathes W, Buus RJ, Verdugo R a, Baric RS, Ferris MT, Frelinger J a, Heise M, Frieman MB, Gralinski LE, Bell T a, Didion JD, Hua K, Nehrenberg DL, Powell CL, Steigerwalt J, Xie Y, Kelada SNP, Collins FS, Yang I V, Schwartz D a, Branstetter L a, Chesler EJ, Miller DR, Spence J, Liu EY, Mcmillan L, Sarkar A, Wang J, Wang W, Zhang Q, Broman KW, Korstanje R, Durrant C, Mott R, Iraqi F a. 2011. Genetic analysis of complex traits in the emerging Collaborative Genetic analysis of complex traits in the emerging Collaborative Cross. *Genome Res* 21:1213–1222.
 40. Threadgill DW, Miller DR, Churchill G a, de Villena FP-M. 2011. The

collaborative cross: a recombinant inbred mouse population for the systems genetic era. *ILAR J* 52:24–31.

41. Price A, Okumura A, Haddock E, Feldmann F, Meade-White K, Sharma P, Artami M, Lipkin WI, Threadgill DW, Feldmann H, Rasmussen AL. 2020. Transcriptional Correlates of Tolerance and Lethality in Mice Predict Ebola Virus Disease Patient Outcomes. *Cell Rep* 30:1702–1713.
42. Mathes WF, Kelly SA, Pomp D. 2011. Advances in comparative genetics: influence of genetics on obesity. *Br J Nutr* 106:S1–S10.
43. Welsh CE, Miller DR, Manly KF, Wang J, McMillan L, Morahan G, Mott R, Iraqi FA, Threadgill DW, De Villena FPM. 2012. Status and access to the Collaborative Cross population. *Mamm Genome* 23:706–712.
44. Philippi J, Xie Y, Miller DR, Bell TA, Zhang Z, Lenarcic AB, Aylor DL, Krovi SH, Threadgill DW, de Villena FP-M, Wang W, Valdar W, Frelinger JA. 2014. Using the emerging Collaborative Cross to probe the immune system. *Genes Immun* 15:38–46.
45. Abu Toamih Atamni H, Nashef A, Iraqi FA. 2018. The Collaborative Cross mouse model for dissecting genetic susceptibility to infectious diseases. *Mamm Genome* 29:471–487.
46. Graham JB, Swarts JL, Mooney M, Choonoo G, Jeng S, Miller DR, Ferris MT, McWeeney S, Lund JM. 2017. Extensive Homeostatic T Cell Phenotypic Variation within the Collaborative Cross. *Cell Rep* 21:2313–2325.
47. Raberg L, Sim D, Read AF. 2007. Disentangling Genetic Variation for Resistance

- and Tolerance to Infectious Disease in Animals. *Science* (80-) 318:812–814.
48. Raberg L, Graham AL, Read AF. 2009. Decomposing health: tolerance and resistance to parasites in animals. *Philos Trans R Soc B Biol Sci* 364:37–49.
49. Medzhitov R, Schneider DS, Soares MP, Caldwell RM, Schafer JF, Compton LE, Patterson FL, Schafer J, Råberg L, Graham AL, Read AF, Råberg L, Sim D, Read AF, Read AF, Graham AL, Råberg L, Schneider DS, Ayres JS, Kavaliers M, Choleris E, Agmo A, Pfaff DW, Liberles SD, Rivière S, Challet L, Fluegge D, Spehr M, Rodriguez I, Tizzano M, Pradel E, Zhang Y, Lu H, Bargmann CI, Cremer S, Sixt M, Kiesecker JM, Skelly DK, Beard KH, Preisser E, Curtis V, Barra M de, Aunger R, Graham A, Allen J, Read A, Casadevall A, Pirofski LA, Ayres JS, Freitag N, Schneider DS, Ayres JS, Schneider DS, Shinzawa N, Richardson CE, Kooistra T, Kim DH, Sun J, Singh V, Kajino-Sakamoto R, Aballay A, Ferreira A, Balla J, Jeney V, Balla G, Soares MP, Gozzelino R, Jeney V, Soares MP, Ferreira A, Seixas E, Pamplona A, Larsen R, Bente D, Gren J, Strong JE, Feldmann H, Matzinger P, Kamala T, Balch WE, Morimoto RI, Dillin A, Kelly JW, Kensler TW, Wakabayashi N, Biswal S, Walter P, Ron D, Foster SL, Hargreaves DC, Medzhitov R, Durieux J, Wolff S, Dillin A, Prahla V, Cornelius T, Morimoto RI, Sapolsky RM, Romero LM, Munck AU, Pamplona R, Costantini D, Hart BL, Gromkowski SH, Yagi J, Janeway CA, Ayres JS, Schneider DS, Playfair JH, Taverne J, Bate CA, Souza JB de, Schofield L, Hewitt MC, Evans K, Siomos MA, Seeberger PH, Peiris JS, Hui KP, Yen HL, Little TJ, Shuker DM, Colegrave N, Day T, Graham AL, Tscherne DM, García-Sastre A,

- Miller MR, White A, Boots M, Roy BA, Kirchner JW, Miller RA, Shaw AC, Joshi S, Greenwood H, Panda A, Lord JM, Kurtz CC, Lindell SL, Mangino MJ, Carey H V., Kenyon CJ. 2012. Disease tolerance as a defense strategy. *Science* 335:936–41.
50. Sarkar S, Heise MT. 2019. Mouse Models as Resources for Studying Infectious Diseases. *Clin Ther* 1–11.
51. Graham JB, Thomas S, Swarts J, McMillan AA, Ferris MT, Suthar MS, Treuting PM, Ireton R, Gale M, Lund JM. 2015. Genetic diversity in the collaborative cross model recapitulates human west nile virus disease outcomes. *MBio* 6:1–11.
52. Graham JB, Swarts JL, Wilkins C, Thomas S, Green R, Sekine A, Voss KM, Ireton RC, Mooney M, Choonoo G, Miller DR, Treuting PM, Pardo Manuel de Villena F, Ferris MT, McWeeney S, Gale M, Lund JM. 2016. A Mouse Model of Chronic West Nile Virus Disease. *PLoS Pathog* 12:1–23.
53. Ferris MT, Aylor DL, Bottomly D, Whitmore AC, Aicher LD, Bell TA, Bradel-Tretheway B, Bryan JT, Buus RJ, Gralinski LE, Haagmans BL, McMillan L, Miller DR, Rosenzweig E, Valdar W, Wang J, Churchill GA, Threadgill DW, McWeeney SK, Katze MG, Pardo-Manuel de Villena F, Baric RS, Heise MT. 2013. Modeling Host Genetic Regulation of Influenza Pathogenesis in the Collaborative Cross. *PLoS Pathog* 9.
54. Maurizio PL, Ferris MT, Keele GR, Miller DR, Shaw GD, Whitmore AC, West A, Morrison CR, Noll KE, Plante KS, Cockrell AS, Threadgill DW, Pardo-Manuel de Villena F, Baric RS, Heise MT, Valdar W. 2017. Bayesian Diallel

Analysis Reveals *Mx1* -Dependent and *Mx1* -Independent Effects on Response to Influenza A Virus in Mice. *Genes|Genomes|Genetics* 8:g3.300438.2017.

55. Kollmus H, Pilzner C, Leist SR, Heise M, Geffers R, Schughart K. 2018. Of mice and men: the host response to influenza virus infection. *Mamm Genome* 0:1–25.
56. Rasmussen AL, Okumura A, Ferris MT, Green R, Feldmann F, Kelly SM, Scott DP, Safronetz D, Haddock E, Lacasse R, Thomas MJ, Sova P, Carter VS, Weiss JM, Miller DR, Shaw GD, Korth MJ, Heise MT, Baric RS, Villena FP De, Feldmann H, Katze MG. 2014. Host genetic diversity enables Ebola hemorrhagic fever pathogenesis and resistance. *Science* (80-) 346:987–991.
57. Price A, Okumura A, Haddock E, Feldmann F, Meade-White K, Sharma P, Artami M, Lipkin WI, Threadgill DW, Feldmann H, Rasmussen AL. 2020. Transcriptional Correlates of Tolerance and Lethality in Mice Predict Ebola Virus Disease Patient Outcomes. *Cell Rep* 30:1702-1713.e6.
58. Brinkmeyer-Langford CL, Rech R, Amstalden K, Kochan KJ, Hillhouse AE, Young C, Welsh CJ, Threadgill DW. 2017. Host genetic background influences diverse neurological responses to viral infection in mice. *Sci Rep* 7:1–17.
59. Gralinski LE, Ferris MT, Aylor DL, Whitmore AC, Green R, Frieman MB, Deming D, Menachery VD, Miller DR, Buus RJ, Bell TA, Churchill GA, Threadgill DW, Katze MG, McMillan L, Valdar W, Heise MT, Pardo-Manuel de Villena F, Baric RS. 2015. Genome Wide Identification of SARS-CoV Susceptibility Loci Using the Collaborative Cross. *PLoS Genet* 11:1–21.

60. Gralinski LE, Menachery VD, Morgan AP, Totura AL, Beall A, Kocher J, Plante J, Harrison-shostak DC, Schäfer A, Villena FP De, Ferris MT, Baric RS. 2017. Allelic Variation in the Toll-Like Receptor Adaptor Protein Ticam2 Contributes to SARS-Coronavirus Pathogenesis in Mice. *Genes Genomes Genet* 7:1653–1663.
61. Vered K, Durrant C, Mott R, Iraqi FA. 2014. Susceptibility to klebsiella pneumoniae infection in collaborative cross mice is a complex trait controlled by at least three loci acting at different time points. *BMC Genomics* 15:865.
62. Lorè NI, Iraqi FA, Bragonzi A. 2015. Host genetic diversity influences the severity of *Pseudomonas aeruginosa* pneumonia in the Collaborative Cross mice. *BMC Genet* 16:6–11.
63. Nashef A, Qabaja R, Salaymeh Y, Botzman M, Munz M, Dommisch H, Krone B, Hoffmann P, Wellmann J, Laudes M, Berger K, Kocher T, Loos B, van der Velde N, Uitterlinden AG, de Groot LCPGM, Franke A, Offenbacher S, Lieb W, Divaris K, Mott R, Gat-Viks I, Wiess E, Schaefer A, Iraqi FA, Haddad YH. 2018. Integration of Murine and Human Studies for Mapping Periodontitis Susceptibility. *J Dent Res* 002203451774418.
64. Smith CM, Proulx MK, Olive AJ, Laddy D, Mishra BB, Moss C, Gutierrez NM, Bellerose MM, Barreira-Silva P, Phuah JY, Baker RE, Behar SM, Kornfeld H, Evans TG, Beamer G, Sasseti CM. 2016. Tuberculosis susceptibility and vaccine protection are independently controlled by host genotype. *MBio* 7:1–13.
65. Zhang J, Malo D, Mott R, Panthier J, Montagutelli X, Jaubert J. 2018.

- Identification of new loci involved in the host susceptibility to *Salmonella* Typhimurium in collaborative cross mice. *BMC Genomics* 19:1–13.
66. Zhang J, Teh M, Kim J, Eva MM, Cayrol R, Meade R, Nijnik A, Montagutelli X, Malo D, Jauberta J. 2019. A Loss-of-Function Mutation in the Integrin Alpha L (Itgal) Gene Contributes to Susceptibility to *Salmonella enterica* Serovar Typhimurium Infection in Collaborative Cross Strain CC042. *Infect Immun* 88:1–19.
67. Plant JE, Glynn AA. 1982. Genetic control of resistance to *Salmonella* typhimurium infection in high and low antibody responder mice. *Clin Exp Immunol* 50:283–290.
68. Kover PX, Schaal BA. 2002. Genetic variation for disease resistance and tolerance among *Arabidopsis thaliana* accessions. *Proc Natl Acad Sci* 99:11270–11274.
69. Howick VM, Lazzaro BP. 2014. Genotype and diet shape resistance and tolerance across distinct phases of bacterial infection. *BMC Evol Biol* 14:1–13.
70. Merkl SH, Bronkhorst AW, Kramer JM, Overheul GJ, Schenck A, Van Rij RP. 2015. The Epigenetic Regulator G9a Mediates Tolerance to RNA Virus Infection in *Drosophila*. *PLoS Pathog* 11:1–25.
71. Louie A, Song KH, Hotson A, Thomas Tate A, Schneider DS. 2016. How Many Parameters Does It Take to Describe Disease Tolerance? *PLoS Biol* 14:1–21.
72. Read AF, Graham AL, Råberg L. 2008. Animal defenses against infectious agents: Is damage control more important than pathogen control? *PLoS Biol*

- 6:2638–2641.
73. Martins R, Carlos AR, Braza F, Thompson JA, Bastos-Amador P, Ramos S, Soares MP. 2019. Disease Tolerance as an Inherent Component of Immunity. *Annu Rev Immunol* 37:405–437.
 74. Ayres JS, Schneider DS. 2008. Two ways to Survive an Infection: What Resistance and Tolerance Can Teach Us About Treatments for Infectious Diseases. *Nat Rev Immunol* 8:889–895.
 75. McCarville JL, Ayres JS. 2018. Disease tolerance: concept and mechanisms. *Curr Opin Immunol* 50:88–93.
 76. Chervonsky A V. 2017. Just a Spoonful of Sugar Helps the Tolerance Go Up. *Cell* 169:1170–1172.
 77. Ganeshan K, Nikkanen J, Man K, Chagwedera DN, Cox JE, Chawla A, Ganeshan K, Nikkanen J, Man K, Leong YA, Sogawa Y, Maschek JA. 2019. Article Energetic Trade-Offs and Hypometabolic States Promote Disease Tolerance. *Cell* 177:399–413.
 78. Schieber AMP, Ayres JS. 2016. Thermoregulation as a disease tolerance as a defense strategy. *Pathog Dis* 74.
 79. Alexandria M, Palaferri Schieber¹, Lee¹ YM, Chang MW, Leblanc M, Collins B, Downes M, Evans RM, Ayres JS. 2015. Disease tolerance mediated by commensal *E. coli* via inflammasome and IGF-1 signaling. *Science* (80-) 350:558–563.
 80. Horns F, Hood ME. 2012. The evolution of disease resistance and tolerance in

- spatially structured populations. *Ecol Evol* 2:1705–1711.
81. Kortha MJ, Tchitcheka N, Benecke A, Katzea MG. 2013. Systems approaches to influenza-virus host interactions and the pathogenesis of highly virulent and pandemic viruses. *Semin Immunol* 25:1–7.
 82. Green R, Wilkins C, Thomas S, Sekine A, Ireton RC, Ferris MT, Hendrick DM, Voss K, de Villena FP-M, Baric R, Heise M, Gale M. 2016. Identifying protective host gene expression signatures within the spleen during West Nile virus infection in the collaborative cross model. *Genomics Data* 10:114–117.
 83. Smith CM, Proulx MK, Villena FP De, Lai R, Kiritsy MC, Bell TA, Hock P, Ferris MT, Baker RE, Behar SM. 2019. Functionally Overlapping Variants Control Tuberculosis Susceptibility in Collaborative Cross Mice. *MBio* 10:1–15.
 84. Smarr BL, Grant AD, Zucker I, Prednergast BJ, Kriegsfeld LJ. 2017. Sex differences in variability across timescales in BALB/c mice. *Biol Sex Differ* 8:1–7.
 85. Sanchez-Alavez M, Alboni S, Conti B. 2011. Sex- and age-specific differences in core body temperature of C57Bl/6 mice. *Age (Omaha)* 33:89–99.
 86. Geurs TL, Hill EB, Lippold DM, French AR. 2012. Sex Differences in Murine Susceptibility to Systemic Viral Infections. *J Autoimmun* 38.
 87. Boivin GA, Pothlichet J, Skamene E, Brown EG, Loredó-Osti JC, Sladek R, Vidal SM. 2012. Mapping of Clinical and Expression Quantitative Trait Loci in a Sex-Dependent Effect of Host Susceptibility to Mouse-Adapted Influenza H3N2/HK/1/68. *J Immunol* 188:3949–3960.

88. Failla KR, Connelly CD. 2017. Systematic Review of Gender Differences in Sepsis Management and Outcomes. *J Nurs Scholarsh* 312–324.
89. Aminian M, Andrews-Polymenis H, Gupta J, Kirby M, Kvinge H, Ma X, Rosse P, Scoggin K, Threadgill D. 2020. Mathematical methods for visualization and anomaly detection in telemetry datasets. *Interface Focus* 10.
90. Konganti K, Ehrlich A, Rusyn I, Threadgill D. 2018. gQTL : A Web Application for QTL Analysis Using the Collaborative Cross Mouse Genetic Reference Population. *Genes Genomes Genet* 8.
91. Caron J, Loredó-Osti JC, Laroche L, Skamene E, Morgan K, Malo D. 2002. Identification of genetic loci controlling bacterial clearance in experimental *Salmonella enteritidis* infection: An unexpected role of *Nramp1* (*Slc11a1*) in the persistence of infection in mice. *Genes Immun* 3:196–204.
92. Caron J, Loredó-Osti JC, Morgan K, Malo D. 2005. Mapping of interactions and mouse congenic strains identified novel epistatic QTLs controlling the persistence of *Salmonella Enteritidis* in mice. *Genes Immun* 6:500–508.
93. Plaza JJG, Hulak N, Zhumadilov Z, Akilzhanova A. 2016. Fever as an important resource for infectious diseases research. *Intractable Rare Dis Res* 5:97–102.
94. Vlach KD, Boles JW, Stiles BG. 2000. Telemetric evaluation of body temperature and physical activity as predictors of mortality in a murine model of staphylococcal enterotoxic shock. *Comp Med* 50:160–166.
95. Elhadad D, McClelland M, Rahav G, Gal-Mor O. 2015. Feverlike temperature is a virulence regulatory cue controlling the motility and host cell entry of typhoidal

- Salmonella. *J Infect Dis* 212:147–156.
96. McLaughlin PA, Bettke JA, Tam JW, Leeds J, Bliska JB, Butler BP, van der Velden AWM. 2019. Inflammatory monocytes provide a niche for Salmonella expansion in the lumen of the inflamed intestine. *PLoS Pathog* 15:1–17.
 97. Bingle CD, Bingle L, Craven CJ. 2011. Distant cousins: Genomic and sequence diversity within the BPI fold-containing (BPIF)/PLUNC protein family. *Biochem Soc Trans* 39:961–965.
 98. Chen S, Bonifati S, Qin Z, Gelais CS, Kodigepalli KM, Barrett BS, Kim SH, Antonucci JM, Ladner KJ, Buzovetsky O, Knecht KM, Xiong Y, Yount JS, Guttridge DC, Santiago ML, Wu L. 2018. SAMHD1 suppresses innate immune responses to viral infections and inflammatory stimuli by inhibiting the NF- κ B and interferon pathways. *Proc Natl Acad Sci U S A* 115:E3798–E3807.
 99. Li Z, Huan C, Wang H, Liu Y, Liu X, Su X, Yu J, Zhao Z, Yu X, Zheng B, Zhang W. 2020. TRIM 21-mediated proteasomal degradation of SAMHD 1 regulates its antiviral activity . *EMBO Rep* 21:1–18.
 100. Bogomolnaya LM, Santiviago CA, Yang HJ, Baumler AJ, Andrews-Polymenis HL. 2008. “Form variation” of the O12 antigen is critical for persistence of Salmonella Typhimurium in the murine intestine. *Mol Microbiol* 70:1105–1119.
 101. Iraqi FA, Mahajne M, Salaymah Y, Sandovski H, Tayem H, Vered K, Balmer L, Hall M, Manship G, Morahan G, Pettit K, Scholten J, Tweedie K, Wallace A, Weerasekera L, Cleak J, Durrant C, Goodstadt L, Mott R, Yalcin B, Aylor DL, Baric RS, Bell TA, Bendt KM, Brennan J, Brooks JD, Buus RJ, Crowley JJ,

Calaway JD, Calaway ME, Cholka A, Darr DB, Didion JP, Dorman A, Everett ET, Ferris MT, Mathes WF, Fu CP, Gooch TJ, Goodson SG, Gralinski LE, Hansen SD, Heise MT, Hoel J, Hua K, Kapita MC, Lee S, Lenarcic AB, Liu EY, Liu H, McMillan L, Magnuson TR, Manly KF, Miller DR, O'Brien DA, Odet F, Pakatci IK, Pan W, de Villena FPM, Perou CM, Pomp D, Quackenbush CR, Robinson NN, Sharpless NE, Shaw GD, Spence JS, Sullivan PF, Sun W, Tarantino LM, Valdar W, Wang J, Wang W, Welsh CE, Whitmore A, Wiltshire T, Wright FA, Xie Y, Yun Z, Zhabotynsky V, Zhang Z, Zou F, Powell C, Steigerwalt J, Threadgill DW, Chesler EJ, Churchill GA, Gatti DM, Korstanje R, Svenson KL, Collins FS, Crawford N, Hunter K, Samir N, Kelada P, Peck BCE, Reilly K, Tavarez U, Bottomly D, Hitzeman R, Mcweeney SK, Frelinger J, Krovi H, Phillippi J, Spritz RA, Aicher L, Katze M, Rosenzweig E, Shusterman A, Nashef A, Weiss EI, Houry-Haddad Y, Soller M, Williams RW, Schughart K, Yang H, French JE, Benson AK, Kim J, Legge R, Low SJ, Ma F, Martinez I, Walter J, Broman KW, Hallgrimsson B, Klein O, Weinstock G, Warren WC, Yang Y V., Schwartz D. 2012. The genome architecture of the collaborative cross mouse genetic reference population. *Genetics* 190:389–401.

102. Korth MJ, Tchitchek N, Benecke A, Katze MG. 2013. Systems approach to influenza-virus host interactions and the pathogenesis of highly virulent and pandemic viruses. *Semin Immunol* 25.
103. Monack DM, Bouley DM, Falkow S. 2004. *Salmonella typhimurium* Persists within Macrophages in the Mesenteric Lymph Nodes of Chronically Infected

- Nramp1^{+/+} Mice and Can Be Reactivated by IFN γ Neutralization. *J Exp Med* 199:231–241.
104. Lough G, Kyriazakis I, Bergmann S, Lengeling A, Doeschl-Wilson AB. 2015. Health trajectories reveal the dynamic contributions of host genetic resistance and tolerance to infection outcome. *Proc R Soc B Biol Sci* 282.
105. Hui WW, Hercik K, Belsare S, Alugubelly N, Clapp B, Rinaldi C, Edelmann MJ. 2018. *Salmonella enterica* serovar Typhimurium alters the extracellular proteome of macrophages and leads to the production of proinflammatory exosomes. *Infect Immun* 86.
106. Martin GS. 2012. Sepsis, severe sepsis and septic shock: changes in incidence, pathogens and outcomes. *Expert Rev Anti Infect Ther* 10:701–706.
107. Chaudhry H, Zhou J, Zhong Y, Ali MM, McGuire F, Nagarkatti PS, Nagarkatti M. 2015. Role of Cytokines as a Double-edged Sword in Sepsis. *PMC* 27:669–684.
108. Rowell DL, Eckmann L, Dwinell MB, Carpenter SP, Raucy JL, Yang SK, Kagnoff MF. 1997. Human hepatocytes express an array of proinflammatory cytokines after agonist stimulation or bacterial invasion. *Am J Physiol - Gastrointest Liver Physiol* 273.
109. Ram R, Mehta M, Balmer L, Gatti DM, Morahan G. 2014. Rapid identification of major-effect genes using the collaborative cross. *Genetics* 198:75–86.
110. Ao TT, Feasey NA, Gordon MA, Keddy KH, Angulo FJ, Crump JA. 2015. Global burden of invasive nontyphoidal salmonella disease, 2010. *Emerg Infect Dis*

21:941–949.

111. Peters LC, Jensen JR, Borrego A, Cabrera WHK, Baker N, Starobinas N, Ribeiro OG, Ibañez OM, De Franco M. 2007. Slc11a1 (formerly NRAMP1) gene modulates both acute inflammatory reactions and pristane-induced arthritis in mice. *Genes Immun* 8:51–56.
112. Blackwell JM, Goswami T, Evans CAW, Sibthorpe D, Papo N, White JK, Searle S, Miller EN, Peacock CS, Mohammed H, Ibrahim M. 2001. SLC11A1 (formerly NRAMP1) and disease resistance. *Cell Microbiol* 3:773–784.
113. Ramirez-Carrozzi V, Sambandam A, Luis E, Lin Z, Jeet S, Lesch J, Hackney J, Kim J, Zhou M, Lai J, Modrusan Z, Sai T, Lee W, Xu M, Caplazi P, Diehl L, De Voss J, Balazs M, Gonzalez L, Singh H, Ouyang W, Pappu R. 2011. IL-17C regulates the innate immune function of epithelial cells in an autocrine manner. *Nat Immunol* 12:1159–1166.
114. Mayuzumi H, Inagaki-Ohara K, Uyttenhove C, Okamoto Y, Matsuzaki G. 2010. Interleukin-17A is required to suppress invasion of *Salmonella enterica* serovar Typhimurium to enteric mucosa. *Immunology* 131:377–385.
115. Muñoz-García J, Cochonneau D, Télétchéa S, Moranton E, Lanoe D, Brion R, Lézot F, Heymann MF, Heymann D. 2021. The twin cytokines interleukin-34 and CSF-1: Masterful conductors of macrophage homeostasis. *Theranostics* 11:1568–1593.
116. Fritz JM, Weaver TE. 2014. The BiP cochaperone ERdj4 is required for B cell development and function. *PLoS One* 9:1–10.

117. Gade P, Ramachandran G, Maachani UB, Rizzo MA, Okada T, Prywes R, Cross AS, Mori K, Kalvakolanu D V. 2012. An IFN- γ -stimulated ATF6-C/EBP- β -signaling pathway critical for the expression of death associated protein kinase 1 and induction of autophagy. *Proc Natl Acad Sci U S A* 109:10316–10321.
118. Deiss LP, Feinstein E, Berissi H, Cohen O, Kimchi A. 1995. Identification of a novel serine/threonine kinase and a novel 15-kD protein as potential mediators of the γ interferon-induced cell death. *Genes Dev* 9:15–30.
119. Ingram JP, Brodsky IE, Balachandran S. 2017. Interferon- γ in Salmonella pathogenesis: New tricks for an old dog. *Cytokine* 98:27–32.
120. Sigmon JS, Blanchard MW, Baric RS, Bell TA, Brennan J, Brockmann GA, Wesley Burks A, Mauro Calabrese J, Caron KM, Cheney RE, Ciavatta D, Conlon F, Darr DB, Faber J, Franklin C, Gershon TR, Gralinski L, Gu B, Gaines CH, Hagan RS, Heimsath EG, Heise MT, Hock P, Ideraabdullah F, Charles Jennette J, Kafri T, Kashfeen A, Kulis M, Kumar V, Linnertz C, Livraghi-Butrico A, Kent Lloyd KC, Lutz C, Lynch RM, Magnuson T, Matsushima GK, McMullan R, Miller DR, Mohlke KL, Moy SS, Murphy CEY, Najarian M, O'Brien L, Palmer AA, Philpot BD, Randell SH, Reinholdt L, Ren Y, Rockwood S, Rogala AR, Saraswatula A, Sasseti CM, Schisler JC, Schoenrock SA, Shaw GD, Shorter JR, Smith CM, St. Pierre CL, Tarantino LM, Threadgill DW, Valdar W, Vilen BJ, Wardwell K, Whitmire JK, Williams L, Zylka MJ, Ferris MT, McMillan L, Manuel de Villena FP. 2020. Content and performance of the MiniMUGA genotyping array: A new tool to improve rigor and reproducibility in mouse

- research. *Genetics* 216:905–930.
121. Broman KW, Gatti M, Simecek P, Furlotte N, Prins P, Sen S, Yandell B, Churchill G. 2019. R/qtl2: Software for Mapping Quantitative Trait Loci with High-Dimensional Data and Multiparent Populations *Karlsberg Genetics* 211:495–502.
 122. Marzel A, Desai PT, Goren A, Schorr YI, Nissan I, Porwollik S, Valinsky L, McClelland M, Rahav G, Gal-Mor O. 2016. Persistent infections by nontyphoidal salmonella in humans: Epidemiology and genetics. *Clin Infect Dis* 62:879–886.
 123. Ohad Gal-Mora B. 2019. Persistent Infection and Long-Term Carriage of Typhoidal and Nontyphoidal Salmonellae. *Clin Microbiol Rev* 32:1–31.
 124. Broz P, Ohlson MB, Monack DM. 2012. Innate immune response to *Salmonella typhimurium*, a model enteric pathogen. *Gut Microbes* 3:62–70.
 125. Coiffard B, Diallo AB, Mezouar S, Leone M, Mege J-L. 2021. A Tangled Threesome: Circadian Rhythm, Body Temperature Variations, and the Immune System. *Biology (Basel)* 10.
 126. Leon LR, Walker LD, DuBose DA, Stephenson LA. 2004. Biotelemetry transmitter implantation in rodents: Impact on growth and circadian rhythms. *Am J Physiol - Regul Integr Comp Physiol* 286:967–974.
 127. Summers C, Rankin SM, Condliffe AM, Singh N, Peters AM, Chilvers ER. 2010. Neutrophil kinetics in health and disease. *Trends Immunol* 31:318–324.
 128. Ulloa L, Tracey KJ. 2005. The “cytokine profile”: A code for sepsis. *Trends Mol Med* 11:56–63.
 129. Tetta C, Bellomo R, D’Intini V, De Nitti C, Inguaggiato P, Brendolan A, Ronco

- C. 2003. Do circulating cytokines really matter in sepsis? *Kidney Int Suppl* 63:69–71.
130. Roy B, Kirchner J. 2000. Evolutionary dynamics of pathogen resistance and tolerance. *Evolution (N Y)* 54:51–63.

APPENDIX A

Table A 1: Histopathology scoring matrix with descriptions.

Final score per organ corresponds to whichever section has the highest score. Scoring matrix from Dr. Garry Adams.

Score	Tissue Injury	PMN Infiltrate*	Mononuclear Infiltrate*	Microgranuloma Formation*	Necrosis Cellular or Zonal	Abscessation or Zonal Infarction
0	None	No changes, 0-3	No changes, 0-5	No changes	No changes	No changes
1	Mild	3-5	6-10	1-2	Single cells	None
2	Moderate	6-15	11-80	3-5	Multiple cells	Small, rare
3	Marked	16-150	81-200	6-12	Islands of cells	Moderate, occasional
4	Severe	>150	>200	>12	Broad zones	Massive, common

*Number of cells or microgranulomas per high power field (400X).

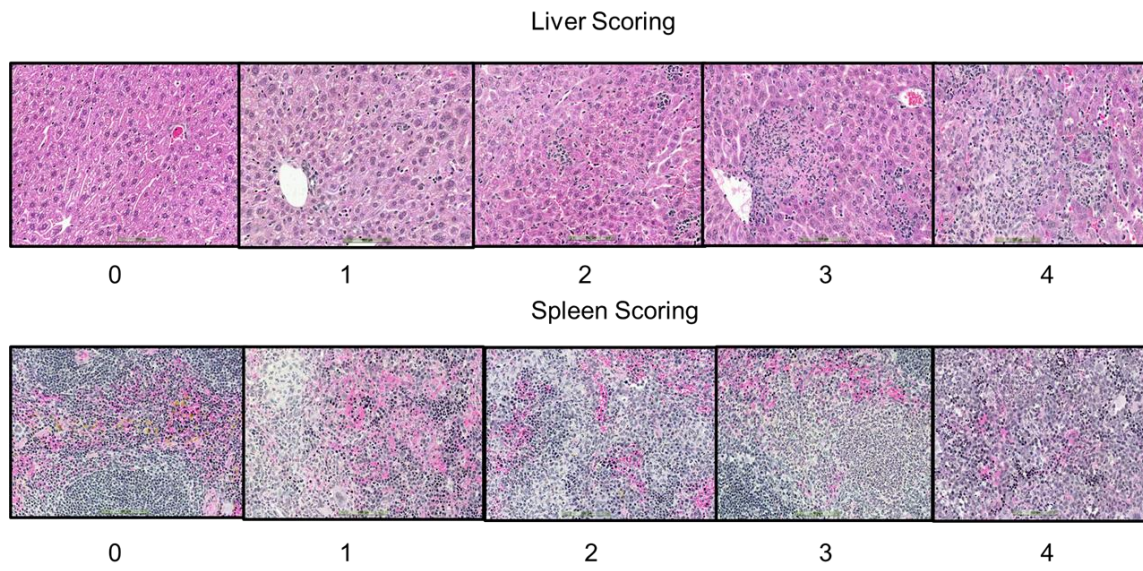


Figure A 1: Representative images of spleen and liver histology scoring matrix. Tissues were sectioned and stained with H&E before being analyzed. Images from Dr. Garry Adams illustrating scoring matrix.

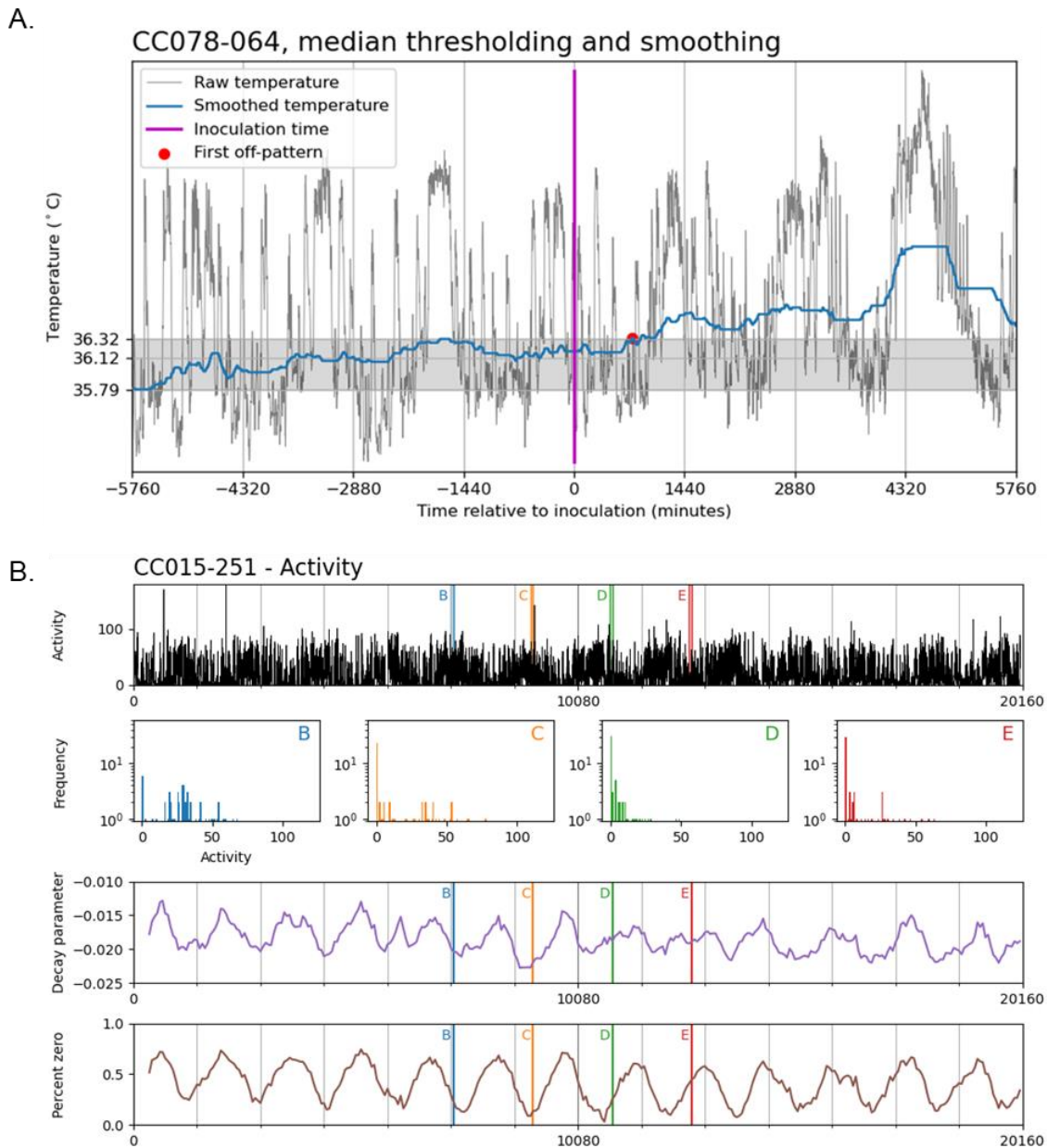


Figure A 2: Graphical representation of how telemetry models were run. Examples of how A. temperature and B. activity calculations were determined. Specifically maximum, median, minimum pre-infection temperature and activity as well “off-pattern” for post-infection.